Formulation, Optimisation and Characterisation of pH Gradient Niosomes: Active Loading of Bromocresol Green and Doxorubicin

Altaee, Mohammed Ahmad Tarik

A thesis submitted in partial fulfilment of the requirements of the University of Sunderland for the degree of Doctor of Philosophy

Faculty of Health Sciences and Wellbeing

July 2026

Abstract

Background: The active loading of drugs into liposomes was proven to be a very successful technique in drug loading to enhance the percentage of drug loaded. However, numerous knowledge gaps have been identified in active drug loading in niosomes. The purpose of this thesis is to investigate the effect of different co-surfactants (Solutol HS-15, Cremophor ELP, and Cremophor RH 40) on the niosomal membrane stability and their effect on active drug loading and niosomes' physicochemical properties. **Methods:** A new technique to study pH gradient in nanovesicles was developed utilising the pH indicator bromocresol green (BCG). BCG was used as a probe to investigate the presence and stability of the pH gradient across the niosomal membrane, as it undergoes colour changes at different pH values. It helps studying the effects of different parameters on active drug loading via a pH gradient, including buffer types, surfactants, and co-surfactants. The optimised formulations were used to actively load doxorubicin using an ammonium sulfate pH gradient. Preliminary studies included the formulation of niosomes using the thin-film hydration technique. However, the microfluidic technique was also used to formulate optimised niosomes for active pH-gradient doxorubicin loading, as this has not been studied before. **Results:** The results demonstrated that the compatibility between the main surfactant and the co-surfactant is critical for maintaining pH gradient stability. For instance, Span 65 showed greater compatibility with Cremophor RH 40, maintaining a pH gradient for more than 1 hour, compared to Solutol HS-15, which maintained a pH gradient for less than 15 minutes. In contrast, Span 60 exhibited the opposite behaviour, maintaining a longer pH gradient with Solutol HS 15 than with Cremophor RH 40. Additional factors influencing the entrapment efficiency of actively loaded drugs and the size of niosomes included the buffer system used, the vesicle size and morphology, the temperature during drug loading, and the cholesterol content of the formulation.

Among the formulations tested, Span 65 niosomes exhibited smaller vesicle size and greater stability than Span 60 niosomes. Doxorubicin was successfully loaded into Span 65–Cremophor RH 40 niosomes with high entrapment efficiency using the pH gradient method, reaching 78.79 % EE, and achieved a size of 237.8 nm after sonication when 5% of Cremophor RH 40 was included as the co-surfactant and 76.99% EE and 191.9

nm after sonication when 10% of Cremophor RH 40 was included as the co-surfactant with size distribution PDI for both formulations was 0.27 and 0.28 respectively. Given the promising performance of this formulation, a microfluidic technique was employed to prepare it, yielding niosomes with smaller sizes and a more controlled size distribution. The microfluidic approach produced Span 65 niosomes with controlled size and narrow size distribution when 0.3 mg/mL of doxorubicin was loaded (~ 108 nm, PDI = 0.12) and 0.5mg/mL of doxorubicin was loaded (~ 140 nm, PDI = 0.11) while maintaining high entrapment efficiency (~ 70% in both drug loading concentrations) through active drug loading, resulting in a stable niosomal formulation (no significant size change over 3 months period with both drug loading concentrations.

Key words: niosomes, span 60, span 65, cremophor RH40, solutol HS-15, pH gradient, active drug loading, doxorubicin, bromocresol green, pH indicator, thin film hydration, microfluidic, niosomes stability.

Acknowledgement

I would like to express my sincere gratitude to my wife and family for standing with me and supporting me throughout this journey. My deepest appreciation goes to my supervisors, Prof. Amal Ali Elkordy and Dr. Ahmed Mostafa Faheem for their invaluable guidance, insightful feedback, and continuous encouragement throughout the course of this research. Their expertise, patience, and support have greatly contributed to the development and completion of this work. I am also grateful to the university staff for their assistance and professionalism during my time at the university. Their support in both academic and administrative matters has been greatly appreciated.

Research activity

Open Access Publication:

Altaee, M.; Faheem, A.M.; Elkordy, A.A. pH Gradient-Driven Loading of Doxorubicin into Niosomes: A Comparative Study Using Bromocresol Green as a Visual Indicator. Pharmaceutics 2025, 17, 862. https://doi.org/10.3390/pharmaceutics17070862[1]

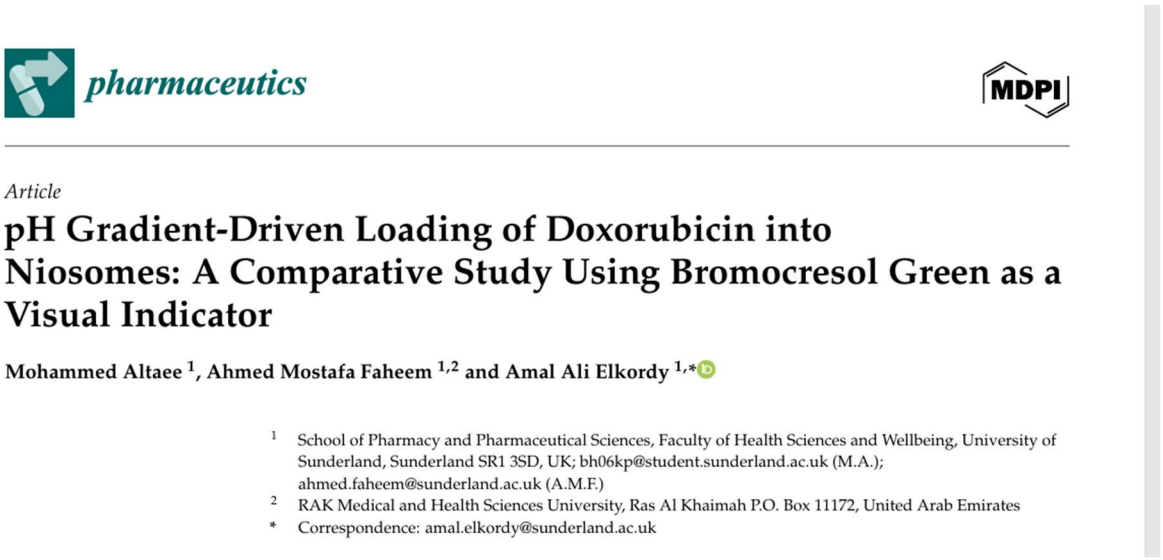

pharmaceutics

MDPI

Article

pH Gradient-Driven Loading of Doxorubicin into Niosomes: A Comparative Study Using Bromocresol Green as a Visual Indicator

Mohammed Altaee [1], Ahmed Mostafa Faheem [1,2] and Amal Ali Elkordy [1,*]

[1] School of Pharmacy and Pharmaceutical Sciences, Faculty of Health Sciences and Wellbeing, University of Sunderland, Sunderland SR1 3SD, UK; bh06kp@student.sunderland.ac.uk (M.A.); ahmed.faheem@sunderland.ac.uk (A.M.F.)
[2] RAK Medical and Health Sciences University, Ras Al Khaimah P.O. Box 11172, United Arab Emirates
* Correspondence: amal.elkordy@sunderland.ac.uk

Poster Presentation:

Title: Liposomes: Methods of Preparation and Their Uses

University of Sunderland Research Conference, University of Sunderland (21/06/2023)

Abbreviations

%EE: percentage entrapment efficiency

AMF: alternating magnetic field stimulus

BCG: bromocresol green

BCP: bromocresol purple

BNF: British National Formulary

CPP: critical packing parameter

DLS: differential light scattering

DMF: Dimethyl formamide

DMSO: Dimethyl sulfoxide

DNA: deoxyribonucleic

DSC: Differential Scanning Colourimetry

FDA: Food and Drug Administration

FT-IR: Fourier Transform Infrared Spectroscopy

GA: Gambogic Acid

HCl: hydrochloric acid

HLB: hydrophilic lipophilic balance

HSPC: hydrogenated phosphatidylcholine

kDa: kilodalton

LUV: large unilamellar vesicle

MLV: multilamellar vesicle

NMP: N-Methylpyrrolidone

PDI: polydispersity index

RNA: ribonucleic acid

ROS: Reactive oxygen species

SUV: small unilamellar vesicle

Tm: phase transition temperature

λmax: lambda max

Table of Contents

List of Figures

List of Tables

Thesis Structure

The thesis consists of the following chapters:

Chapter 1 provides an introduction to the field of niosomes and establishes the scientific background for the area of research covered in this thesis.

Chapter 2 explains the methods and techniques used in the laboratory to develop the thesis.

Chapter 3 demonstrates how bromocresol green, a pH indicator, can be a useful tool for studying pH gradients in niosomes. It also demonstrates the properties of different niosomal formulations for establishing and maintaining a pH gradient.

Chapter 4 will rely on the data generated in Chapter 3 to make a niosomal formulation capable of actively loading doxorubicin.

Chapter 5 focuses on using the microfluidic technique to further optimise the formulations from Chapter 4.

Chapter 6 summarises the key findings and suggests future work to build on this thesis.

Chapter 7 includes the references used throughout the thesis.

Chapter One: Introduction

1.1 Background

Several drugs currently available, as well as many others under research, have significant pharmacokinetic limitations that hinder their therapeutic use, reducing effectiveness, safety, and patient compliance. These drugs face numerous challenges, including poor water solubility and bioavailability, rapid degradation and clearance, nonspecific distribution and side effects, poor patient compliance due to frequent dosing or inconvenient delivery routes, and incompatibility with certain routes of administration. Several solutions have been proposed to solve these challenges including the use of nanovesicles[1–4].

These challenges limit the use of many potent drugs in practice. Many drugs, such as chemotherapy agents, are poorly water-soluble, which results in reduced absorption when administered orally, leading to low bioavailability and inconsistent therapeutic outcomes[5]. Certain drugs are rapidly degraded in the bloodstream or stomach, or are quickly cleared by the kidneys or liver, which limits their therapeutic window, such as the delivery of genetic materials like deoxyribonucleic acid (DNA) and ribonucleic acid (RNA)[6,7]. Many drugs, such as chemotherapy and antibiotics, act systemically and affect both diseased and healthy tissues, causing side effects[8]. Some drugs require frequent dosing due to short half-lives[9]. This leads to poor adherence and fluctuating drug levels.

Nanovesicles have been employed to deliver various drugs, addressing key pharmaceutical challenges such as solubility, stability, targeting, and patient adherence [10,11]. Examples of nanovesicles include niosomes, which are the focus of this thesis, as well as liposomes, transferosomes, ethosomes, cubosomes, and polymersomes[12–15]. The key feature in all these vesicles is that they contain a bilayer membrane similar in structure to that found in cells, and an aqueous core. What distinguishes these vesicles from one another is the structure and composition of their bilayer membranes. A hydrophobic bilayer membrane allows vesicles to solubilise hydrophobic molecules such as curcumin, thereby increasing their concentration in the formulation. Having an aqueous core surrounded by a bilayer membrane protects the entrapped drugs in the aqueous core from the surrounding environment, thereby reducing rapid degradation and clearance[12–15].

1.2 Niosomes: Definition and Background

Niosomes were first developed by researchers from L'Oréal (France), and the first patent was released in 1975 for cosmetic use. Niosomes, also known as non-ionic surfactant vesicles, are nanovesicles consisting of a bilayer membrane and an aqueous core (figure 1.1). The bilayer membrane is formed from non-ionic surfactant(s) and cholesterol lipid[16]. Co-surfactants, such as Cremophore RH40[17] and Solutol HS-15[18], are sometimes added to stabilise the niosomal formulation and improve its properties.

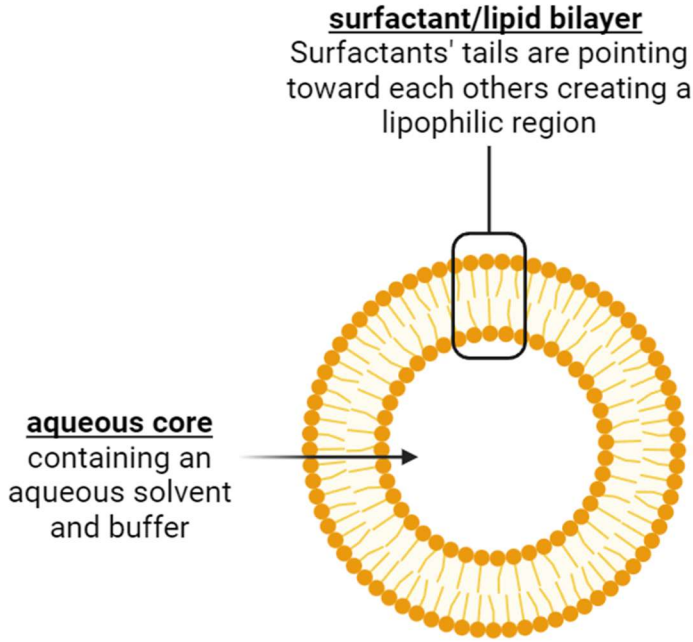

Figure 1.1: Structure of niosomes (created using BioRender)

Currently, various niosomal formulations are being developed as alternatives to liposomes. Liposomes have been proven to be highly effective drug delivery systems that have reached the market and are used to treat various medical conditions, including cancers and infections[19]. However, only a few niosomal formulations have progressed to pre-clinical and clinical trials, with a primary focus on topical delivery in the cosmetics field[16]. This means that niosomes require more work to reach clinical use in drug delivery.

Niosomes offer several advantages over liposomes, including greater stability and lower cost. In addition, lipids used in liposome production have the problem of variable purities, which is avoided in niosomes[16].

1.3 Classification of Niosomes Based on Size and Shape

Niosomes can be classified into different categories based on their size and shape: small unilamellar vesicles (SUV), large unilamellar vesicles (LUV), and multilamellar vesicles (MLV). Multilamellar vesicle niosomes are vesicles consisting of multiple bilayer membranes. This appears to be a structure of niosomes within niosomes, featuring multiple bilayers and multiple aqueous cores. On the other hand, unilamellar vesicles consist of only one bilayer membrane and one aqueous core (figure 1.2). Multilamellar niosomal vesicles typically have a diameter> 5000 nm. Unilamellar vesicles can be divided into two categories based on size: SUV (10 – 100 nm), and LUV (100 – 3000 nm)[20].

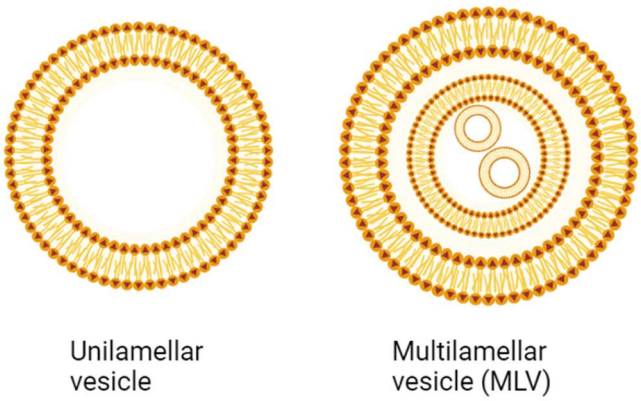

Figure 1.2: Unilamellar vs multilamellar niosomal vesicles (created using BioRender)

Size and shape are crucial factors that influence the amount of drug encapsulated within the niosomes[21]. They are also essential factors to consider in certain dosage forms. For example, the desirable size for intravenous injection of doxorubicin liposomes is 80 – 150 nm to enhance the blood circulation half-life[22].

However, it is vital to consider the methods to be used for reducing the size of the niosomes, as size reduction techniques can result in the leakage of the entrapped drug[23], as will be discussed later.

1.4 Composition of Niosomes

As previously discussed, niosomes are mainly composed of non-ionic surfactants and cholesterol. Niosomes can also contain other additives that help stabilise them. These are known as co-surfactants, such as charge-inducing compounds, surfactants with high hydrophilic lipophilic balance (HLB) and molecules containing polyethylene glycol (PEG)[17,18].

1.4.1 Surfactants

A surfactant is an amphiphilic compound that has a hydrophilic head and a hydrophobic tail. In the niosomal bilayer membrane, the hydrophilic head faces the aqueous environment in the niosome aqueous core and the medium surrounding the niosomes. In contrast, the hydrophobic tails face each other away from the aqueous surroundings.

Different types of non-ionic surfactants have been used in niosomes. These surfactants can have various characteristics depending on their properties, including their chemical structure, HLB, critical packing parameter (CPP) and phase transition temperature (Tm)[21,24].

1.4.1.1 Surfactant Chemical Structures

The common feature in all surfactants used in niosomal formulations is that they contain a hydrophilic head group and a hydrophobic tail to allow the assembly of a bilayer membrane in niosomes. However, different surfactants have distinct head groups, tail groups, and types of linkers that connect the head group to the tail group[10]. These differences can impact the properties of the niosomal bilayer membrane, including permeability, thickness, fluidity, and the loading capacity of hydrophobic drugs, among others[16]. Table 1.1 below shows examples of different surfactants used in niosomes.

Surfactants are classified into families such as sorbitans, polysorbates and Brij surfactants. The different members of these surfactant families have distinct structures, resulting in niosome membranes with varying properties. The length of the alkyl chain, the degree of saturation, the size of the head group, and the number

of alkyl chains in the surfactant all play crucial roles in determining the properties of the niosomal membrane[25].

Span 60 has a longer alkyl chain than Span 40 and Span 20 (table 1.1). The length of the alkyl chain increases membrane rigidity, entrapment efficiency, and stability, while shorter alkyl chains can form more permeable and leaky vesicles. This can be explained by the fact that longer chains can form thicker and denser bilayer membranes, which create a more substantial barrier that separates the niosomal aqueous core from the buffer surrounding the niosomes[26].

Moreover, the degree of saturation in the alkyl chain affects membrane fluidity and permeability, where unsaturated surfactants (such as Span 80 which is monounsaturated) form a more fluid and leaky membrane, while saturated surfactants (such as Span 60) result in a rigid, less permeable membrane[26]. Span 80 is liquid at room temperature, while Span 60 is solid[27]. The interaction between the alkyl chains is called the van der Waals force. Unsaturated alkyl chains are known to form weaker van der Waals forces compared to saturated alkyl chains[28]. This can explain why unsaturated surfactants, such as Span 80, form less rigid and leakier membranes.

The number of alkyl chains in a surfactant can also play a crucial role in membrane stability, entrapment efficiency, and vesicle size. For example, Span 65, which has three alkyl chains, forms smaller niosomes with higher entrapment efficiency of curcumin than Span 60 niosomes[29].

Table 1.1: The different families of surfactants used for niosomes preparation. The families are classified by the linker group that connects the surfactant's hydrophilic head to its lipophilic tails.

Linker group	Surfactant families - examples of members	Examples of surfactant structures
Fatty alcohols	**Fatty alcohols**[30] - Cetyl alcohol - Stearyl alcohol - Oleyl alcohol	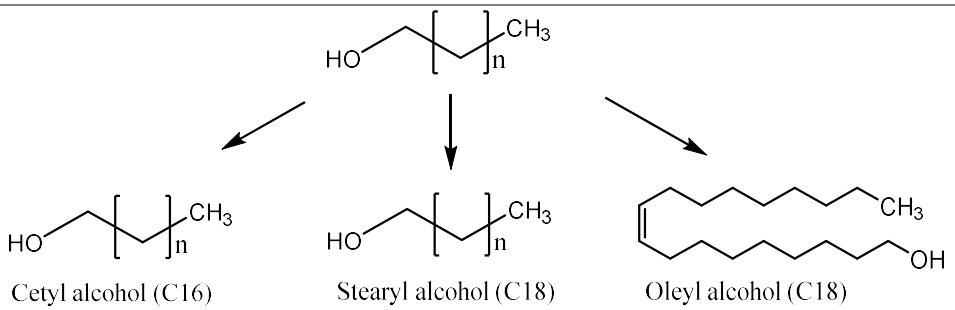
Ether	**Brij series**[10,31] - Brij 30 - Brij 35 - Brij 52 - Brij 56 - Brij 58 - Brij 72 - Brij 76 - Brij 78 - Brij 721 - Brij 78 - Brij 700 - Brij 92 - Brij 97 - Brij 98 **Glycosides**[26] - Octyl glucoside - Lauryl glucoside - Decyl glucoside	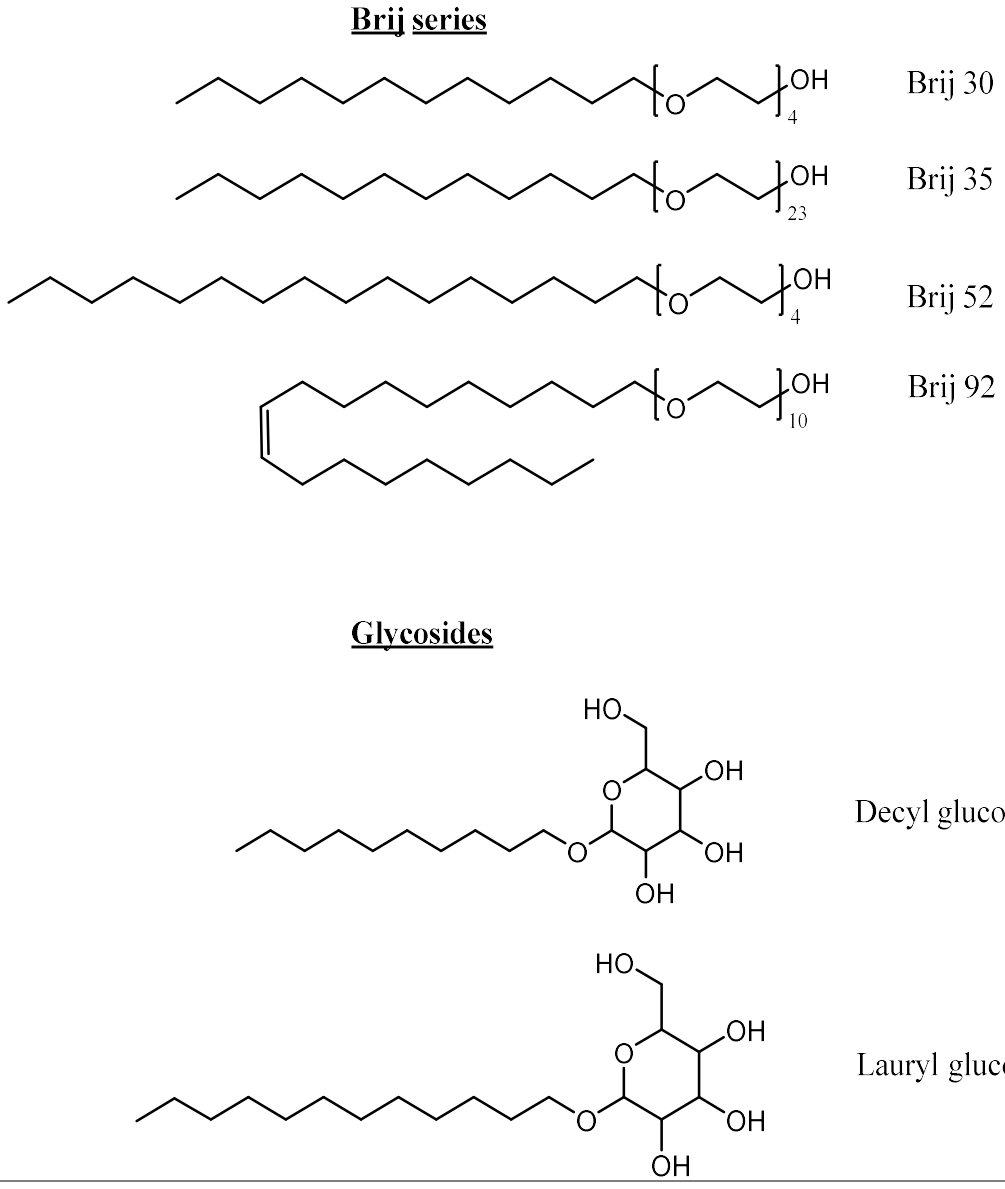

Esters	**Span series (sorbitan esters)**[30] - Span 20 - Span 40 - Span 60 - Span 80 - Span 65 - Span 85 **Tween series (polysorbates)**[32] - Tween 20 - Tween 40 - Tween 60 - Tween 65 - Tween 80	**Span series** 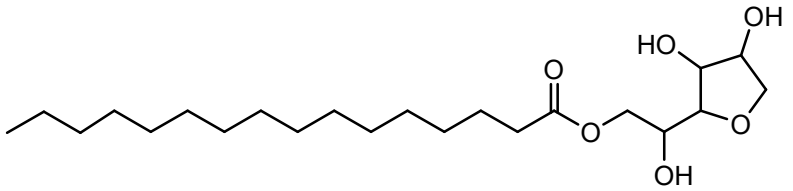 Span 40 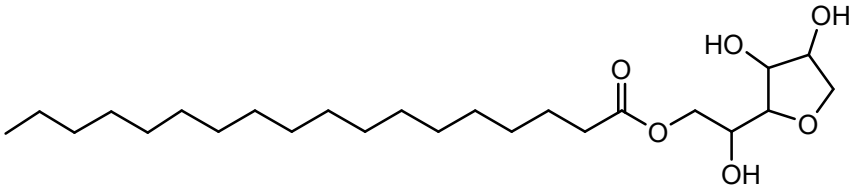 Span 60 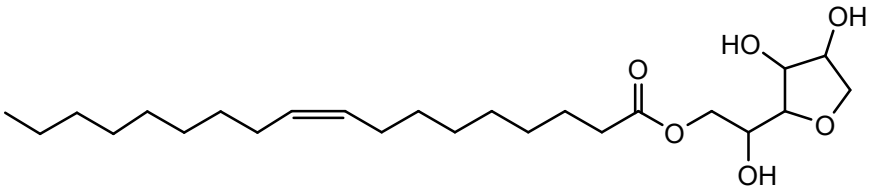 Span 80 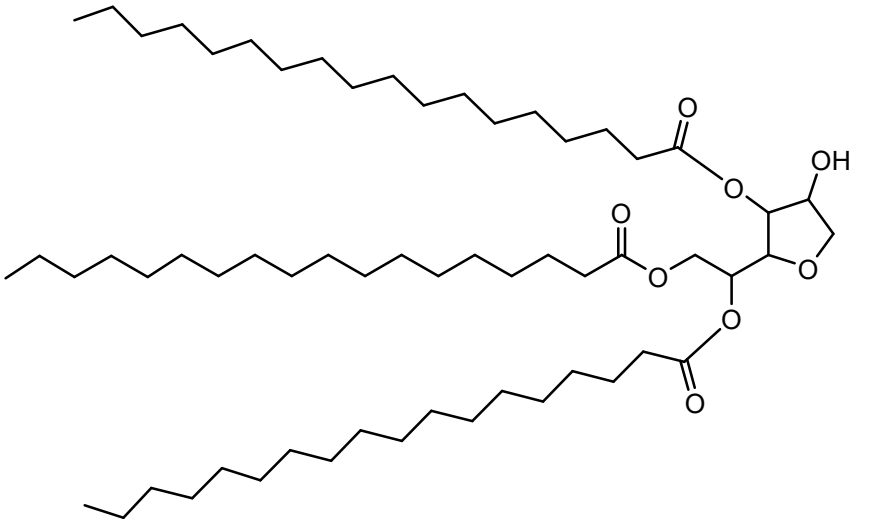 Span 65

Tween series

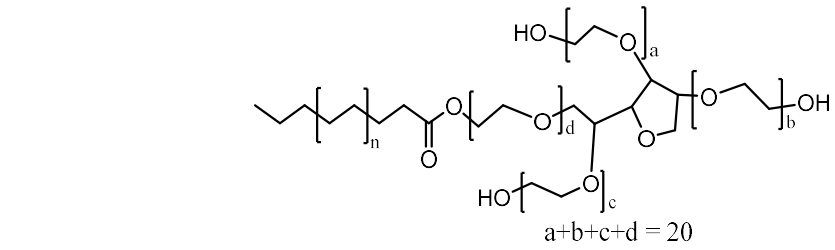

Tween 20 (n = 3)
Tween 40 (n = 5)
Tween 60 (n = 6)

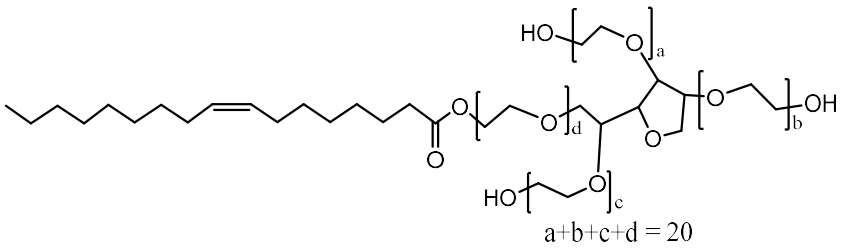

Tween 80

1.4.1.2 Surfactants' Hydrophilic Lipophilic Balance

To measure the degree of hydrophilicity or lipophilicity of surfactants, an HLB equation is used. The equation compares the molar mass of the surfactant's hydrophobic region to that of the hydrophilic region.

$$HLB = 20 \text{ x } \frac{\text{Mh}}{\text{Mt}} \qquad \text{eq. 1.1}$$

Where Mh is the molar mass of the hydrophilic part of the surfactant, while Mt is the total molar mass of the surfactant. HLB is an arbitrary scale ranging from 0 to 20. Lower values indicate that the surfactant is more lipophilic in character, while higher values indicate that the surfactant is more hydrophilic[33].

It can be concluded from equation 1.1 that surfactants with longer alkyl chains have lower HLB values than those with shorter tails. For example, Span 60 has a lower HLB compared to Span 40 (4.7 vs 6.7)[20]. Also, surfactants with multiple alkyl chains, like Span 65, have a lower HLB than those with a mono alkyl chain, like Span 60 (2.1 vs 4.7)[34].

Surfactants with high HLB values tend to form micelles rather than bilayers in aqueous media. The right HLB must be achieved for niosomes to form. It was found

that surfactants with high HLB could only form niosomes in the presence of cholesterol, while niosomes were formed, without cholesterol, by surfactants with low HLB. HLB values above 14 are not suitable for the production of niosomes. Cholesterol must be added to surfactants with HLB > 6 to be able to form niosomes, while cholesterol is added to surfactants with HLB < 6 to enhance vesicles' stability[35].

1.4.1.3 Phase Transition Temperature

The phase transition temperature (Tm) is a key physical property of the surfactant used to prepare niosomes, as it significantly affects their stability, permeability, and drug retention. Tm is the temperature at which the surfactant's hydrophobic tail undergoes a transition from an ordered (gel) phase to a disordered (liquid-crystalline) phase. Below Tm, tails are tightly packed in the vesicle membrane, and the vesicle membrane is rigid. Above Tm, tails are more mobile, resulting in the membrane becoming more fluid and flexible[26].

Below Tm, the vesicle membrane is more rigid and less permeable, thereby enhancing vesicle stability and drug retention and reducing vesicle fusion and drug leakage. Above the Tm, the membrane becomes more fluid, potentially leading to drug leakage, vesicle fusion, or degradation. For long-term storage, the niosomes should be stored below the main surfactant Tm to maintain stability. Choosing a surfactant with a high Tm, such as Span 60 (Tm = 53 °C), will form rigid vesicles that are beneficial for stability[26].

1.4.1.4 Critical Packing Parameter

Critical packing parameter (CPP) is a calculated value that is used to predict the geometry of the vesicle that surfactants and amphiphilic molecules will form in solution (e.g. micelles, inverted micelles, bilayers). It is a crucial parameter when selecting a surfactant for designing niosomes[36]. Table 1.2 below describes the structures linked to the surfactant CPP value.

Table 1.2: The relationship between CPP value and the structure of the nanovesicles containing the surfactants[21].

CPP Value Range	Expected Structure
< 1/3	**Spherical micelles**
≈ 1/3 – 1/2	**Cylindrical micelles**
≈ 1/2 – 1	**Bilayers or vesicles**
≈ 1	**Planar bilayers (lamellae)**
> 1	**Inverse structures** (e.g., inverted micelles)

CPP can be calculated using the following equation[36]:

$$CPP = \frac{V}{a_0 .lc} \quad \text{eq. 1.2}$$

Where V is the volume of the hydrophobic tail(s), a_0 is the optimal headgroup area, and lc is the length of the hydrophobic tail.

The volume of the hydrophobic tail(s), V, can be calculated using the following formula, which is based on the number of carbon atoms[37]:

$$V = 27.4 + 26.9 \cdot \mathrm{n} \quad \text{eq. 1.3}$$

Where n is the number of carbon atoms in the hydrophobic tail.

The optimal headgroup area, a_0, represents the area occupied by the hydrophilic headgroup at the interface between the hydrophobic and hydrophilic regions.

To measure the length of the hydrophobic tail, lc, the Tanford equation can be used[37]:

$$\mathrm{lc} = 1.5 + 1.265 \cdot \mathrm{n} \quad \text{eq. 1.4}$$

Where n is the number of carbon atoms in the alkyl chain

1.4.2 Cholesterol

Cholesterol is an amphiphilic steroid that is white, waxy and solid at room temperature[16]. It is found in animal cell membranes, which modulates the

permeability, fluidity, and structure of cell membranes, and organises lipid rafts for signal transduction in cells[38,39]. Before niosomes, cholesterol was added to liposomes in the 1970s as a membrane stabiliser and was found to improve membrane stability, reduce permeability, and prevent the leakage of hydrophilic drugs. When niosomes were developed in the 1980s as a cost-effective alternative to liposomes, cholesterol was also incorporated into the niosomal vesicle composition[40].

Adding cholesterol was found to improve the rigidity and stability of niosome membranes. In some formulations, cholesterol was found to enhance drug entrapment efficiency in niosomes[41]. Cholesterol incorporates itself into the bilayer membrane and aligns itself next to the lipophilic tail of the surfactants. It forms hydrogen bonds with the surfactant, as shown in figure 1.3. By intercalating between surfactant molecules and interacting with their hydrophilic tails, cholesterol can modify membrane fluidity, especially at temperatures above the phase transition temperature. Cholesterol increases membrane cohesion and limits the movement of the surfactant alkyl chains[35].

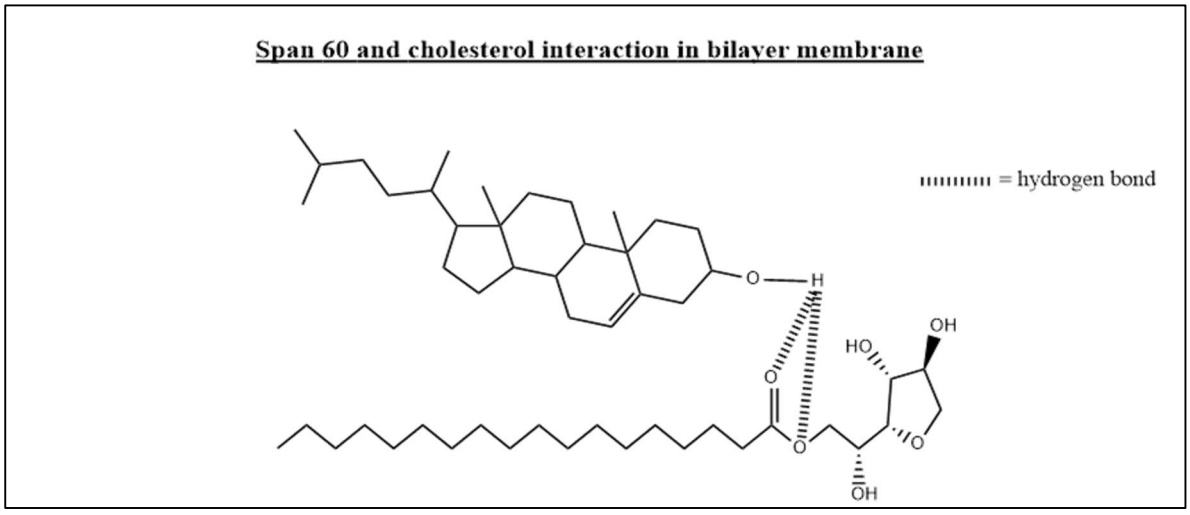

Figure 1.3: interaction of cholesterol with Span 60 surfactant in niosome bilayer membrane. Note that one hydrogen atom does not form hydrogen bonds with two oxygen atoms at the same time. However, this figure illustrates the oxygen atoms with which the hydrogen atom can form hydrogen bonds, one at a time. All structures were generated using ChemDraw 22.2.0[1].

Cholesterol is an essential component in the formation of niosomes when surfactants with HLB > 6 are used (such as Span 20 and tweens)[25]. This is because surfactants

with an HLB value greater than 6 increase hydrophilicity, which can decrease niosome stability and prevent their formation.

1.4.3 Co-surfactants

Co-surfactants are surfactants that are added to the niosomes, in addition to the main non-ionic surfactant, to enhance the niosomes' membrane stability and flexibility, improve percentage entrapment efficiency (%EE), and adjust the niosomes' size, membrane charge and drug release profile[23].

There are several types of co-surfactants, which can be classified as charge-inducing or neutral. There are two types of charge-inducing surfactants: those that are permanently charged[42] and those that are ionisable[43]. Permanently charged surfactants are those that will always be ionised regardless of the pH of the media, while ionisable surfactants are those whose ionisation depends on the pH of the media. The use of ionisable lipids in niosomes is not widely employed, and it remains an important research area for future exploration.

Negatively charged surfactants, such as DCP, and positively charged surfactants, like stearyl amine and stearyl pyridinium chloride, are widely used in niosomal formulations to prevent niosome aggregation and improve colloidal stability. Positively or negatively charged niosomal vesicles repel each other via electrostatic repulsive forces, which prevent vesicles from coming close enough to aggregate or fuse[24,26].

Neutral surfactants, such as Solutol HS-15, Cremophor RH 40 and Cremophor ELP, can also stabilise niosomes. These surfactants have hydrophobic tails that can embed themselves in the niosomal bilayer membrane and a large hydrophilic head group that can sterically stabilise the niosomes (table 1.3). The head group of these surfactants is a long polyethylene glycol chain. For example, each molecule of Solutol HS-15 contains 15 ethylene glycol molecules. Cremophor RH 40 and Cremophor ELP contain 40 and 35 ethylene glycol molecules, respectively. However, Cremophor RH 40 and Cremophor ELP contain three hydrophobic tails, while Solutol HS-15 contains only one hydrophobic tail[18,44–46]. This produces different abilities of these surfactants to stabilise the membrane.

Table 1.3: Examples of charge-inducing and neutral co-surfactants that can be used in conjunction with the main surfactant in niosomes.

Type of co-surfactant	Example	Charge	Structure
Permanently charged	stearyl amine	Positive	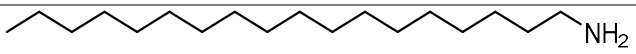
	Dicetyl phosphate (DCP)	Negative	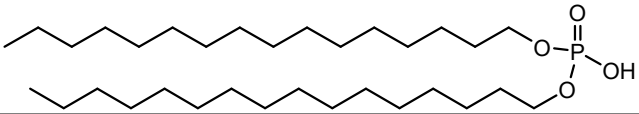
Ionisable	1,2-Dioleyl-3-dimethylammonium propane (DODAP)	At pH 7.4 (neutral) At pH 5.5 (positively charged)	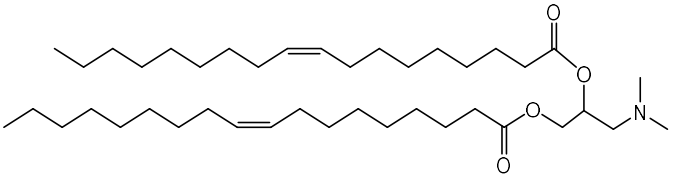
Neutral	Solutol HS-15	Neutral	(Contains two main compounds) 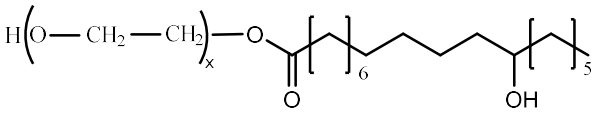 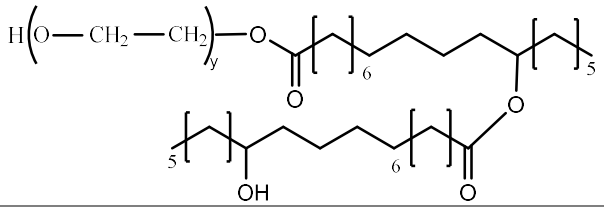
	Cremophor RH 40	Neutral	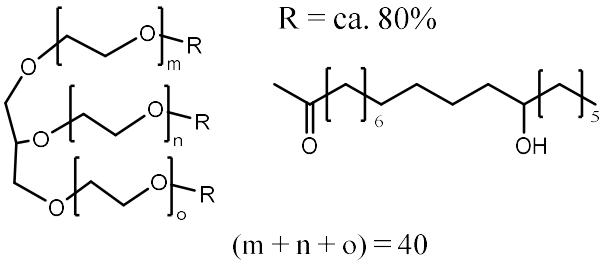 R = ca. 80% (m + n + o) = 40
	Cremophor ELP		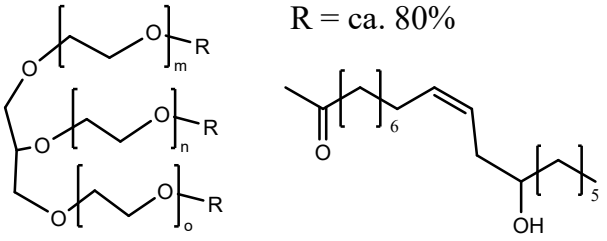 R = ca. 80% (m + n + o) = 35

DSPE-PEG 2000, the gold standard pegylated lipid used in many liposomal formulations currently on the market, has also been used in niosomes[47,48]. This lipid

contains forty-four ethylene glycol molecules that extend linearly in front of the lipid, as shown in figure 1.4 below[49].

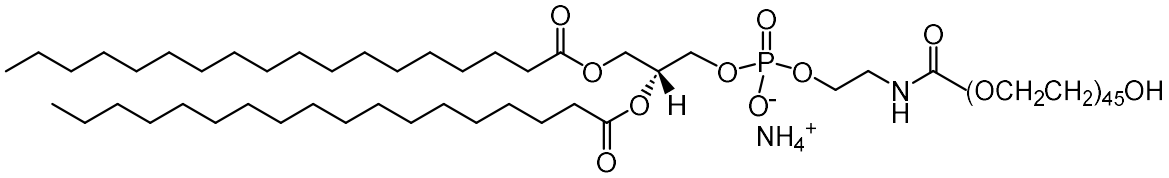

Figure 1.4: Structure of DSPE-PEG 2000-OH

Ionisable lipids, such as DODAP (table 1.3), have been used in the entrapment and delivery of genetic materials, including DNA and mRNA. These lipids become ionised in acidic media (e.g., pH 6.5), whereas they remain neutral at physiological pH (7.4). Positively charged lipids can cause toxicity and side effects. For this reason, ionisable lipids are suitable, as during niosome preparation the suspension pH can be reduced to 5.5 to ionise the lipid, facilitating its interaction with negatively charged mRNA or DNA and enhancing entrapment efficiency. The pH of the niosomal suspension is raised to 7.4 to deionise the ionisable lipid and prevent toxicity[50,51].

1.5 Methods of Formulating Niosomes

There are several methods for formulating niosome vesicles, each with its advantages and disadvantages. Several factors should be considered when selecting a production method, including the size of the niosomes to be produced after synthesis, the presence of organic solvents in the final product, the production scale, and associated costs.

1.5.1 Thin Film Hydration

The thin film hydration (figure 1.5) technique was developed by Bangham et al.[52] for liposomes preparation, but it was then used to develop niosomes. The thin-film hydration technique is one of the most commonly used and the simplest methods for forming niosomes. The method involves creating a thin film of surfactants and cholesterol, with or without a co-surfactant, at the bottom of a round-bottom flask. The film is then hydrated with an aqueous solution to form niosomes. The film is formed by dissolving the ingredients in an organic solvent such as methanol or

chloroform. The solvent is then evaporated at elevated temperatures and under reduced pressure, while the round-bottom flask is rotated at an angle. The formed thin film is then hydrated at a temperature above the main surfactant's phase transition temperature. This will produce multilamellar vesicles (MLVs)[53].

There are two ways to entrap the drug in the niosomes, depending on the solubility of the drug. Hydrophilic drugs are typically added to the aqueous hydration medium to enable niosomes to entrap them as they form. Hydrophobic drugs are added to the organic solvent along with surfactants and cholesterol, and they become part of the thin film. Upon hydration of the film, the niosomes will incorporate the hydrophobic drug as they form[26].

The advantages of the thin-film hydration technique include its simplicity and well-established nature, making it suitable for both hydrophilic and hydrophobic drugs. It is also compatible with a wide range of surfactants and co-surfactants. However, there are disadvantages to its use, including batch-to-batch variation, low encapsulation efficiency (especially for hydrophilic drugs), a risk of residual organic solvent, a time-consuming process, and small-scale production. Most importantly, it produces multilamellar vesicles that often require additional size-reduction steps[54].

Solutions to some of these challenges, such as the low drug entrapment efficiency and the need for size reduction, will be discussed in section 1.6.

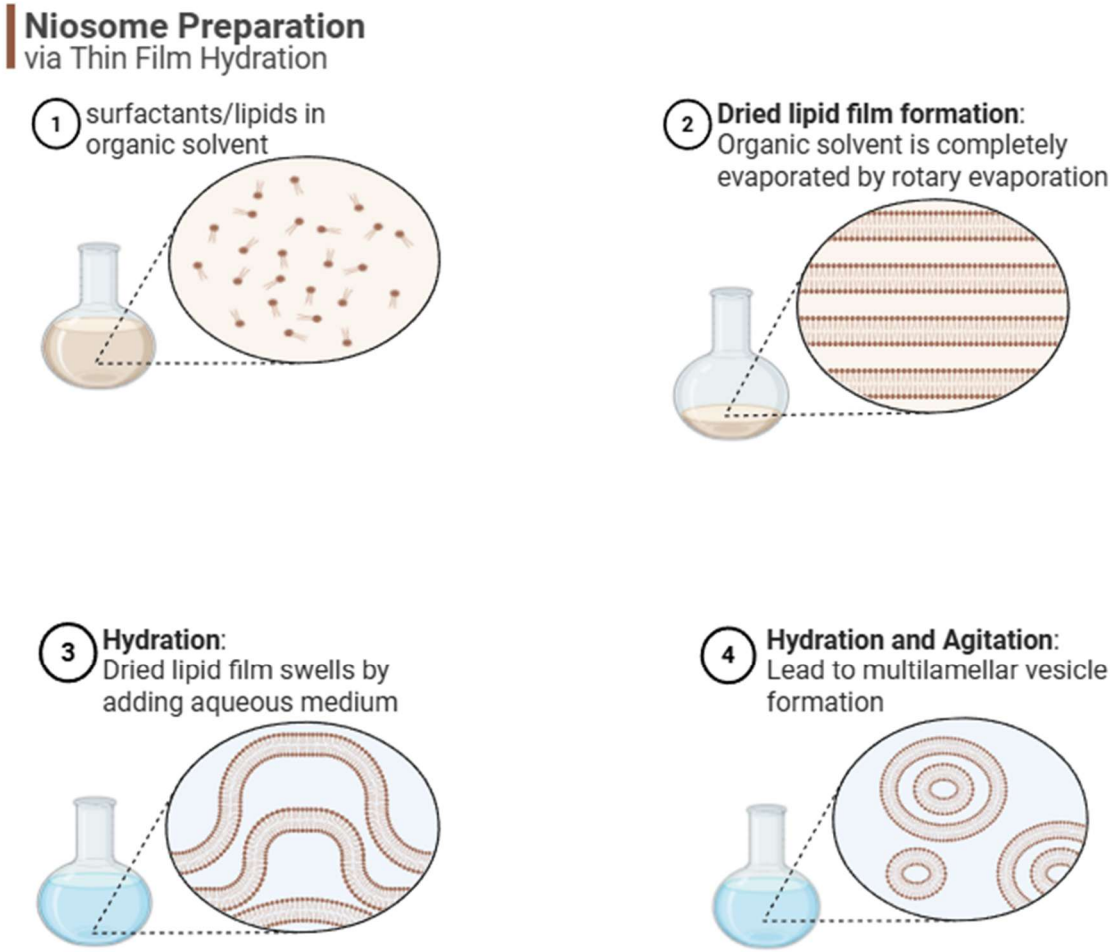

Figure 1.5: Summary of thin film hydration technique (generated using BioRender)

1.5.2 Microfluidic

Microfluidic techniques are modern, highly controlled, and scalable methods for producing nanovesicles such as niosomes and liposomes (figure 1.6). The technique involves dissolving surfactants, cholesterol, and co-surfactants in an organic solvent, typically ethanol or methanol. The organic solvent is rapidly mixed with an aqueous solvent in microchannels. The aqueous solvent is either pure water or a buffer. At the junction, the phases meet and mix rapidly due to laminar flow and diffusive mixing. This results in the self-assembly of niosomes. This method enables precise control over size and size distribution, representing a significant advancement over the traditional thin-film hydration technique[55,56].

Hydrophilic drugs are usually added to the aqueous phase, while hydrophobic drugs are added to the organic solvent with the surfactant mixture. Several factors should

be controlled to achieve a good size, a uniform size distribution, and a high entrapment efficiency. The total flow rate (TFR), the flow rate ratio (FRR), surfactant/lipid concentration in the organic phase, temperature, choice of organic solvent, and aqueous buffer are all factors that can significantly affect the outcomes of niosomes[56].

TFR is the combined flow rate of aqueous and organic phases, while FRR is the ratio of aqueous phase to organic phase. Both TFR and FRR affect the particle size and size distribution of niosomes. The concentration of surfactant/lipid is crucial in controlling the number of niosome particles in the final solution and can also influence the size of the niosomes. To increase the solubility of the surfactant/lipid, a heating block can be used to raise and maintain the solvent's temperature during the mixing process[56,57].

There are several advantages to using the microfluidic technique. The main benefits include excellent size control, reproducibility, and the ability to scale up to meet industry demands. However, the disadvantages of this technique include the fact that the produced niosomes contain an organic solvent that must be extracted from the niosomal suspension, as it can be toxic upon administration and affect the long-term stability of the niosomal suspension. The technique is also limited in its use of certain solvents and acids, which can affect the cartridge and inner tubes of the microfluidic instrument. Also, the process required specialised equipment, which can be costly[56].

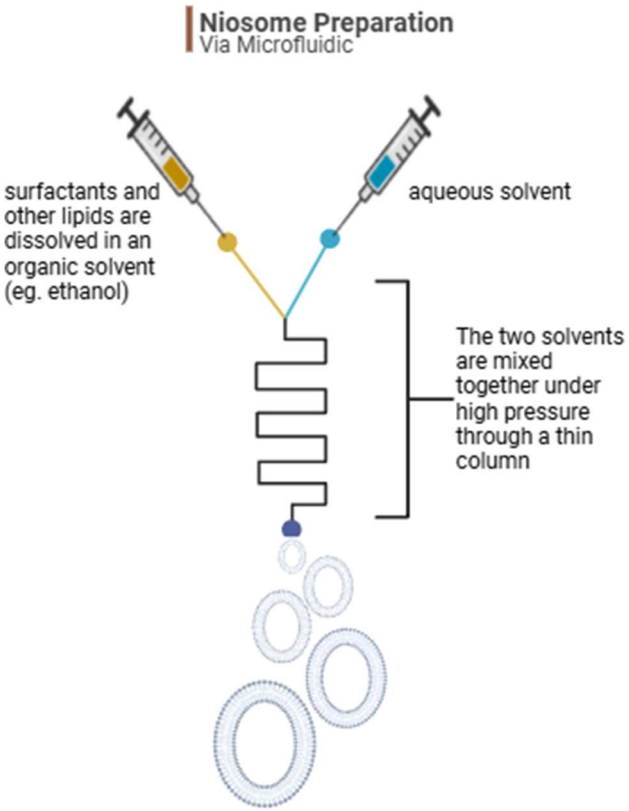

Figure 1.6: Summary of microfluidic techniques (generated using BioRender)

1.5.3 Organic Solvent Injection

During this technique, an organic phase, such as ethanol or ether, containing the surfactant/lipid mixture is slowly injected into an aqueous phase that is stirred and heated to facilitate evaporation of the organic solvent. Upon contact with the aqueous solution, the surfactant/lipid will assemble into niosomes. Hydrophilic drugs are usually added to the aqueous phase, while hydrophobic drugs are added to the organic phase[24].

The advantages of using this technique include its straightforwardness, simplicity, scalability, and suitability for loading both hydrophilic and hydrophobic drugs. However, it has challenges. Removal of organic solvent residue is necessary to prevent toxicity. Hydrophilic drugs have low entrapment efficiency. This technique can produce a broad size distribution, and, without optimisation, the size distribution can vary [24].

1.5.4 Reverse Phase Evaporation

The method involves dissolving surfactants/lipids in an organic solvent (such as chloroform or ethyl ether) and then mixing the organic solvent with an aqueous solvent. The two immiscible solvents are then homogenised and sonicated to form a water-in-oil emulsion (W/O). The organic solvent is then removed by reducing the pressure and increasing the temperature of the emulsion using a rotary evaporator, which forms the niosomes[32].

This technique is suitable for both hydrophilic and hydrophobic drugs, where hydrophilic drugs are added to the aqueous phase, while hydrophobic drugs are added to the organic phase. The disadvantage of this technique includes the presence of residual organic solvents that can be toxic[24,32].

1.5.5 Sonication

This technique is a green technology that produces small niosomes without the use of an organic solvent. The surfactants/lipids are added to an aqueous phase and are sonicated at elevated temperatures, such as 60 °C, using probe sonication. The two main advantages of this technique are that it produces small niosomes and does not require an organic solvent. However, not using an organic solvent makes this technique unsuitable for hydrophobic drugs[58,59].

1.5.6 Ball Milling Method

The ball-milling method is an old technique that has been recently employed for preparing niosomes. In this method, surfactant and cholesterol are added to deionised water or a suitable aqueous phase, and the pharmaceutical agent is dissolved in a separate container containing deionised water. Both liquids are then mixed in a milling container that contains spherical balls. The milling container is then rotated, initiating a mechanistic cascade that applies a rotational force. The force exerts pressure on the surfactant particles and the drug. This leads to compression and fracturing, which subsequently result in niosome formation[24].

1.5.7 Lipid Injection

During this technique, the surfactants and cholesterol are melted at high temperature and quickly injected into a heated aqueous phase under continuous agitation. This results in the formation of niosomes. The aqueous phase contains the drug dissolved. This technique is not suitable for heat-labile drugs[36].

1.6 Optimisation of Niosomes Postproduction

Several challenges arise during niosome manufacturing, as discussed in the section on methods for formulating niosomes. The most common challenges are niosome size and entrapment efficiency. Many manufacturing methods, such as the thin-film hydration technique and organic solvent injection, produce large vesicles that are unsuitable for therapeutic use and exhibit low entrapment efficiency. For this reason, several size reduction techniques have been developed and tested. Also, several approaches have been designed to enhance entrapment efficiency.

1.6.1 Niosomes Size Reduction

Reducing the size of niosomes is crucial for their use in clinical applications. Controlling the size is essential to avoid batch-to-batch variation. Niosomes' size can determine their site of accumulation and rate of clearance from the body, and thus their circulation time. Niosomes in the 10-100 nm size range have reduced clearance by the reticuloendothelial system (RES) and improved tissue penetrability. This enhances their accumulation at target sites and prolongs their circulation time. However, nanoparticles smaller than 10nm might exhibit rapid kidney clearance[60]. Nanoparticles larger than 200 nm are more likely to be trapped in the spleen due to the spleen's large fenestrations (200-500 nm) and the slow blood flow at the spleen. The liver has a capillary fenestration of 100-150 nm, allowing particles less than 150 nm to be preferentially taken up by the liver[61].

Moreover, the gold standard for sterilising injectable nanovesicles is filtration through a 0.22 μm filter. For this reason, the niosome size should be less than 200 nm for this process to be efficient, with niosome loss and, consequently, the entrapped drug. Heat and steam sterilisation can be destructive for the niosomes and result in drug leakage after entrapment due to membrane disruption[62].

Two parameters must be considered when studying niosome size: the average diameter and the polydispersity index (PDI). The average diameter indicates the size of the niosomes, while the PDI is a measure of the distribution of niosome sizes and thus the uniformity or diversity of the niosomes. The PDI value is between 0 – 1, with the smaller values indicating a more monodispersed size distribution[63].

To obtain niosomes with a specific size and low PDI, several size-reduction techniques can be used post-production to control their size. Below are examples of the most common methods used for size reduction.

1.6.1.1 Extrusion

Extrusion is a technique used to produce small, uniform, and stable niosomes by forcing them through a membrane with a specific pore size. The niosomes will possess the size of the membrane they passed through. This is a prevalent technique used in industry to produce small and uniform nanovesicles[64].

Three components are usually needed to perform extrusion: the extruder, which is a manual or high-pressure device, a polycarbonate membrane with a specific pore size for niosomes to pass through to reduce their size, and a heating block which is optional as it is recommended that the nanovesicle suspension temperature should be above the phase transition temperature of the main lipid/surfactant to prevent blockage and damage to the membrane and to facilitate more efficient size reduction[65,66].

There are two types of extruders: manual and automated. Manual extruders are used in research and development and consist of two syringes, a heating block, and a membrane. The two syringes are joined at the middle by a metal casing that holds the membrane filter, as shown in figure 1.7. The heating block, which holds the syringe and metal casing, requires heating by an external heat source, such as a laboratory hot plate. The heating block also features a hole that accommodates a glass thermometer, allowing temperature monitoring[65].

The main limitation of using a manual extruder is that it relies on hand pressure, which provides low and inconsistent shear force, resulting in batch-to-batch variation and sometimes ineffective size reduction. It is also not suitable for concentrated, viscous formulations or formulations containing large MLVs, and sometimes the

formulation can clog the membrane if not used appropriately. Moreover, when a syringe is used, the volume of the formulation is limited to the syringe size[67].

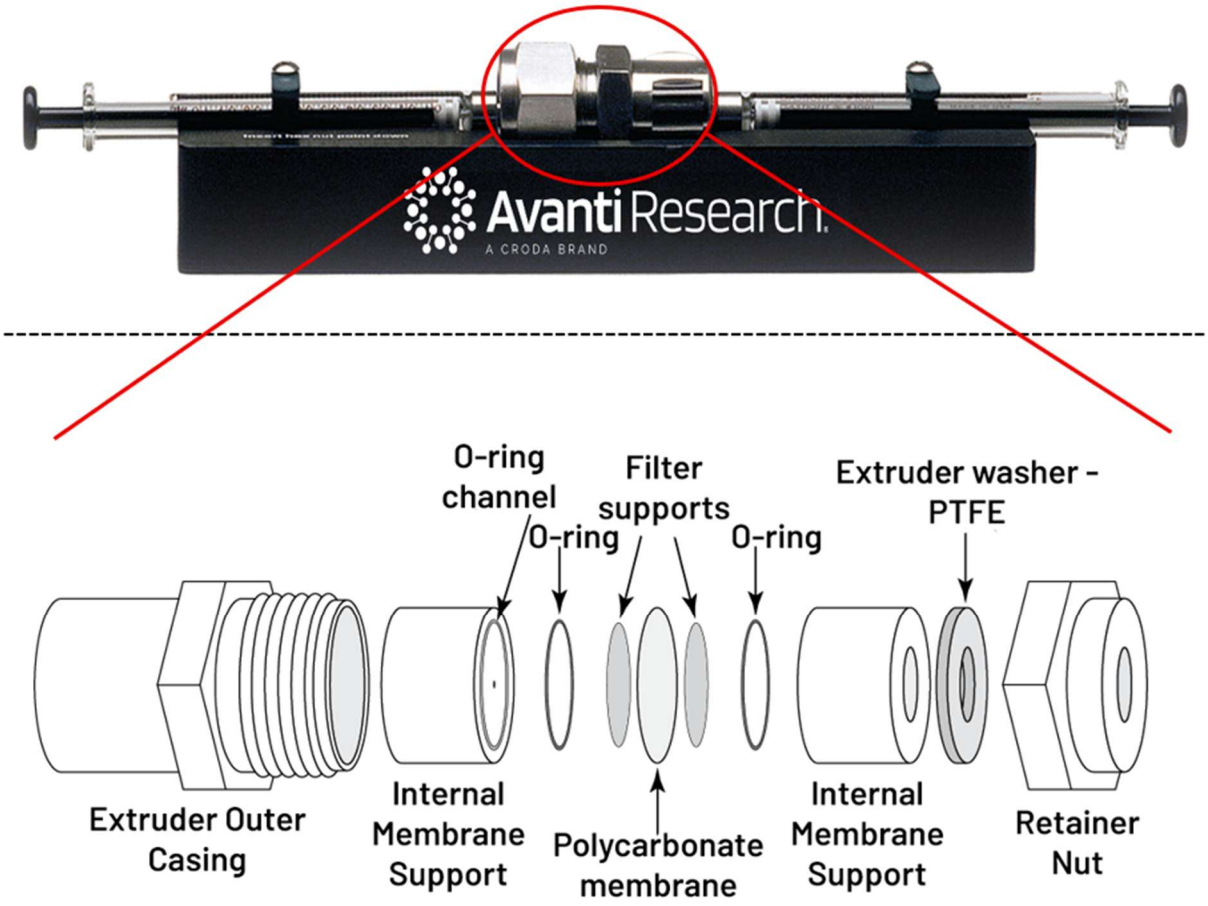

Figure 1.7: Composition of a manual extruder provided by Avanti Polar Lipids.

An alternative option to manual extruders is the automated extruder (figure 1.8). Automated extruders consist of a stainless-steel container and a stack of membrane filters. Filters of different sizes are typically used to allow niosomes to pass through membranes in a size order (from the highest pore size to the lowest), enabling more efficient size reduction and preventing membrane clogging (e.g., 400 → 200 → 100 nm). After filling the container with niosomes, the formulation is forced through the stack of membranes using a pressurised gas (such as nitrogen) or a piston. The formulation is then either collected or recirculated for additional passes. The container temperature can also be controlled to enable more efficient size reduction

and prevent clogging. Parameters such as pressure, number of cycles, and temperature are often monitored and recorded digitally[66,68,69].

Automated extrusion solutions can be used to support production of as little as 1mL formulations for research and development purposes to hundreds of litres for commercial scale. Figure 1.8 below shows examples of automated extruders of different sizes provided by Evonik[66].

Figure 1.8: Different sizes of automated extruders provided by Evonik.

1.6.1.2 Homogenisation

Homogenisation is a mechanical process that applies high shear forces, usually under high pressure, by forcing vesicles through a narrow gap. The intense mechanical forces break large MLV nanoparticles into more uniform, smaller unilamellar vesicles. The process can be repeated several times to achieve further size reduction [70].

A homogeniser might not achieve a satisfactory particle size and particle size distribution for nanovesicles to be acceptable for clinical use. For this reason, a homogeniser can be combined with an extrusion membrane to enhance efficiency and better control the size and size distribution of the nanovesicles (figure 1.9-A). This powerful combination can result in high output production of niosomes with an acceptable average size and PDI[71].

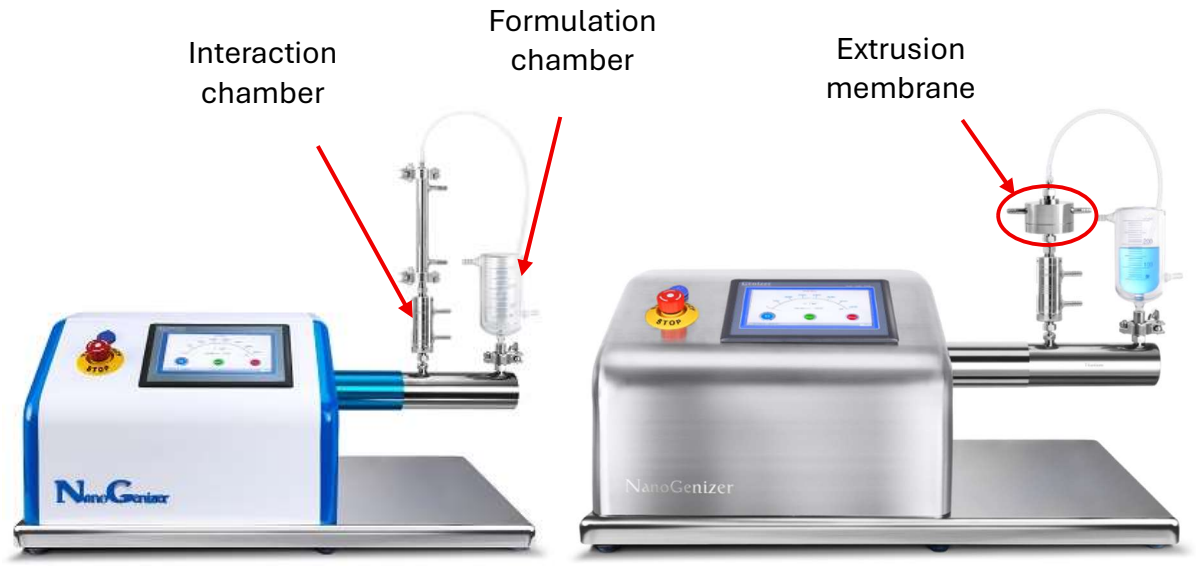

Figure 1.9: Two types of homogenisers: a homogeniser without an extrusion membrane (A) and a homogeniser with an extrusion membrane (B). The formulation will be added to the chamber as shown in figure A. The formulation will travel clockwise and reach the interaction chamber where homogenisation occurs. Then the formulation continues travelling clockwise and reaches the formulation chamber again. The cycle is repeated several times until the desired outcome is reached and that depends on the nature of the formulation. The red circle in figure B shows the location of the extrusion membrane which is added to the interaction chamber. Figures were obtained from NanoGenizer website (genizer.com)[71].

1.6.1.3 Sonication

Sonication is a technique that reduces the size of niosomes by applying ultrasonic energy to break large MLVs into smaller unilamellar vesicles. A sonicator emits ultrasound waves that pass through the niosome suspension. The ultrasonic waves cause rarefaction and compression of the liquid medium, creating microscopic bubbles that rapidly grow and collapse. The collapse of the cavitation bubbles generates high local temperatures, high pressure and strong shockwaves. These forces break open the nanovesicles and convert them into smaller vesicles, thus forming smaller unilamellar vesicles[72].

There are two types of sonicators: bath sonicators and probe sonicators. Probe sonicators apply ultrasound waves directly into the niosomal suspension by inserting a metal probe in the formulation, while bath sonicators deliver ultrasound waves indirectly through a water bath. As a result, probe sonicators are considered more

potent than bath sonicators. Additionally, probe sonicators generate heat, so the sample should be placed in ice to prevent damage to the formulation. Bath sonication is considered faster than probe sonication, where multiple vials can be put in a water bath. Bath sonication also poses a lower contamination risk, as there is no direct contact with the sonicator[72,73]. Figure 1.10 below shows examples of bath and probe sonicators.

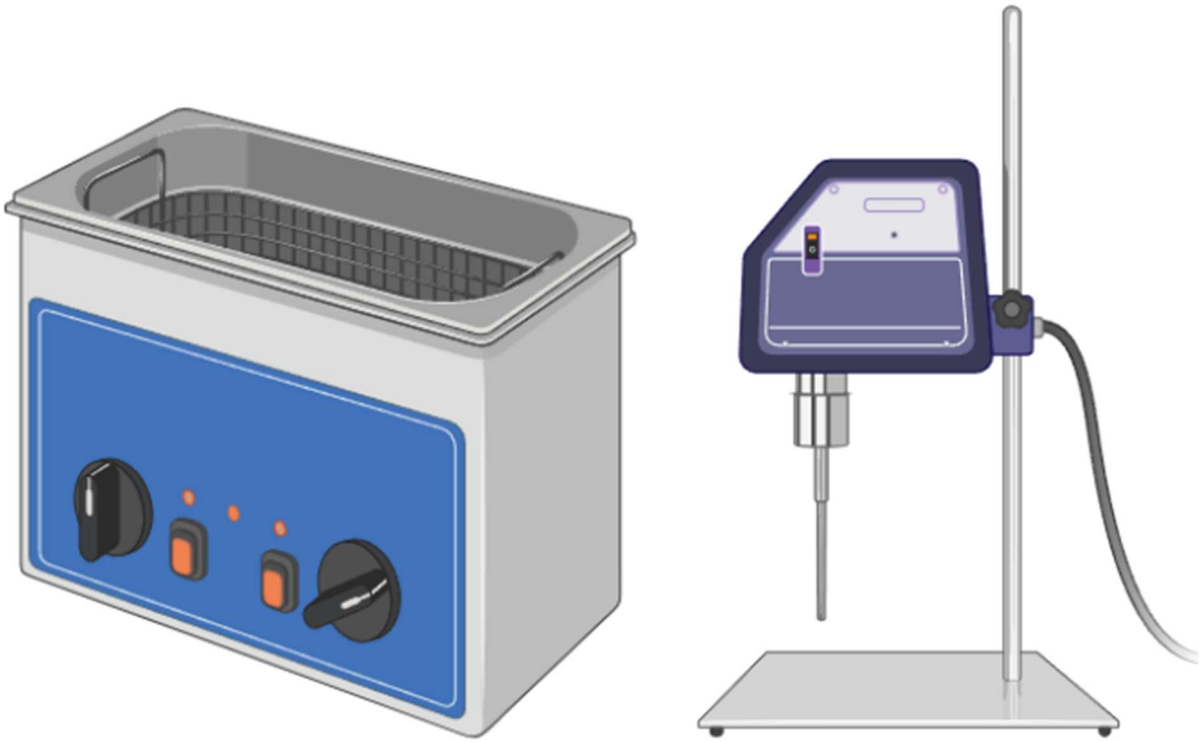

Figure 1.10: Diagram showing bath sonicator (left) and probe sonicator (right). Generated using BioRender.com.

During size reduction, niosomes are exposed to certain forces (such as ultrasonic energy, physical deformation through extrusion or shear forces of homogenisation). These forces break the membrane, allowing the reformation of smaller niosomes. During these processes, the drug entrapped in niosomes might leak outside, and the entrapment efficiency will be reduced[23]. For this reason, several drug entrapment techniques have been used to load the drug after optimising the niosome size.

1.6.2 Enhancing Entrapment Efficiency

There are two methods to entrap drugs inside niosomes: passive drug loading and active drug loading. During passive drug loading, the drug is added during the formation of niosomes. For example, during thin film hydration, hydrophobic drugs are mixed with the organic phase to be part of the lipid/surfactant thin film, while hydrophilic drugs are added to the aqueous phase to hydrate the thin film. During the hydration of the thin film, niosomes are formed, and hydrophobic drugs will embed themselves in the bilayer membrane, while hydrophilic drugs will incorporate themselves in the aqueous phase. There are two main limitations to this technique of drug loading. The first limitation is the lower entrapment efficiency and lower drug loading capacity. Passive drug loading does not always allow high entrapment of the drug inside the niosomes, especially for hydrophilic drugs[29]. The second limitation is the batch-to-batch variability in entrapment efficiency, especially after size reduction of niosomes using techniques such as sonication, extrusion, or homogenisation[23]. For these two reasons, active drug loading techniques were invented.

There are different techniques to load drugs actively. One technique that can be considered active loading is coacervation. This technique is applied to proteins such as albumin and to aminoglycosides such as amikacin. During this technique, the loaded molecules aggregate to form microscopic droplets suspended in the liquid when exposed to certain conditions, such as pH changes or alcohol addition. The liposomes will form around the coacervated particles and enhance their entrapment[74].

Another technique relies on the use of a pH gradient to entrap drugs[75]. Other formulations rely on pH and ionic gradients to facilitate drug loading[76]. In both cases, the drug being loaded must have an ionisable functional group such as an amine. This allows the drug to be entrapped and becomes ionised inside the niosomes while it is unionised outside the niosomes. Once ionised, the drug will not be able to pass back through the hydrophobic bilayer membrane and will accumulate within the niosomes[75,76].

Drug ionisation depends mainly on three factors: the type of the ionisable functional group (weak acidic or weak basic), the pKa of the functional group, and the pH of the medium in which the molecule carrying the functional group is dissolved. There are

two types of ionisable functional groups, which are acidic (groups that can release a H^+ ion) and basic (groups that can accept a H^+ ion). The pKa of the functional group and the pH of the medium can determine the percentage of ionisation of the compounds. This can be explained by the Henderson-Hasselbalch equation, which states for a weak acid:

$$\mathrm{pH} = \mathrm{pKa} + \log\left(\frac{[\mathrm{A}-]}{[\mathrm{HA}]}\right) \qquad \text{eq. 1.5}$$

Where pH is a measure of hydrogen ion concentration in the solution, pKa is the negative logarithm of the acid dissociation constant (Ka), [HA] is the concentration of the unionised form of the acid, and [A-] is the concentration of the ionised form of the acid.

The equation also states for weak basic functional groups:

$$\mathrm{pH} = \mathrm{pKa} + \log\left(\frac{[\mathrm{B}]}{[\mathrm{BH}\ ]}\right) \qquad \text{eq. 1.6}$$

Where [B] is the concentration of the unionised form of the base, while BH+ is the concentration of the ionised form of the base[77,78].

These two equations help determine the percentage of ionisation of the ionisable functional groups. For an acidic functional group, the percentage ionisation can be measured with the following equation:

$$\%\text{ionisation (acid)} = \frac{100}{1+10^{(\mathrm{pK}\quad)}} \qquad \text{eq. 1.7}$$

While for a basic functional group, the following equation determines the percentage ionisation:

$$\%\text{ionisation (base)} = \frac{100}{1+10^{(\mathrm{pH}-\mathrm{pKa})}} \qquad \text{eq. 1.8}$$

As a rule of thumb, when the pH of the medium equals the pKa of the functional group, 50% of the functional group is ionised. When pH > pKa, an acidic functional group will be mainly ionised, while a basic functional group will mainly be unionised. If pH < pKa, an acidic functional group will be primarily unionised, while a basic functional group will mainly be ionised[77,78].

1.6.2.1 Active Drug Loading – pH Gradient

During the pH gradient technique, the nanovesicles are formulated in an aqueous buffer that enables drug ionisation. This results in the pH of the vesicles' aqueous cores being similar to that of the surrounding buffer. Then, a buffer exchange is performed to replace the buffer surrounding the niosomes with a buffer at a different pH that does not ionise the drug. This results in a net flow of the drug into the niosomes[75]. Figure 1.11 below explains this process.

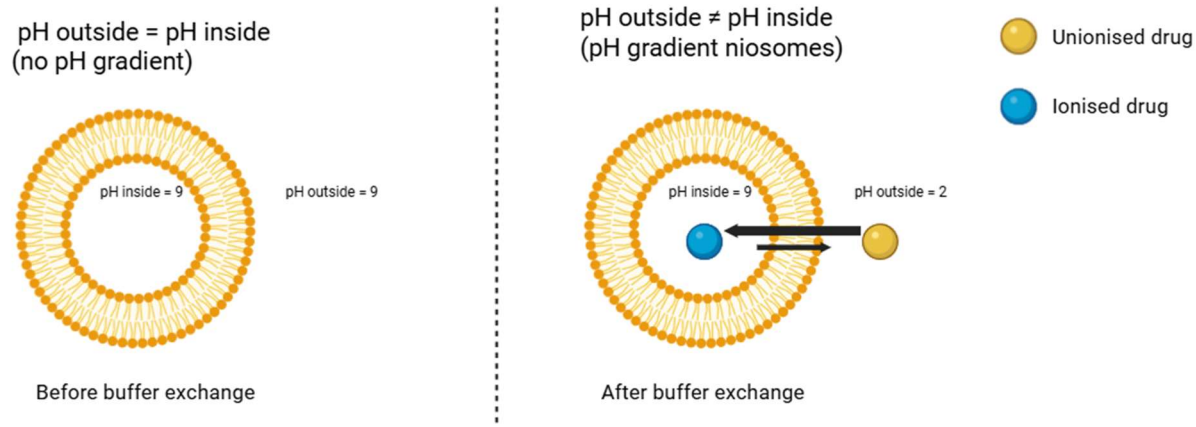

Figure 1.11: Creating a pH gradient in niosomes. After buffer exchange, the net migration of the drug will be to the inside of the niosomes.

There are four main techniques for adjusting the pH of the media surrounding the niosomes: adding acids or bases, using gel columns, employing membrane filters, and pelleting.

A straightforward method to change the pH of the buffer surrounding the nanovesicles and create a pH gradient is to add an acid or base to the nanovesicle suspension. For example, nanovesicles can be prepared in an acidic medium, such as a citric acid solution, where the pH is acidic. Then, a basic solution such as sodium carbonate is added to the nanovesicle suspension to increase the pH of the medium surrounding the niosomes. This technique creates a pH gradient, allowing drugs with a basic functional group, such as an amine, to be unionised in the outer media while ionised in the nanovesicle core. This technique is used in the liposomal doxorubicin formulation known as Myocet[79].

Myocet comes in three vials, where vial 1 contains lyophilised doxorubicin with lactose, vial 2 contains liposomes prepared in citric acid, and vial 3 contains an

alkaline buffer made from sodium carbonate. To prepare the medicine for administration, a volume of NaCl solution is added to vial 1 to dissolve the doxorubicin. Then, 1.9mL of vial 2 containing the liposomes is added to vial 1. Then, vial 3 is added to them to create a pH gradient, allowing the doxorubicin to be entrapped in the liposomes, as described in figure 1.11 above[79]. The doxorubicin structure is illustrated in figure 1.12 below.

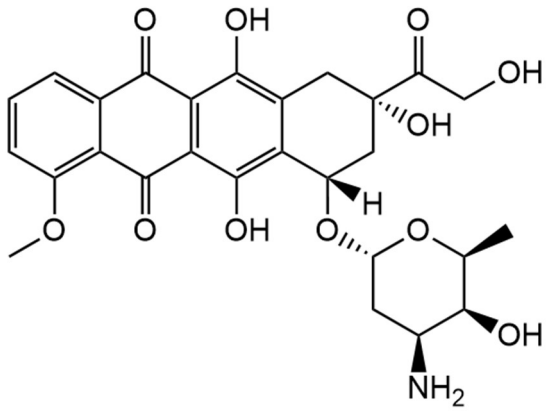

Figure 1.12: Structure of doxorubicin. (Generated using ChemDraw 22.2.0)

Gel columns are also used to generate pH gradients. This technique relies on size-based filtration, where large molecules, such as liposomes and niosomes, pass through the column faster than small molecules. One type of gel column utilises Sephadex beads. Sephadex is a cross-linked dextran gel with pores of defined sizes. Molecules larger than the pore size cannot pass through the beads' pores and thus pass quickly through the column. However, small molecules enter the beads' pores and are retained longer. As a result, large molecules elute first. The size is determined by the type of Sephadex used. For example, Sephadex G-25 excludes molecules with a molecular weight (MW) greater than 5 kDa (kilodaltons), while Sephadex G-50 excludes those with an MW greater than 30 kDa. In buffer exchange, liposomes and niosomes will elute first in the buffer used to prepare the Sephadex column. In contrast, the old buffer, composed of small molecules, will remain in the column for a longer period. This will result in a buffer exchange and the formation of a pH gradient[80–82].

A third technique involves using filtration to alter the buffer of the media. During this technique, a semipermeable membrane with a specific pore size is used. The

membrane retains Niosomes/liposomes, while small solutes diffuse through it. Common methods used include the use of dialysis bags[83], centrifugal filter and tangential flow filtration (TFF)[84].

The dialysis bag technique is a simple method that utilises a semipermeable bag with a known pore size to contain the niosomal suspension. The bag containing the niosomal suspension is then immersed in a large volume of the desired buffer, allowing small molecules and ions to diffuse across the membrane. The new buffer will gradually replace the original buffer surrounding the niosomes. The centrifugal filters enable buffer removal via low-speed centrifugation while retaining the nanoparticles. This results in the nanoparticles being concentrated. The niosomes/liposomes are then diluted with a new buffer. The process is repeated several times until the original buffer is completely exchanged[83].

TFF is a membrane-filtration technique in which the solution flows parallel to the membrane surface, allowing small molecules and buffer components to pass through the membrane while retaining large nanoparticles, enabling efficient buffer exchange[85].

With pelleting, the niosomes/liposomes are centrifuged at a high speed to pellet and separate them from the buffer in which they were suspended. The supernatant is removed, and the pellet is resuspended in a new buffer[75].

Besides enhancing entrapment efficiency, active loading can aid in dialysis and treating drug toxicity. Some liposomal formulations have been developed to scavenge weakly basic drugs, such as the antidepressant amitriptyline[86] and the calcium channel blocker verapamil[87] and eliminate them from the circulation to treat their toxicity. A liposomal formulation with a pH gradient has also been used to treat severe hyperammonaemia in rats[88]. In all cases, the liposomes' inner core is acidic, drawing these weakly basic molecules into the liposomes and reducing their effect on the organs. The use of pH-gradient vesicles to mitigate drug toxicity is not common in niosomes and warrants further exploration.

1.6.2.2 Drug Loading of Hydrophobic Drugs

Techniques other than pH gradient have also been used to enhance drug loading in niosomes. Hydrophobic molecules, such as curcumin, can achieve entrapment

efficiencies exceeding 90% in niosomes. This is because hydrophobic drugs will reside in the niosome's hydrophobic membrane away from the water surrounding the niosome’s membrane. Hadjipour et al. formulated niosomes containing curcumin using Span 65, cholesterol, and Cremophor RH 40. The niosomes' size was 197.4 nm (±3.0) with a PDI of 0.46 (±0.02), which can be further improved through extrusion or by formulating the niosomes using other techniques such as microfluidics. The formulation entrapment efficiency was 91.2% (±1.5)[29].

1.7 Assessing Niosomes Properties Postproduction

When manufacturing niosomes, several parameters can be studied to assess their properties and predict their in vivo performance. Properties such as size and size distribution, drug loading, surface charge, vesicle morphology, and stability studies can help predict the in vivo success of the formulation.

1.7.1 Niosomes Size and Size Distribution

Depending on the route of administration, the target size of niosomes should be determined, as particle size can determine the site of accumulation in the body. Two important size parameters should be measured when studying niosomes: average size and the polydispersity index (PDI). For niosomes to be suitable for injection, their size distribution should be uniform and considered monodispersed. According to the industry, a PDI of ≤0.3 is acceptable, and the niosomes will be considered monodispersed[89].

The most common technique for measuring niosome size is dynamic light scattering (DLS). DLS is used to measure the size distribution of small particles in suspension, such as niosomes, liposomes, proteins, polymers, and other colloidal systems. It involves shining a laser onto a colloidal suspension of particles. The particles undergo a random movement in a liquid due to collisions with solvent molecules. This movement is called Brownian motion. The light from the laser scatters in different directions as the particles move in the liquid. The fluctuations in scattered light intensity over time depend on the speed of particle movement. In turn, the speed of particle movement depends on the particle size. Smaller particles move

faster and exhibit faster intensity fluctuations, while larger particles move more slowly, resulting in slower fluctuations[90].

1.7.2 Entrapment Efficiency

Entrapment efficiency (%EE) is a measure of the amount of available drug entrapped in niosomes. It is measured using the following equation[91]:

$$\%\mathrm{EE} = \frac{amount\ of\ drug\ entrapped}{total\ amount\ of\ drug}\ x\ 100 \qquad \text{eq. 1.9}$$

Entrapment efficiency can be measured either directly by determining the amount of drug inside the niosomes and comparing it to the total amount of drug, as per equation 9, or indirectly by measuring the amount of drug unentrapped and then calculating the amount of drug entrapped, as per equation 10 below[92].

$$\%\mathrm{EE} = \frac{total\ amount\ of\ drug - amount\ of\ drug\ unentrapped}{total\ amount\ of\ drug}\ x\ 100 \qquad \text{eq. 1.10}$$

To measure %EE, the free drug must first be separated from the drug incorporated into vesicles. Various techniques can be used to achieve this separation. The methods used to establish a pH gradient, as explained in Section 1.6.2.1, can also be employed to separate the entrapped drug from the unentrapped drug.

For example, size exclusion chromatography can be used with a Sephadex G-50 column to separate the entrapped drug from the unentrapped drug. A drug containing niosomes will travel faster through the Sephadex column than the free drug[29].

Another technique is to utilise a filtration membrane to remove the free drug. The nanoparticle suspension is dialysed against a drug-free solution, allowing the unentrapped drug to leave through a membrane. In contrast, the entrapped drug will be retained with the nanoparticles behind the dialysis membrane. TFF can be used for this purpose[93].

A third technique involves pelleting niosomes via centrifugation, thereby separating niosomes containing the drug from free, unentrapped drug. Unentrapped drug molecules will remain in the supernatant[92].

To measure the amount of drug in niosomes, the niosomes must be disrupted to release the amount of drug inside them. Isopropanol is commonly used for this

purpose by adding it to a niosomal suspension, as it breaks down and dissolves the niosomes to release the entrapped drug, and it is water-miscible[29].

1.7.3 Zeta Potential

Zeta potential (ζ) is an indicator of the surface charge of the nanoparticle. Surface charge of nanoparticles is an important parameter for colloidal stability[94]. Zeta potential can be positive when the nanoparticle contains amphiphiles with a positively charged head group, such as amines, negatively charged when the nanoparticle contains amphiphiles with a negatively charged head group, such as carboxylic acid, or neutral when the nanoparticle contains amphiphiles with a neutral head group (such as alcohols).

The greater the zeta potential value, the stronger the electrostatic repulsion between the nanoparticles, resulting in better colloidal stability. As a rule of thumb, a zeta potential value of greater than 30mV or less than – 30mV will usually result in stable nanoparticle vesicles that will prevent aggregation[95].

The charge of nanovesicles can be kept neutral while maintaining colloidal stability through steric stabilisation. In liposomes, pegylated lipids such as DSPE-PEG 2000 are used to maintain this stability[96]. In niosomes, Solutol HS 15, Cremophor RH 40 and Cremophor EL have been used to enhance steric stability[23,55].

1.7.4 Morphological Examination

Microscopic examination can reveal the size and shape of the nanovesicles. It can also be used to demonstrate the formation of nanovesicles and to assess their quality, including aggregation and surface morphology. A transmission electron microscope is used to reveal the shape and size of the nanovesicles[23]. A scanning electron microscope provides a 3-D shape of the niosome to better understand its structure[97]. A light microscope, although its resolution is much lower than that of electron microscopes, can also be used to demonstrate niosome formation and detect aggregation [55].

1.7.5 Stability Study

One of the biggest challenges facing the niosomal colloidal system is physicochemical instability, in which niosomes can aggregate and precipitate. A long-term stability study is required to ensure the formulation remains stable during its intended shelf-life and to demonstrate its suitability for administration to patients. The most important factors to study during a stability study are the niosome size and size distribution[23]. Some studies also add zeta potential measurements and the amount of drug remaining entrapped after stability[98].

1.7.6 Studying pH Gradient Across the Nanovesicle Membrane

In pH-gradient nanovesicle formulations, the pH gradient across the membrane can be studied. In a pH gradient nanovesicle, the pH inside the nanovesicle is different from that outside the nanovesicle. To measure the pH inside the nanovesicles, a pH probe can be used. A pH probe is a compound that undergoes chemical changes in response to different pH conditions. A change in the probe chemical structure will affect its excitation-emission characteristics. This change can be used to study the pH inside the nanovesicles.

The pH probe excitation-emission response is calibrated in known standards. The pH probe is then loaded into the nanovesicle, and any unentrapped pH probe molecules are removed from the buffer. Changes in the excitation-emission characteristics are linked to the calibration curve and thus indicate the pH inside the nanovesicle.

In pH gradient liposomes, fluorescent probes such as pyranine (HPTS)[99,100], BCECF[100,101], SNARF-1[100,102], and Porphyrin dendrimer[103] have been used to study pH gradients.

1.8 Loading of Doxorubicin in Liposomes

Doxorubicin has been successfully loaded into liposomal formulations that have reached the market. Doxorubicin was loaded into liposomes at high entrapment efficiency, reaching almost 100% in some formulations. Sun Pharma (India) has published a patent that describes a technique with almost 100% entrapment efficiency[104].

There are two types of liposomal doxorubicin formulations: pegylated and non-pegylated. Pegylated liposomes contain a pegylated lipid, such as DSPE-PEG 2000, whereas non-pegylated liposomes do not. Pegylated liposomes were found to circulate in the blood for a longer period than non-pegylated liposomes, thereby increasing their blood shelf life. However, pegylated doxorubicin liposomes can cause a side effect called palmar-plantar erythrodysesthesia. This occurs due to their accumulation in the blood capillaries of the hands and feet, resulting in redness, swelling, tingling, pain, and blistering. However, non-pegylated liposomes have less risk of causing this side effect[105].

There are two standard techniques for loading doxorubicin in liposomes: pH gradient using citric acid and the pH gradient using ammonium sulfate. For the citric acid technique, the liposomes are prepared in a citric acid solution, and then a sodium carbonate solution is added to increase the pH of the surrounding medium. This results in doxorubicin being unionised in the external media while being ionised inside the liposomes. Another technique is the use of an ammonium sulfate gradient. During this technique, liposomes are formed in an acidic ammonium sulfate solution. Then, the ammonium sulfate in the media surrounding the liposomes is removed and replaced with another buffer, such as sodium chloride (NaCl) or sucrose. Doxorubicin will start to enter the liposomes and get entrapped. The technique is explained in figure 1.13 below[106].

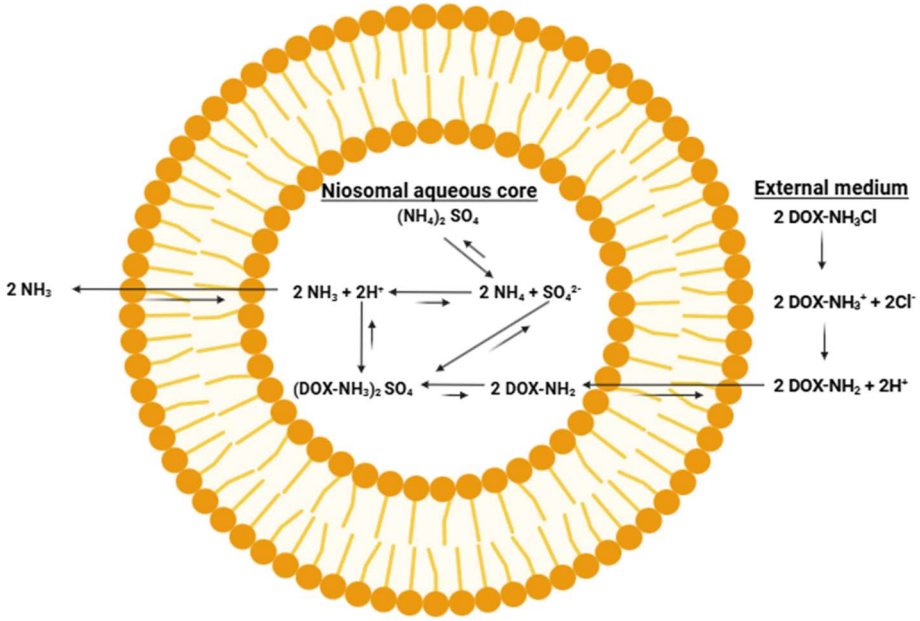

Figure 1.13: Active loading of doxorubicin using ammonium sulfate gradient. Concentration of ammonium sulfate in the liposomal core is much higher than that outside the liposomes. DOX-NH_3Cl is doxorubicin hydrochloride. Doxorubicin will become de-ionised in the external medium and cross the liposomal membrane. In the liposomal aqueous core, doxorubicin amine will receive one hydrogen from ammonia and become positively charged. Two of the positively charged doxorubicin molecules will form a complex with the negatively charged sulfate (SO_4^{2-}) ion. This complex is not soluble, and doxorubicin will precipitate within the liposomes, allowing more doxorubicin to enter the liposomal core. In exchange for doxorubicin entry, ammonia will leave the liposomes through the liposomal membrane, becoming neutral after donating its hydrogen to the doxorubicin amine (created using BioRender)[1].

The liposomal doxorubicin formulations have faced some challenges, including batch-to-batch variation. The first FDA-approved liposomal doxorubicin formulation was Doxil in 1995. In 2011, the FDA issued a warning to the company responsible for Doxil production for failing to comply with manufacturing practices. This was due to difficulties in reproducibility across devices used to manufacture Doxil. In 2013, the FDA approved a new technique to manufacture Doxil due to a shortage. Research has now focused on formulating doxorubicin liposomes using improved methods to minimise batch-to-batch variation. At the University of Strathclyde in 2020, C. Roces and colleagues formulated liposomes using microfluidic techniques and achieved an

entrapment efficiency of over 90% through the ammonium sulfate pH gradient technique. The advantage of using the microfluidic technique is that it produces liposomes with controlled size, thereby avoiding batch-to-batch variation and allowing for scalable production. To date, no microfluidic doxorubicin liposome formulations have been marketed. However, the results obtained by C. Roces and colleagues are promising[93].

The lesson learnt from liposomes will be studied in this thesis but applied to niosomes. This will help us overcome the challenges that the liposomes face during their development.

1.9 Loading of Doxorubicin in Niosomes

Niosomes offer several benefits over liposomes, including reduced manufacturing costs and improved stability. Furthermore, the issue of inconsistent lipid purity found in liposome preparation is not encountered with niosomes. These factors make niosomes a more advantageous option than liposomes.[16]. Additionally, niosomes loaded with doxorubicin can be engineered with targeting components, enabling them to selectively deliver doxorubicin to cancer cells and thereby improve the overall effectiveness of these nanocarriers[107,108]. Niosomes can deliver multiple anticancer agents simultaneously, thereby enhancing effectiveness against multidrug-resistant cancer cells. They can also be engineered to be responsive to different stimuli—such as pH, temperature, ultrasound, electric fields, light, and enzymes—allowing controlled drug release specifically at tumour sites[16].

There have been previous attempts to load doxorubicin into niosomes, each with a different purpose. Drake et al. have formulated niosomes using Span 60 and cholesterol with dextran-coated iron oxide nanoparticles. The purpose of adding iron oxide is to enable the release of the loaded drug upon application of an external alternating magnetic field stimulus (AMF). AMF will heat the nanoparticles, thereby releasing doxorubicin. The niosomes co-loaded iron oxide nanoparticles with doxorubicin in the aqueous core achieved a 61% doxorubicin entrapment efficiency[109]. I aim to achieve higher entrapment efficiency at higher doxorubicin concentrations in the final product.

Another study conducted by Bragagni et al. loaded doxorubicin into niosomes functionalised with the glucose-derivative N-palmitoylglucosamine (NPG) to target the brain. The niosomal formulation containing doxorubicin was prepared using the thin-film hydration technique. The maximum entrapment efficiency achieved was 57.8%[110].

Other studies have also attempted to load doxorubicin in niosomes for various purposes. For example, Zaer et al. loaded doxorubicin into niosomes functionalised with gelatine-alginate. However, they have prepared the niosomes in PBS buffer (1x, pH 7.4). This can cause a serious problem as doxorubicin is unstable in PBS and can cause its dimerisation and significant reduction in its function[111,112]. In 1984, Janssen et al. studied the effect of different buffer pH on the stability of doxorubicin in liposomes. They have concluded that loading doxorubicin into liposomes using PBS at pH 7.4 results in the decomposition of the doxorubicin due to pH instability[113]. PBS can be used to actively load doxorubicin; however, PBS in active loading of doxorubicin remains outside the liposomes, while ammonium sulfate or similar salts are usually kept inside the liposomes, mediating active drug loading[93].

1.10 Aim and Novelty of the Research

The aim of this thesis is to address knowledge gaps in the field of active drug loading (pH and salt gradients) in niosomes and to contribute to the understanding of this field.

The first knowledge gap identified is that several techniques have been used to study pH gradients in liposomes (as per section 1.7.6), which can also be applied to niosomes. However, there is no single technique that uses a pH probe to visualise a pH gradient and actively load the probe to study its entrapment efficiency. For this reason, a pH indicator called bromocresol green (BCG) will be used, with dual benefits: to study the entrapment efficiency of active drug loading and to visualise the pH gradient in niosomes.

The effect of using affordable co-surfactants to pegylate niosomes on niosome stability and the entrapment efficiency of doxorubicin using a pH gradient has not been studied before, and thus, it represents another knowledge gap in niosomes.

Pegylated co-surfactants Cremophor RH 40, Cremophor ELP, and Solutol HS-15 will be used to prepare pegylated niosomes, and their effects on entrapment efficiency and niosome stability under a pH gradient will be studied. The compatibility of the co-surfactants with Span 40, Span 60 and Span 65 surfactants will be studied using FTIR, niosomes size and size distribution (PDI), pH gradient formation and stability, and zeta potential.

Another knowledge gap is that the use of the microfluidic technique to prepare niosomes for active drug loading has not been previously studied. For this reason, the microfluidic technique will be used to prepare niosomes with controlled size to enable active loading of doxorubicin, thereby assessing its feasibility for future industrial-scale production of pH-gradient doxorubicin niosomes. The long-term stability of these niosomes will also be studied.

1.11 Objectives

There are three main objectives for this thesis. The first objective is to develop a new technique to study the ability of different niosomes to create and maintain a pH gradient. The new technique will use the pH indicator bromocresol green as a pH probe to indicate the formation of a pH gradient, the ability of the niosomes to actively load an ionisable drug using a pH gradient, and the ability of niosomes to maintain the pH gradient.

The second objective is to use the data generated from the bromocresol green study and the established knowledge of the optimised parameters for active loading of ionisable compounds into niosomes to actively load drugs such as doxorubicin and, potentially, other drugs such as methotrexate, salicylic acid, and ketorolac.

The third objective is to formulate the niosomes that successfully load doxorubicin using the microfluidic technique. Given that the microfluidic technique has not been used previously to formulate niosomes for active drug loading, the objective is to optimise it, as it can improve formulation properties and reduce production time compared to other techniques. The objective is also to formulate a stable and optimised niosomal formulation with a specific size to enable its use in injection dosage forms.

Collectively, these objectives seek to advance our understanding of pH-gradient niosomes and assess their capacity for active doxorubicin loading with high entrapment efficiency, as well as their stability during storage.

Chapter 2: Materials and Methods

The materials and methodology described in this chapter were used in my open-access published article[1]. All methods and their exact step-by-step explanations were carried out and written by the author of this thesis in both the publication and the thesis.

Open Access Publication:

Altaee, M.; Faheem, A.M.; Elkordy, A.A. pH Gradient-Driven Loading of Doxorubicin into Niosomes: A Comparative Study Using Bromocresol Green as a Visual Indicator. Pharmaceutics 2025, 17, 862. https://doi.org/10.3390/pharmaceutics17070862

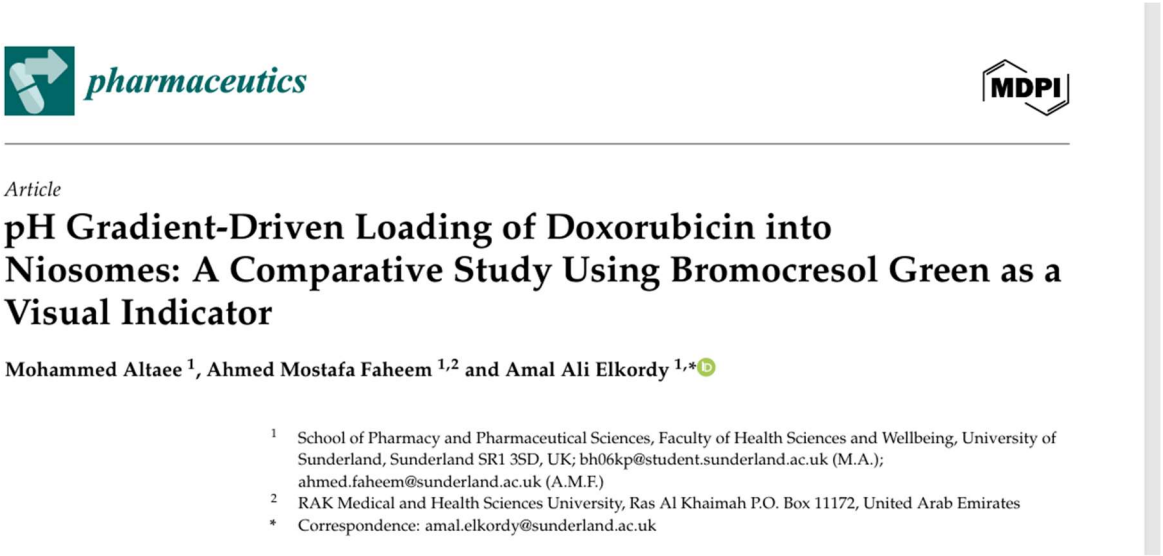

pharmaceutics

MDPI

Article

pH Gradient-Driven Loading of Doxorubicin into Niosomes: A Comparative Study Using Bromocresol Green as a Visual Indicator

Mohammed Altaee [1], Ahmed Mostafa Faheem [1,2] and Amal Ali Elkordy [1,*]

[1] School of Pharmacy and Pharmaceutical Sciences, Faculty of Health Sciences and Wellbeing, University of Sunderland, Sunderland SR1 3SD, UK; bh06kp@student.sunderland.ac.uk (M.A.); ahmed.faheem@sunderland.ac.uk (A.M.F.)
[2] RAK Medical and Health Sciences University, Ras Al Khaimah P.O. Box 11172, United Arab Emirates
* Correspondence: amal.elkordy@sunderland.ac.uk

2.1. Materials

2.1.1 Sources and Molar Masses of Materials Used

Doxorubicin HCl (Molecular weight: 579.98 g/mol), citric acid (Molecular weight: 192.12 g/mol), Ketorolac (Molecular weight: 255.27 g/mol), and 4-2(2-hydroxyethyl)-1-piperazineethanesulfonic acid (HEPES) (Molecular weight: 238.30 g/mol) were obtained from Flourochem, UK. Span 40 (Molecular weight: 402.57 g/mol), Span 60 (Molecular weight: 430.62 g/mol) and Span 65 (Molecular weight: 963.55 g/mol) were obtained as free samples from Croda, Spain. Cremophor RH-40 (Molecular weight: ~ 2700 g/mol), Cremophor ELP (Molecular weight: ~ 2500 g/mol) and Solutol HS-15 (Molecular weight: ~ 960 g/mol) were obtained as free samples from BASF, Germany. Bromocresol green (Molecular weight: 698.05 g/mol) was purchased from Sigma-Aldrich (Switzerland), while cholesterol (Molecular weight: 386.65 g/mol) was purchased from Sigma-Aldrich (USA). Trizma base (Molecular weight: 121.14 g/mol), trizma hydrochloride (Molecular weight: 157.60 g/mol), Chloroform (Molecular weight: 119.38 g/mol), Hydrochloric acid (HCl) and polyethersulfone (PES) 0.2 µm filters were purchased from Fisher Scientific, UK. Sephadex G50 was purchased from GE Healthcare (Sweden). Methotrexate (Molecular weight: 454.44 g/mol) was obtained from Apollo Scientific, UK. All reagents were of analytical grade. Dicetyl phosphate (DCP) (Molecular weight: 546.8 g/mol) was obtained from Avanti Polar, USA.

2.1.2 Characteristics of the Surfactants Used to Formulate the Niosomes

The following table summarises the properties of the surfactants selected for this project. The properties of these surfactants have been discussed in detail in Chapter 1.

Table 2.1: Summary of characteristics of Span 40, Span 60 and Span 65 surfactants.

Name	No. of hydroxyl groups in the surfactant head	Molar mass (g/mol)	Number of hydrophobic tails	Phase transition temperature (°C)	HLB
Span 40	3	402.57	1	42	6.7
Span 60	3	430.62	1	53	4.7
Span 65	1	963.55	3	53	2.1

Span 60 surfactant is one of the most commonly used in niosomal formulations. Span 40, with a shorter hydrophobic tail, was chosen to study the effect of hydrophobic chain length on entrapment efficiency. Span 65 is more hydrophobic than Span 60 due to its having three hydrophobic tails instead of one and one hydroxyl head group, rather than three. Thus, it can form a thicker hydrophobic membrane layer. Figure 2.1 illustrates their structures.

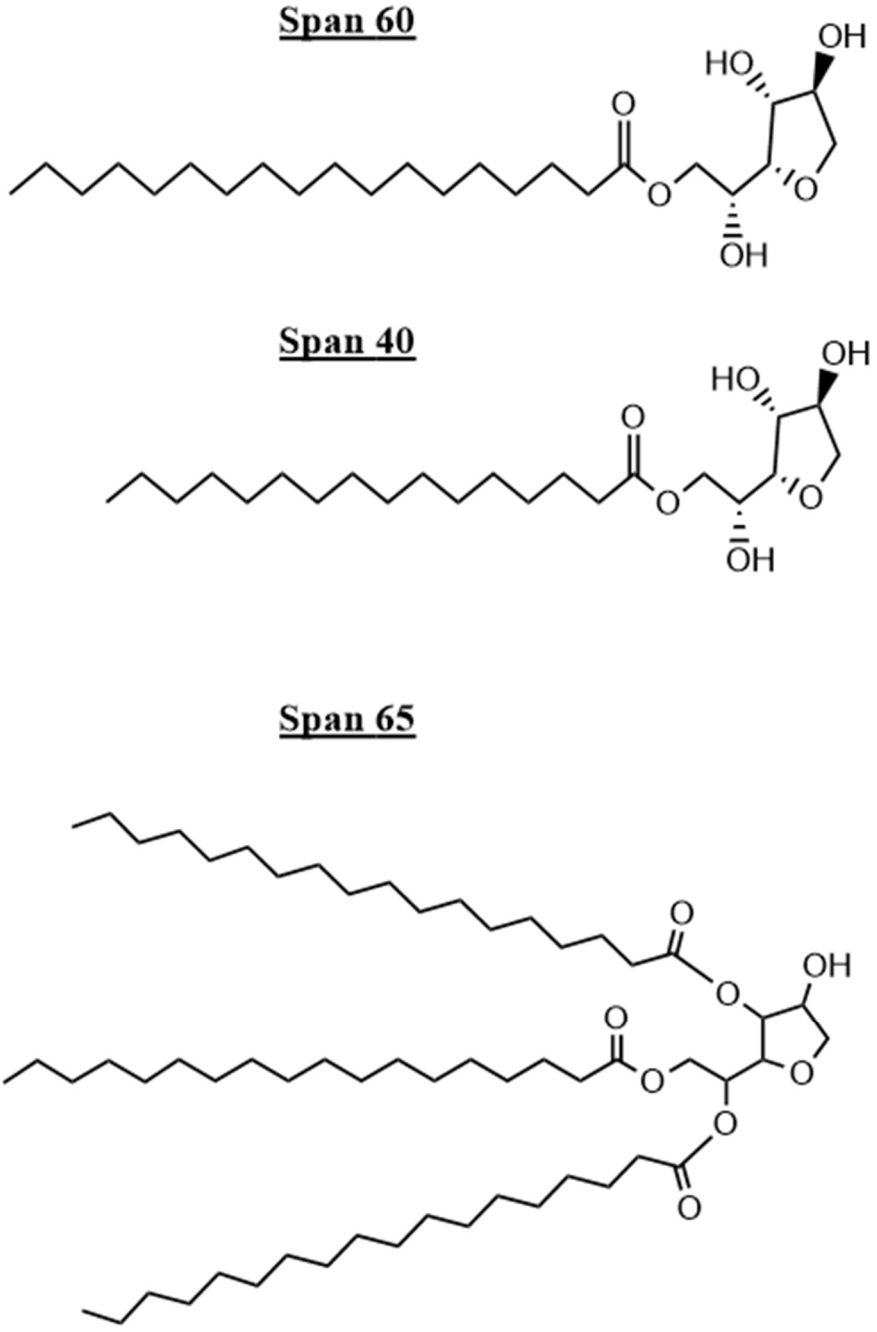

Figure 2.1: Structure of Span 60, Span 40 and Span 65.

2.1.3 Characteristics of the Co-surfactants

Three co-surfactants were selected to assess their ability to maintain a pH gradient in niosomes: Solutol HS-15, Cremophor RH40, and Cremophor ELP. The three co-surfactants have different hydrophilic-lipophilic balances, structures, and sizes, as summarised in table 2.2 and shown in figure 2.2. None of these co-surfactants has been used before in niosomes to maintain a pH gradient. I theorise that the addition of these co-surfactants will pegylate the niosomes, enhancing their colloidal stability and making them stealth from white blood cells when administered by injection, thereby prolonging their circulation time in the body.

The FDA approved Solutol HS-15 for inclusion in parenteral formulations[114]. It was also found that Solutol HS-15 has low haemolytic activity when tested in vitro. Moreover, it can inhibit P-glycoprotein (P-GP) in cancer cells, enabling the accumulation of cytotoxic drugs[115,116].

Cremophor RH40 and Cremophor ELP both have the same structure, but they differ in the size of the polyethylene glycol group and the saturation of the hydrophobic alkyl chain (figure 2.2). Cremophor RH 40 has more PEG groups than Cremophor ELP, which makes Cremophor RH 40 more hydrophilic with a higher HLB than Cremophor ELP. Cremophor ELP has unsaturated hydrophobic tails, while Cremophor RH 40 has saturated hydrophobic tails. Cremophor RH 40 and ELP have both been tested in commercially available oral formulations for drug solubilisation. Cremophor ELP has been used in injectable formulations, while Cremophor RH 60, similar to Cremophor RH 40 but with twenty more PEG groups, has been used in injectable formulations, which also suggests the safety of Cremophor RH 40 in injectable formulations. This indicates the safety of Cremophor RH 40 and Cremophor ELP when administered parenterally, such as in chemotherapy. Cremophor RH40 has also been reported to inhibit p-GP, a glycoprotein that can enhance the accumulation of cytotoxic drugs in cancer cells[46,117].

The formulation's ability to inhibit the p-GP glycoprotein is an added advantage, as one of this project's goals is to load doxorubicin, a cytotoxic drug.

Table 2.2: Summary of characteristics of co-surfactants

Co-surfactant	HLB	Molar mass (g/mol)
Solutol HS-15	14-16	~ 960
Cremophor ELP	12-14	~ 2500
Cremophor RH40	14-16	~ 2700

Cremophor RH 40

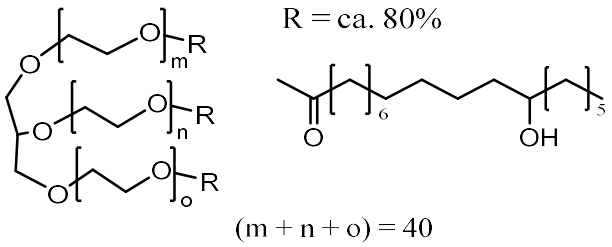

Cremophor ELP

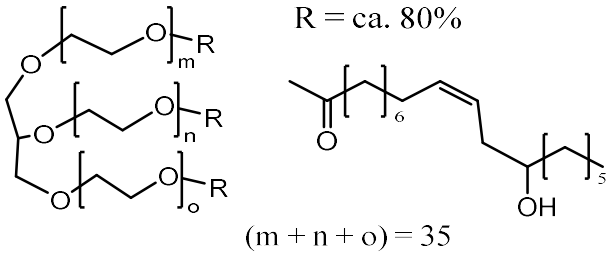

Solutol HS 15

(Contains two main compounds)

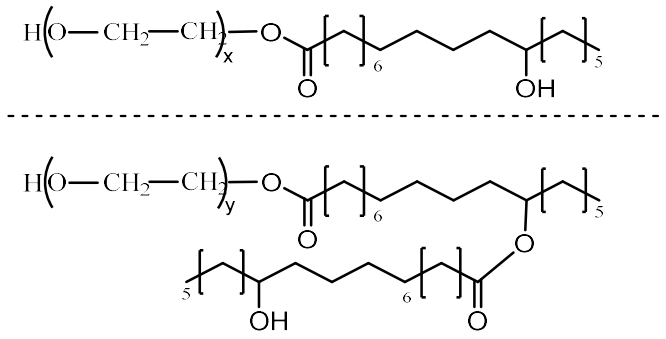

Figure 2.2: Structure of co-surfactants Cremophor RH 40 (hydrogenated polyoxyl 40 castor oil), Cremophor ELP (polyoxyl 35 castor oil) and solutol HS 15 (polyoxyl 15 hydroxystearate).

2.2 Methods

2.2.1 Studying Niosomes pH Gradient Properties Using Bromocresol Green

The ability of niosomes to create and maintain a pH gradient, and how different parameters can affect the stability of the pH gradient and other niosome properties, such as size and zeta potential, will be studied using bromocresol green, a pH indicator. The parameters to be studied include buffer type, surfactant and co-surfactant types, cholesterol concentration in the formulation, loading temperature, and niosomal size.

2.2.1.1 Niosomes Preparation Using Thin Film Hydration for Loading Bromocresol Green Using a pH Gradient

Niosomes were prepared using the thin film hydration technique. Surfactants (Span 60 or Span 40) and cholesterol with or without co-surfactants (Cremophor RH40, Cremophor ELP or Solutol HS-15) were used to formulate the niosomes. The ingredients (as summarised in table 2.3) were dissolved in 3 mL of chloroform in a 25 mL round-bottom flask. The chloroform was then removed under vacuum using a rotary evaporator (Rotavapor R-210, Buchi, Switzerland) at 40 °C. The pressure was reduced to 400 mbar and kept for 5 minutes to warm the chloroform. Then, the pressure was gradually reduced to 200 mbar to ensure chloroform evaporation without solvent bubbling. Once a thin film is formed, the round-bottom flask containing it is detached from the rotary evaporator and left in the fume cupboard to dry overnight.

The thin films of BCG formulations (table 2.3) were hydrated with a buffer of choice (Trizma or HEPES) at 60°C for 1 hour using a shaking water bath (NB-303 model, N-Biotek, South Korea). The thin films in formulations F1 to F5 were hydrated with 5 mL of 0.1 M Trizma buffer (pH 9.0) containing BCG at 0.1 mg/mL to assess the efficiency of passive drug loading. However, in formulations F6 to F15, the formulations were hydrated with 4.5 mL of Trizma or HEPES buffer without adding BCG to test for active BCG loading by adding the drug after niosome formation. All BCG formulations were prepared in triplicate. Trizma buffer was prepared by

dissolving Trizma hydrochloride (6.4 mM) and Trizma base (93.6 mM) in deionised water. The pH was then adjusted to 9.0 using NaOH and HCl as required.

Unless otherwise stated, the suspension was then sonicated in an ultrasound bath sonicator (Hilsonic, UK) for 30 minutes to convert the niosomes from multilamellar vesicles (MLV) to large uni-lamellar vesicles (LUV).

Table 2.3: Niosomes compositions for encapsulation of bromocresol green (BCG) via pH gradient.

Formulation code	Co-surfactant used	Span surfactant used	Total number of moles of ingredients (μmol)	molar ratio of Span surfactant : cholesterol : co-surfactant	Thin film hydration buffer
F1	Cremophor RH40	Span 60	60	45:45:10	5mL of trizma (0.1M, pH 9.0, 0.1mg/mL BCG)
F2*	Cremophor ELP	Span 60	60	46.5 : 46.5 : 7.0	5mL of trizma (0.1M, pH 9.0, 0.1mg/mL BCG)
F3	Solutol HS15	Span 60	60	45:45:10	5mL of trizma (0.1M, pH 9.0, 0.1mg/mL BCG)
F4	N/A	Span 60	60	50:50:0	5mL of trizma (0.1M, pH 9.0, 0.1mg/mL BCG)
F5	N/A	Span 40	60	50:50:0	5mL of trizma (0.1M, pH 9.0, 0.1mg/mL BCG)
F6	Solutol HS15	Span 60	60	45:45:10	4.5mL of trizma (0.1M, pH 9.0)
F7	Solutol HS15	Span 40	60	45:45:10	4.5mL of trizma (0.1M, pH 9.0)
F8	Solutol HS15	Span 60	60	45:45:10	4.5mL of trizma (0.1M, pH 9.0)
F9	Solutol HS15	Span 40	60	45:45:10	4.5mL of trizma (0.1M, pH 9.0)
F10	Solutol HS15	Span 60	60	45:45:10	4.5mL of HEPES (0.1M, pH 8.0)
F11	Solutol HS15	Span 60	60	45:45:10	4.5mL of HEPES (0.1M, pH 8.0)
F12	Solutol HS15	Span 60	60	35:55:10	4.5mL of trizma (0.1M, pH 9.0)
F13	Solutol HS15	Span 60	60	55:35:10	4.5mL of trizma (0.1M, pH 9.0)
F14	Solutol HS15	Span 65	60	45:45:10	4.5mL of trizma (0.1M, pH 9.0)
F15	Solutol HS15 + Cremophor RH 40 (1:1 molar ratio)	Span 65	60	45:45:10	4.5mL of trizma (0.1M, pH 9.0)
F16	Cremophor RH 40	Span 65	60	45:45:10	4.5mL of trizma (0.1M, pH 9.0)

*** In formulation F2, the ratio of 45:45:10 of span 60:cholesterol:Cremophor ELP has been tried. Still, it did not produce large unilamellar vesicles (LUV) niosomes after sonication, which is one of the targets for these formulations to study the effect of size on %EE. The ratio shown in this table (46.5:46.5:7.0) has been tested and produced LUV niosomes upon sonication. For this reason, it has been chosen.**

2.2.1.2 Bromocresol Green (BCG) Loading

A 1mg/mL BCG solution was prepared in 0.1 M Trizma buffer (pH 9.0). The BCG drug model was either loaded into niosomes by adding 0.5mL of BCG solution to 4.5mL of hydration media (for passive loading of niosomes like in formulations F1 to F5) or by adding the BCG solution to the niosomal suspension after niosomes were formed (for active loading of niosomes like in formulations F6 to F13 by adding the drug after the formation of niosomes).

Achieving pH gradient and thus starting active loading of BCG into niosomes was performed by the addition of either 0.1 mL of 1 M HCl to 1 mL of the formulation containing BCG (like in formulations F1 to F7, F10, F12 to F16) to reduce the pH to 1.5 (for formulations hydrated with trizma buffer) and to 2.8 (in case of formulation F10 which is hydrated with HEPES buffer) or adding 0.5 mL of 0.25 M citric acid to 1 mL of the formulation containing BCG (like in formulations F4, F5, F8, F9 and F11) to reduce pH to 3.2 (for formulations hydrated with trizma buffer) and to 3.36 (in case of formulation F11 which is hydrated with HEPES buffer). Drug loading took place at either room temperature (RT, ~23 °C), around 23 ^{o}C, or at 40 ^{o}C.

In formulations F1 to F3, active loading was also tested by adding 0.1 mL of 1 M HCl to 1 mL of the formulation, which already contained BCG (0.1 mg/mL) that was passively loaded. HCl was added either before the formulations were sonicated to test the efficiency of active loading via pH gradient on large MLV niosomes or after the formulations were sonicated to study the effect of reducing niosomes' size on %EE via active loading.

For formulations F4 and F5, 0.1 mL of 1 M HCl was added to 1 mL of the formulation to reduce the pH to 1.5 and 0.5 mL of 0.25 M citric acid was added to 1 mL of the formulation to reduce the pH to 3.2, creating a pH gradient.

2.2.1.3 Bromocresol Green Lambda Max and Calibration Graph

Lambda max was measured using a UV/Vis spectrophotometer (Spectrasonic Camspec Ltd, Canada). A wavelength scan was performed on a BCG solution in Trizma buffer (0.1 M, pH 9.0) (blue colour) to identify the λmax between 190 nm and 900 nm.

A wavelength scan has shown that when BCG is in its blue form (pH > 5.8), its λmax is 617nm, as shown in figure 2.3 below.

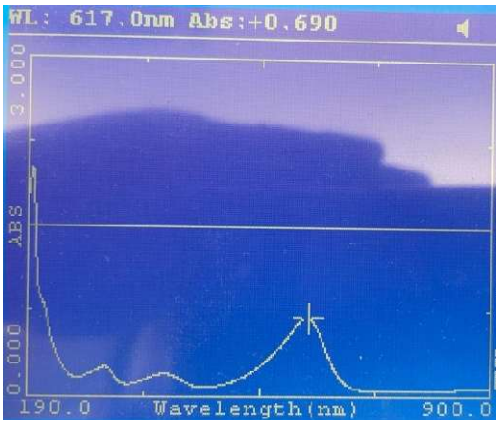

Figure 2.3: Wavelength scan for BCG in its blue form (pH > 5.4)

However, it should be noted that the wavelength scan graph is completely different when BCG is in its yellow form (pH < 3.8), where its lambda max becomes 444nm, as shown in figure 2.4 below.

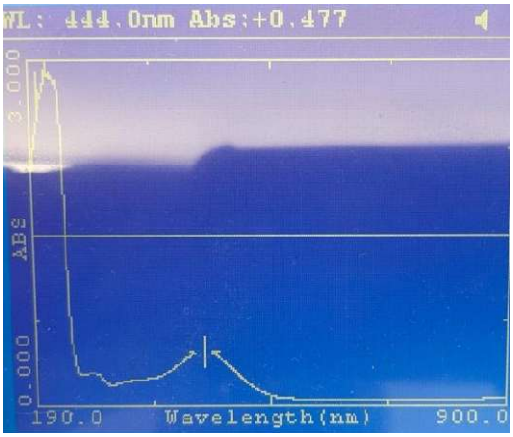

Figure 2.4: wavelength scan for BCG in its yellow form (pH < 3.8)

For this reason, when measuring entrapment efficiency and establishing a calibration graph, the colour of BCG should be either completely yellow or completely blue, as absorbance changes with colour.

This is because when a chemical substance changes colour, it interacts differently with visible light. When white light passes through a coloured material, specific wavelengths are absorbed, depending on the material's properties. The light that is not absorbed is the light we end up seeing—and it appears as the complementary colour of the absorbed wavelength(s). This idea is illustrated by the colour wheel

(figure 2.5 below), where complementary colours sit directly opposite each other. For example, if a substance absorbs light in the 420–430 nm range (which is violet), it will look yellow to our eyes[118,119].

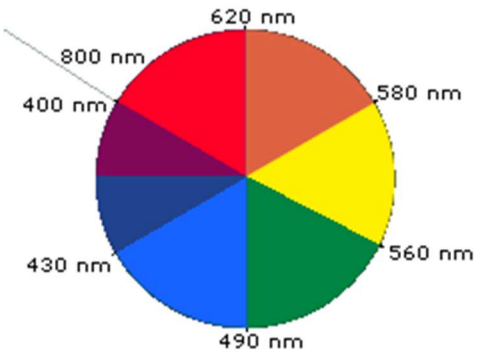

Figure 2.5: Colour wheel showing complementary colours and their wavelengths.

For this reason, when measuring entrapment efficiency and establishing a calibration graph, the BCG should be either completely yellow or completely blue, as absorbance varies with colour. In this study, BCG will always be in its blue form when measuring its concentration.

A calibration graph was then obtained by measuring the absorbance of different concentrations of BCG solution. The absorbance at λmax (617 nm) of four BCG standard solutions was measured. All standards were prepared in a 1:1 ratio of trizma buffer (0.1 M, pH 9.0) to isopropanol to mimic the conditions used to measure BCG entrapment efficiency.

2.2.1.4 Encapsulation Efficiency of Bromocresol Green

The method used to investigate %EE was based on determining the total drug concentration in the formula, rather than relying solely on the theoretical drug quantity, to achieve an accurate measurement. Hence, for pH-gradient niosomes, 0.5 mL of the suspension was collected at 15- and 60-minute intervals during drug loading and mixed with 0.5 mL of the same buffer used to hydrate the niosomal thin film to quench the pH gradient by raising the pH above 5.4. Then, the 1 mL suspension was transferred to a 2 mL Eppendorf tube and centrifuged in a

Centrifuge Mikro 200R (Hettich Zentrifugen, Germany) at 15,000 RPM for 1 hour at 4 °C to pellet the niosomes and separate them from the supernatant. Then, 0.5 mL of the supernatant containing the unentrapped drug was collected and mixed with 1.5 mL of isopropanol. The absorbance of this new solution was measured, and the concentration of the free BCG was calculated. It was found that a 1:1 and a 1:3 ratio of trizma to isopropanol yield similar absorbance values. However, increasing the isopropanol concentration to a 1:3 of trizma: isopropanol ratio was more effective at disrupting the niosomes, as measured by the total BCG content in the formulation.

To measure the total amount of BCG model drug in the formulation loaded via active loading, 0.5 mL of the niosomal suspension was taken and mixed with 0.5 mL of the same buffer used to hydrate the niosomal thin film. Then, 0.5 mL of the suspension was mixed with 1.5 mL of isopropanol to disrupt the niosomes and release the entrapped drug. A homogeneous solution was obtained. The absorbance of the formed solution was measured, and its BCG concentration —the actual total concentration in the formula —was calculated. To avoid any possibility of BCG instability, the total concentration of the drug in the formulation was measured at the beginning of the experiment (as BCG solutions) and after drug loading (as the niosome suspension) to assess drug retention and encapsulation efficiency.

For passively loaded niosomes, 0.5 mL of the suspension was mixed with 0.5 mL of the same buffer used to hydrate the niosomal thin film to dilute the sample for absorbance measurements. The 1 mL suspension was added to 2 mL Eppendorf tubes and centrifuged under the same conditions as above for active loading.

To measure the total amount of drug in the niosome formulation loaded passively, the same steps as above for the active-loaded niosomes were employed.

The percentage of entrapped BCG was measured using the following equation:

$$\%EE = \left(1 - \frac{amount\ of\ drug\ unentrapped}{total\ amount\ of\ drug}\right) \times 100 \qquad \textbf{eq. 2.1}$$

All measurements have been conducted in triplicate.

2.2.2 Doxorubicin Entrapment into Niosomes Via pH Gradient

Niosomal formulations containing Span 60, Solutol HS-15, and cholesterol will be used to prepare pH-gradient niosomes for the remote loading of doxorubicin, after

they have been shown to actively load BCG. However, a different surfactant, Span 65, will also be tested, as it produces niosomes smaller than those made with Span 60[29].

2.2.2.1 Niosomes Preparation Using Thin Film Hydration for Loading Doxorubicin Using Ammonium Sulphate and pH Gradient

Doxorubicin formulations (table 2.4) were treated slightly differently; the F1-D thin film was hydrated with 5 mL of Trizma buffer to assess passive doxorubicin loading. However, formulations F2-D to F5-D, F5-D-E and F6-D to F9-D were hydrated with an ammonium sulfate solution (0.12 M or 0.25 M). All doxorubicin formulations were subjected to bath sonication before the addition of doxorubicin using an ultrasound bath sonicator (Hilsonic, UK) for 30 minutes to convert the multilamellar vesicles (MLV) to large unilamellar vesicles (LUV).

2.2.2.1.1 Extruding Niosomes Using a Manual Extruder

To study the effect of extrusion on the niosomal size and size distribution, formulation F5-D-E was extruded using a mini-extruder (Avanti, USA) with a 100 nm filter. The formulation was heated to 40°C and passed through the filter 11 times immediately after film hydration and sonication. All formulations were prepared in duplicate, as consistent results were obtained.

Table 2.4: Entrapment of anticancer drug (doxorubicin) into niosomes via pH gradient.

Formulation code	Span surfactant	Co-surfactant used	molar ratio of Span surfactant: cholesterol: Co-surfactant 1: Co-surfactant 2 (if present)	Total number of moles of ingredients (μmol)	Hydration buffer	External buffer exchange method
F1-D	Span 60	Solutol HS-15	45:45:10	120	5mL of trizma (0.1M, pH 9.0)	N/A
F2-D	Span 60	Solutol HS-15	45:45:10	120	5mL Ammonium sulfate (0.12M)	Sephadex G50 (in PBS 1x)
F3-D	Span 60	Solutol HS-15	45:45:10	120	5mL Ammonium sulfate (0.12M)	Sephadex G50 (in trizma 0.1M)
F4-D	Span 60	Solutol HS-15	45:45:10	120	5mL Ammonium sulfate (0.25M)	Sephadex G50 (in trizma 0.1M)
F5-D	Span 60	Solutol HS-15	55:35:10	120	5mL Ammonium sulfate (0.12M)	Sephadex G50 (in trizma 0.1M)
F5-D-E*	Span 60	Solutol HS-15	55:35:10	120	5mL Ammonium sulfate (0.12M)	Sephadex G50 (in trizma 0.1M)
F6-D	Span 65	Solutol HS-15 Cremophor RH40	45:40:10:5	120	5mL Ammonium sulfate (0.12M)	Sephadex G50 (in trizma 0.1M)
F7-D	Span 65	Solutol HS-15 Cremophor RH40	45:45:5:5	120	5mL Ammonium sulfate (0.12M)	Sephadex G50 (in trizma 0.1M)
F8-D	Span 65	Cremophor RH40	50:45:5	120	5mL Ammonium sulfate (0.12M)	Sephadex G50 (in trizma 0.1M)
F9-D	Span 65	Cremophor RH40	45:45:10	120	5mL Ammonium sulfate (0.12M)	Sephadex G50 (in trizma 0.1M)

*** Niosomal formulation F5-D-E was extruded after sonication.**

2.2.2.2 Loading of the Anticancer Drug

For passive loading in formulation F1-D, 1 mL of the formulation was diluted to 5 mL to maintain a similar concentration of the niosome ingredients to that in the pH gradient niosomes. Then, 0.9 mL of the formulation was mixed with 0.1 mL of a doxorubicin solution (1 mg/mL in 0.15 M NaCl). Drug loading was left for 1 hour at room temperature, RT, ~23 °C.

To create a pH gradient, the Sephadex G50 gel column technique was used. The Sephadex G50 column was prepared by mixing 1 g of Sephadex G50 powder with 20 mL of either PBS buffer (pH 7.4, the buffer formed from sodium chloride 0.137M, potassium chloride 0.0027M, sodium phosphate dibasic 0.01M and potassium phosphate monobasic 0.0018M) or Trizma (0.1M, pH 9.0). The suspension was then left to equilibrate overnight at room temperature, ~23 °C, allowing the Sephadex resin to swell. The suspension was then loaded into a column. pH gradient was created by passing 1 mL of the niosomal formulation through the Sephadex column pre-equilibrated with either PBS (as in formulation F2-D) or Trizma (as in formulations F3-D to F5-D, F5-D-E and F6-D to F9-D). Then, 5 mL of the new pH gradient niosomal formulation was collected.

To load doxorubicin into formulations F1-D to F5-D, and F5-D-E, 0.9 mL of the pH gradient formulation was taken and mixed with 0.1 mL of doxorubicin solution (1mg/mL dissolved in 0.15 M NaCl). Drug loading was left for 30 or 60 minutes at RT or 60 ^{o}C.

However, formulations F6-D to F9-D were loaded with 0.5mg/mL doxorubicin to assess loading efficiency at higher concentrations. For this purpose, a 2 mg/mL doxorubicin solution was prepared in 0.15 M NaCl. Then, 0.25 mL of the doxorubicin solution was mixed with 0.75 mL of the formulation to achieve a final concentration of 0.5 mg/mL.

2.2.2.3 Calibration Plot of Doxorubicin

The doxorubicin lambda max was determined at pH levels of 9.0 and 5.5. Doxorubicin was dissolved in trizma buffer (0.1 M, pH 9.0) or 0.15 M NaCl solution (pH 5.5) to produce a concentration of 0.025 mg/mL. Knowing from the literature that

the doxorubicin lambda max is around 480nm. A lambda max search was conducted between 190 nm and 650 nm.

The λmax of doxorubicin in both solutions was 482 nm (figure 2.6). Since isopropanol will be used to disrupt the niosomes' bilayer and release the drug, doxorubicin was dissolved in 0.1 M Trizma with isopropanol (1:1 ratio) to obtain the calibration curve.

Figure 2.6: wavelength scan for doxorubicin in the 0.15M NaCl with isopropanol (1:1 ratio) solution at a concentration of 25 mcg/mL.

2.2.2.4 Determination of Entrapment Efficiency for Doxorubicin

Entrapment efficiency was measured by comparing the concentration of unentrapped drug to the total drug concentration in the formulation.

The total concentration of the drug in the formulation was measured at the beginning of the experiment as solutions and after drug loading to assess drug retention and loading efficiency, and to detect/avoid potential drug instability. For this, 0.1 mL of the formulation was mixed with 1 mL of isopropanol. After disrupting the niosomes with isopropanol, 0.9 mL of 0.1M trizma buffer was added. The absorbance was then read at λmax 482nm to determine the actual total drug concentration in the formula.

To measure the concentration of the unentrapped drug for formulations loaded at 0.1 mg/mL, 0.15 mL of the formulation was taken at 30- and 60-minute intervals during drug loading. The collected niosomal suspension was pelleted by centrifugation for 1

hour at 15,000 RPM and 4 °C. Then, 0.1 mL of the supernatant was collected and mixed with 1 mL of isopropanol and 0.9 mL of 0.1 M trizma buffer. The absorbance was taken at λmax of 482 nm.

To measure the concentration of the unentrapped drug for formulations loaded at 0.5 mg/mL of doxorubicin, the loaded niosomes were first separated from the unentrapped drug by gel filtration using a Sephadex G50 column pre-equilibrated with 0.15 M NaCl. Centrifugation was not used because preliminary studies showed that, at high drug concentrations, the drug leaked from the niosomes in significant amounts during centrifugation. For this reason, and to avoid underestimating entrapment efficiency, centrifugation was avoided during drug loading at doxorubicin concentrations greater than 0.1 mg/mL. The percentage of entrapped doxorubicin was measured using equation 2.1. All measurements have been conducted in duplicate.

2.2.3 Entrapment of Acidic Drugs (Methotrexate, Ketorolac and Salicylic acid) in Niosomes Using pH Gradient

Niosomes prepared by thin-film hydration have successfully entrapped the acidic pH indicator BCG. For this reason, the ability of these niosomes to entrap three acidic drugs was tested. Methotrexate, ketorolac, and salicylic acid all have carboxylic acid functional groups that can become ionised at alkaline pH and unionised at acidic pH.

2.2.3.1 Thin Film Hydration for Niosomal Formulations

The niosomal formulations listed in Table 2.4 below were prepared by thin-film hydration. Two buffers were used to hydrate the formulations: trizma buffer (0.1 M, pH 9.0) and HEPES buffer (0.1 M, pH 8.0).

Trizma and HEPES buffers were chosen because they have been shown to entrap the acidic pH indicator BCG. Then, a buffer exchange is performed to remove the alkaline buffer from the environment surrounding the niosomes and replace it with an acidic buffer. Drugs carrying carboxylic acid functional groups will be unionised outside the niosomes and become ionised inside the niosomes. This will increase the drug concentration within the niosomes and enhance entrapment efficiency.

To create a pH gradient in niosomes, 0.1 mL of 1 M HCl solution was added to 1 mL of niosomes prepared with Trizma or HEPES, reducing their pH to 1.5 and 2.8, respectively. Table 2.5 below shows the formulations prepared.

Table 2.5: Methotrexate, ketorolac and salicylic acid entrapment into Niosomal formulations via pH gradient.

Formulation code	molar ratio of Span 60: cholesterol: Solutol HS-15	Total number of moles of ingredients (µmol)	Hydration buffer	Achieving a pH gradient
F1-MKS	45:45:10	120	4.5mL of trizma (0.1M, pH 9.0)	pH was reduced by adding 1 M HCl to 1mL of the formulation to reach 1.5 (and 4.0 for methotrexate).
F2-MKS	45:45:10	120	4.5mL of HEPES (0.1M, pH 8.0)	pH was reduced by adding 1 M HCl to 1mL of the formulation to reach 2.8 (and 4.0 for methotrexate).

Each one of the above formulations was used to entrap methotrexate, ketorolac and salicylic acid individually.

2.2.3.2 Achieving pH Gradient to Load Methotrexate, Ketorolac and Salicylic Acid

Stock solutions of 1 mg/mL of the drugs being loaded (methotrexate, ketorolac and salicylic acid) were prepared in trizma buffer (0.1 M, pH 9.0). To load the drugs into the niosomes, 0.9 mL of each F1-MKS and F2-MKS formulation was mixed with 0.1 mL of 1 mg/mL methotrexate, ketorolac, or salicylic acid, separately. Then, to establish a pH gradient, 0.1 mL of 1 M HCl was added to the F1-MKS and F2-MKS formulations, reducing the pH from 9.0 and 8.0 to 1.5 and 2.8, respectively. This technique follows the same pattern as loading BCG.

Methotrexate and ketorolac precipitated upon the reduction of the pH to 1.5 and 2.8 in formulations F1-MKS and F2-MKS. To solve this problem, a cosolvent was added to enhance the solubility of these drugs. Dimethyl sulfoxide (DMSO) was added to the formulation at a 5%v/v concentration during drug loading to improve drug solubility. Drug loading of methotrexate, ketorolac and salicylic acid was studied with

and without DMSO. Also, drug loading was conducted at room temperature, ~23 °C, and at 40 °C to study the effect of temperature on loading these three drugs with and without DMSO.

2.2.4 Formulating Niosomes Using Microfluidic Technique

A microfluidic technique for niosome formulation can produce small, narrow-size-distribution niosomes (low PDI), meaning they do not require extrusion. The process can also scale up niosome production without the need to extrude the niosomes to reduce their sizes. This technique will be tested to produce small niosomes for loading doxorubicin. The size of the niosomes will be studied both after loading and during long-term storage.

Various parameters can affect the size and size distribution of niosomes. The ingredients used and their concentrations, the buffer and organic solvent used, the temperature, and the total flow rate (TFR) and flow rate ratio (FRR) of the microfluidic instrument are all parameters that can affect niosomes size and their ability to load drugs.

2.2.4.1 Formulations Preparation

Niosomes were formulated using a benchtop microfluidic instrument, NanoAssemblr, provided by Precision NanoSystem Inc (Vancouver, Canada) which was later acquired by the USA company Danaher Corporation. A microfluidic technique forms niosomes by mixing an organic solvent containing surfactants and cholesterol with an aqueous buffer in a microchannel. The organic phase containing the surfactants and cholesterol is added to one syringe, and the aqueous buffer is added to another syringe. The two syringes are fitted into a cartridge that allows the two liquids to mix in a microchannel contained within the cartridge. The instrument will push the syringes at a controlled rate to control the speed of mixing the two phases in the microchannels. The niosomes will exit the cartridge through a third opening and be collected for further processing.

Niosomes were prepared by dissolving the surfactants and cholesterol in ethanol. Different formulations contained different ingredients and were dissolved in 4mL of ethanol. Ethanol was sonicated to help dissolve the ingredients, and the mixture was heated to 60 °C because the ingredients did not dissolve at room temperature, ~23 °C. A heating block was used to maintain a temperature of 60 °C during micromixing to prevent precipitation of ingredients.

The following parameters were studied to obtain the most optimised niosomal formulation for loading doxorubicin using a pH gradient:

a. Different formulation compositions of surfactants, co-surfactants and cholesterol and different FRR.

Table 2.6: Different compositions of niosomes formulated using the microfluidic technique. All formulations were prepared at 60 °C with a TFR of 12mL/min, and three different FRRs (ratio of aqueous phase to organic) for each formulation were tested (5:1, 3:1, and 2:1). The aqueous phase was an ammonium sulfate solution (0.12 M, pH 5.5). All formulations were prepared in duplicate.

Formulation code	Molar % of span 65	Molar % of cholesterol	Molar % of Solutol HS-15	Molar % of Cremophor RH40	Total amount dissolved in 4 mL of ethanol (µmol)
F1-1	45	40	10	5	120
F2-1	45	45	5	5	120
F3-1	45	45	0	10	120
F4-1	50	45	0	5	120
F5-1	45	40	5	10	120
F6-1	45	35	10	10	120
F7-1	45	45	10	0	120

Niosomes in table 2.6 above were prepared to study the effect of different surfactants, co-surfactants and cholesterol compositions on niosome size, size distribution and zeta potential. Each formulation was repeated twice. The surfactant, co-surfactant(s), and cholesterol of each formulation were dissolved in 4 mL of

ethanol, giving a total concentration of 30 µmol/mL. The total flow rate was 12 mL/min, and the aqueous buffer-to-organic solvent ratio, known as the flow rate ratio (FRR), was 5:1, 3:1 or 2:1. This will result in a final surfactant and cholesterol total concentration of 5 µmol/mL for 5:1, 7.5 µmol/mL for 3:1 and 10 µmol/mL for 2:1, assuming ethanol does not evaporate.

b. Different total flow rate

The total flow rate (TFR) determines the speed at which the organic and aqueous phases are pumped through the cartridge's microchannel. Some studies have shown that higher TFR is associated with smaller niosome size. For this reason, two formulations were selected to study the niosome size at five different total flow rates. Table 2.7 below summarises the experiment.

Table 2.7: Studying five different TFRs of two niosomal formulations. The flow rate ratio was 2:1. All experiments were prepared in duplicates.

Formulation code	Total amount dissolved in 4 mL of ethanol (µmol)	FRR	Total flow rate
F3-1	120	2:1	4
			8
			12
			16
			20
F6-1	120	2:1	4
			8
			12
			16
			20

c. Different concentrations of ingredients and different flow rate ratios

The higher the concentration of surfactants and cholesterol dissolved in the ethanol, the more niosomes should be produced by the microfluidic instrument. Another factor that determines the number of niosomes produced is the flow-rate ratio between the aqueous and organic phases. The higher the organic phase, the higher the niosome concentration. Table 2.8 below summarises the formulations prepared.

Table 2.8: Niosomes prepared at different concentrations of surfactants and cholesterol in ethanol. TFR was 1 2mL/min, and three different FRRs for each formulation were tested (5:1, 3:1 and 2:1). The aqueous phase was an ammonium sulfate solution (0.12 M, pH 5.5). All experiments were conducted in duplicates.

Formulation code	% of span 65	% of cholesterol	% of Solutol HS-15	% of Cremophor RH40	Total amount dissolved in 4 mL of ethanol (μmol)
F1-2	45	45	10	5	240
F1-3	45	45	10	5	480
F2-2	45	45	5	5	240
F2-3	45	45	5	5	480
F3-2	45	45	0	10	240
F3-3	45	45	0	10	480
F4-2	50	45	0	5	240
F4-3	50	45	0	5	480
F5-2	45	40	5	10	240
F5-3	45	40	5	10	480
F6-2	45	35	10	10	240
F6-3	45	35	10	10	480
F7-1*	45	45	10	0	120

***** The size of the F7-1 formulation at 5:1, 3:1 and 2:1 FRR was very high, and for this reason, and to avoid clogging the cartridge containing the microchannel, higher concentrations of the F7-1 formulation were not tested as they were not necessary.

2.2.4.2 Passive Drug (Doxorubicin) Loading into Niosomal Suspension via Microfluidic Technique

To assess the ability of niosomes to entrap doxorubicin via passive loading, the F3-3 formulation was used. Doxorubicin was dissolved in a sucrose-histidine buffer solution (10 %w/v sucrose, 10 mM histidine, pH 6.5). The F3-3 ingredients were dissolved in ethanol. Niosomes were prepared by mixing the two solvents at the following settings: TFR of 12mL/min, FRR of 2:1 and at 60 °C. The final doxorubicin concentration in the formulation was 0.5 mg/mL.

The unentrapped drug was separated from the niosomes using Sephadex G50 gel filtration. The Sephadex column was pre-equilibrated with the sucrose-histidine buffer. Entrapment efficiency was measured using equation 2.1.

2.2.4.3 Creating pH Gradient and Drug Loading

Formulation F3-3 was selected for drug loading using a pH gradient. The formulation was made using a microfluidic technique at a TFR of 12 mL/min and a FRR of 2:1. Then, 1 mL of each of the formulated niosomes was passed through a Sephadex column pre-equilibrated with Trizma buffer (0.1M, pH 9.0) to create a pH gradient, where inside the niosomes will be acidic ammonium sulfate, while outside the niosomes will be basic Trizma.

Two solutions of doxorubicin were prepared, one by dissolving doxorubicin in sucrose-histidine buffer (10 %w/v sucrose, 10 mM histidine, pH 6.5) and the other by dissolving doxorubicin in NaCl solution (0.9%). Doxorubicin was loaded into the niosomes at two concentrations: 0.3 mg/mL and 0.5 mg/mL. For a 0.3 mg/mL loading, 0.85 mL of the pH gradient niosomes was mixed with 0.15 mL of 2 mg/mL doxorubicin dissolved in normal saline (0.9% NaCl) or sucrose-histidine buffer solution and for a 0.5 mg/mL loading, 0.75 mL of the pH gradient niosomes was mixed with 0.25 mL of 2 mg/mL doxorubicin.

After 1 hour of adding doxorubicin to the niosomes, the formulation was passed through a Sephadex G50 column pre-equilibrated with NaCl solution for doxorubicin that was already dissolved in NaCl or sucrose-histidine buffer for doxorubicin that was already dissolved in sucrose-histidine to separate the unentrapped drug from

the niosomes, measure entrapment efficiency, and assess niosome stability upon storage in NaCl vs sucrose-histidine solution.

2.2.4.4 Drug Recovery During Sterilisation

In addition to a sterile production environment, the gold standard method for sterilising nanoparticles, such as niosomes and liposomes, is to filter them through a sterile 0.22 µm filter. This is usually the last stage before packaging. For this reason, the niosomes' size and size distribution must be small enough for them to pass through the filter, while microorganisms and other large unwanted particles will be trapped in the filter.

To test the ability of the formulated niosomes to pass through the filter, a 0.20 µm Polyethersulfone (PES) filter was used. 3 mL of the niosomal formulation F3-3, loaded with 0.3 mg/mL and 0.5 mg/mL of drug, were passed through the filter after removing any unentrapped drug.

The total amount of drug in the formulation was measured before and after filtration to study the effect of filtration on niosome retention. To calculate the amount of drug, 0.1 mL of the formulation before filtration and 0.1 mL after filtration were each mixed with 1.9 mL of isopropanol to break the niosomes and release the drug. The amount of drug was measured using a UV/Vis spectrophotometer (Spectrasonic Camspec Ltd, Canada) at a wavelength of 482 nm.

Drug recovery was calculated using the following equation:

$$\% \text{ drug recovered during filtration} = \left(\frac{amount\ of\ drug\ after\ filtration}{amount\ of\ drug\ before\ filtration}\right) \times 100 \qquad \text{eq 2.2}$$

Given that the drug is entrapped in the niosomes, and any unentrapped drug is removed using a Sephadex G50 column, drug recovery is also an indication of the amount of niosomes that passed through the filter and the interaction between the niosomes and the filter to study the suitability of this sterilisation technique.

2.2.5 FT-IR

FT-IR was used to investigate interactions among the niosome components after niosome formation. The FT-IR of Span 60, Span 65, Cremophor RH40, Cremophor ELP and Solutol HS-15 was done individually using Agilent Cary 630 FTIR (CA, USA). Then the FT-IR of the niosomes in table 2.9 below was measured in their pelleted form. However, the water peaks affected the readability of the FT-IR graph; therefore, the FT-IR was measured after lyophilising the formulations. The spectra were recorded over a frequency range of 4000–550 cm^{-1} with a 2 cm^{-1} resolution. The number of scans were 32. The Happ-Genzel function was applied for apodisation.

Table 2.9: Niosomal formulations synthesised for FT-IR study

Formulation code	Co-surfactant used	Span surfactant used	Total number of moles of ingredients (µmol)	molar ratio of Span surfactant : cholesterol : co-surfactant	Thin film hydration solvent
F1-IR	Cremophore RH40	Span 60	60	45:45:10	5mL of Distilled water
F2-IR	Cremophore ELP	Span 60	60	45:45:10	5mL of Distilled water
F3-IR	Solutol HS15	Span 60	60	45:45:10	5mL of Distilled water
F4-IR	Cremophore RH40	Span 65	60	45:45:10	5mL of Distilled water
F5-IR	Solutol HS15	Span 65	60	45:45:10	5mL of Distilled water

2.2.6 Physical Size Using Zetasizer

The niosomal size was measured using Zetasizer ZSP (Malvern Instruments, UK). Each sample was diluted 50-fold with the same buffer in which it was made. All experiments have been conducted in triplicate. Disposable cells were used to measure the sample size. Three measurements were conducted for each sample at room temperature (approximately 23 °C).

2.2.7 Zeta Potential

The zeta potential of the niosomal formulations was measured using a Zetasizer ZSP (Malvern Instruments, UK). Zeta potential is a key factor for determining the stability of a suspension system. One of the key factors that affects zeta potential is the pH of the environment in which the niosomes are suspended. For this reason, the zeta potential of the nanoparticles was measured at three pH values (pH 5, 7, and 9) to predict the effect of pH on the long-term stability of the niosomes. pH 9 was obtained using Trizma buffer (0.1 M, pH 9 adjusted with HCl and NaOH). pH 7 and pH 5 solutions were prepared by adding HCl and NaOH to the pH 9 Trizma buffer until the target pH was reached. To measure zeta potential at different pHs for each formulation, 20 µL of the sample was diluted into 980 µL of the buffer of choice. Each experiment was repeated twice.

2.2.8 Niosomes Morphology

Bioblue.Lab light microscope (Euromex, Netherlands) was used to observe niosomes' morphology under 100x magnification.

2.2.9 Stability Study

The niosome stability study was conducted for 3 months, or until the formulation size significantly increased, indicating the study was unsuccessful. The formulations being tested were stored in the fridge at 4 ± 3°C. Samples from the formulation were taken at predetermined intervals, and the physicochemical niosomal characteristics (particle size and PDI) were measured.

2.2.10 Statistical Analysis

Student *T-Test* was used to calculate the statistical significance, where $p < 0.05$ indicates a significant difference.

Chapter 3: Studying pH Gradient in Niosomes Using pH Indicator Bromocresol Green – a Novel Approach

The data produced form the research and included in this chapter have been open access published[1], cited and referenced in this thesis

Open Access Publication:

Altaee, M.; Faheem, A.M.; Elkordy, A.A. pH Gradient-Driven Loading of Doxorubicin into Niosomes: A Comparative Study Using Bromocresol Green as a Visual Indicator. Pharmaceutics 2025, 17, 862. https://doi.org/10.3390/pharmaceutics17070862

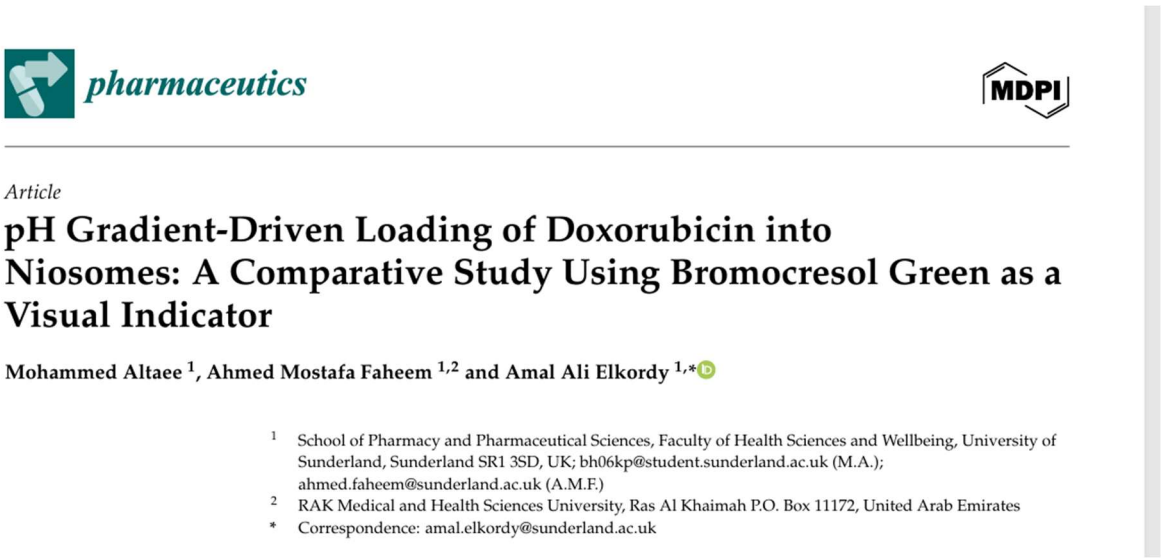

pharmaceutics

MDPI

Article

pH Gradient-Driven Loading of Doxorubicin into Niosomes: A Comparative Study Using Bromocresol Green as a Visual Indicator

Mohammed Altaee [1], Ahmed Mostafa Faheem [1,2] and Amal Ali Elkordy [1,*]

[1] School of Pharmacy and Pharmaceutical Sciences, Faculty of Health Sciences and Wellbeing, University of Sunderland, Sunderland SR1 3SD, UK; bh06kp@student.sunderland.ac.uk (M.A.); ahmed.faheem@sunderland.ac.uk (A.M.F.)
[2] RAK Medical and Health Sciences University, Ras Al Khaimah P.O. Box 11172, United Arab Emirates
* Correspondence: amal.elkordy@sunderland.ac.uk

3.1 Introduction

The main goal of formulating pH gradient niosomes is to enhance the entrapment efficiency of the drug of interest. In pH gradient niosomes, the pH inside the niosomes will be different from that outside the niosomes[62]. This will allow the drug to become unionised and more lipophilic outside the niosomes. It will then cross the niosomal membrane, and once inside the niosome's core, it becomes ionised at the new pH and cannot cross back through the niosomal membrane in its ionised form. Over time, the drug will accumulate and get entrapped inside the niosomes, resulting in better entrapment efficiency[120].

I hypothesise that in niosomes, several factors affect the pH gradient. The most critical factor that controls the pH gradient in niosomes is the niosomal membrane. The niosomal membrane must be rigid enough to control the pH gradient but flexible enough to allow the drug to cross the membrane in its unionised form. The type of the main surfactant can affect the membrane's rigidity. Depending on the phase transition temperature of the surfactant, surfactants with a high phase transition temperature can produce a more rigid membrane than surfactants with a low phase transition temperature[26]. Cholesterol is usually incorporated into the niosomal membrane to stabilise it and improve vesicle stability. Cholesterol is known as a membrane modifier[26]. In cell membranes, it inserts itself between phospholipids, reducing membrane fluidity and enhancing rigidity. The percentage of cholesterol in the niosomal membrane composition can play a crucial role in the membrane integrity and rigidity[121]. Moreover, co-surfactants, which are surfactants with a high hydrophilic lipophilic balance, are sometimes added to the niosomal membrane to improve its properties, such as niosomal stability and drug leakage[23]. Different co-surfactants can have varying effects on membrane stability, thereby affecting the membrane's ability to maintain a pH gradient and to allow the drug of interest to pass through.

From the pH gradient in liposomes, we learnt that other factors can affect the pH gradient and the ability of nanovesicles to actively load drugs, including the choice of buffers and their concentrations, the nanovesicle concentration, and the temperature during drug loading[122].

Several techniques have been used to study the pH gradient across the membrane of a nanovesicle. For example, in pH gradient liposomes, fluorescent probes such as pyranine (HPTS)[99,100], BCECF[100,101], SNARF-1[100,102], and Porphyrin dendrimer[103] have been used to study pH gradients. These techniques rely on the fluorescent probe being encapsulated within the nanovesicle, and the unentrapped probe (external probe) is removed (e.g., via dialysis), leaving only internal fluorescence. These probes emit at two wavelengths depending on the pH of the environment. The ratio of the intensities at the two wavelengths changes with pH, indicating that the pH has changed.

All these techniques lack at least one of the following three criteria: ease of use, the ability to visualise the pH gradient immediately, and the ability to use the probe as a model drug to assess the nanovesicle's ability to entrap drugs efficiently. Some of these probes need to be passively loaded into the nanovesicles such as BCECF[100,101], SNARF-1[100,102], and Porphyrin dendrimer[103]. Then, the amount remaining outside the nanovesicles should be removed using techniques such as gel or membrane filtration. This can introduce uncertainty if the probe is not removed efficiently or leaks during the pH gradient study, leaving the researcher unsure whether the results are due to the pH gradient or to probe leakage outside the nanovesicles. It also means they can only be used to study pH differences across the membrane and will not assess the membrane's ability to load the drug using the pH gradient technique. This is because the probe will be passively loaded into the nanovesicles, and the unentrapped probe is filtered out. Also, the probes mentioned above must be used with an instrument capable of measuring fluorescent signals. This means that the pH gradient and drug loading will not be visible to the naked eye.

For the reasons mentioned above, a novel technique has been established to study the pH gradient across the niosome membrane. The new method relies on a probe, the pH indicator bromocresol green (BCG), which enables the visualisation of the pH gradient as it forms. A pH indicator can be used to assess the niosomal membrane's ability to maintain separation between two environments with differing pH values, namely the internal aqueous core and the surrounding external medium. pH indicators are chemical compounds that exhibit a change in colour in response to variations in pH. This behaviour is attributed to the presence of ionisable functional

groups with defined pKa values, with the observed colour change corresponding to the compound's ionisation state[123].

This study proposes that pH indicators can serve as effective tools for investigating and visualising pH-gradient niosomes, with several practical advantages. For instance, the establishment of a pH gradient across the niosomal membrane can be rapidly confirmed through observable colour changes in the suspension. In addition, pH indicators can act as model compounds representing different classes of active agents and can be readily detected using spectrophotometry due to their distinct colours and characteristic λmax values, which allow clear differentiation from other substances. Furthermore, variations in solution colour may indicate the percentage encapsulation efficiency (%EE). Monitoring colour changes over time can also offer insight into the stability of the pH gradient. Overall, these indicators can contribute to a better understanding of niosomal properties and membrane permeability.

In this chapter, bromocresol green (BCG) was utilised as a pH indicator to examine the characteristics of pH-gradient niosomes. BCG has a molar mass of 698.01 g/mol[124]. BCG is sparingly soluble in water and exists predominantly in a di-anionic, blue form at pH values above 5.4, and in a mono-anionic, yellow form at pH values below 3.8, as illustrated in Figure 3.1-A[125].

When the internal pH of the niosome exceeds 5.4, BCG appears blue, whereas at an external pH below 3.8 it turns yellow (Figure 3.1-B). Consequently, in the presence of BCG, pH-gradient niosomes exhibit both colours simultaneously: blue within the niosomal core and yellow in the surrounding medium. The combination of these colours produces a green appearance in the overall suspension, indicating successful pH gradient formation.

As a greater proportion of BCG becomes encapsulated within the niosomes, the suspension colour gradually shifts towards blue. This change can be used as an indicator of the encapsulation efficiency (%EE) and the effectiveness of the loading process. In addition, %EE can be quantitatively determined using spectrophotometric analysis.

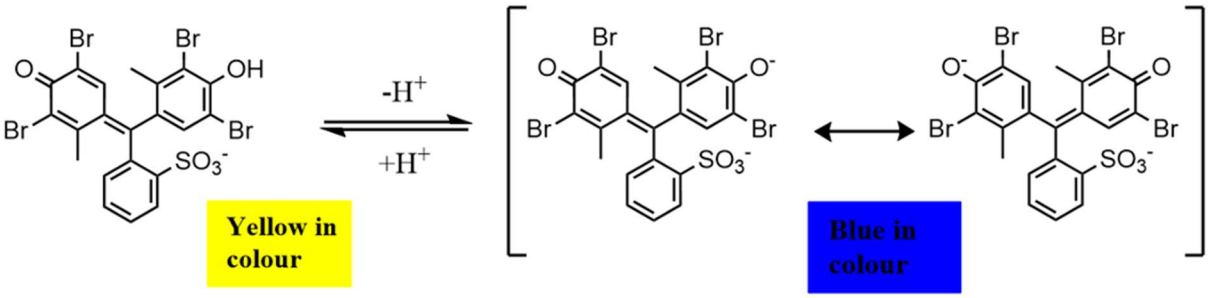

A) Ionisation of BCG in different pH medium

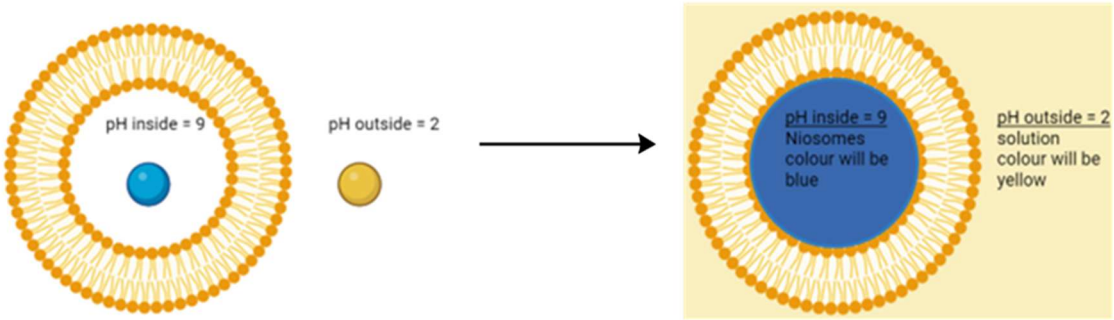

B) The sphere represents a BCG compound where it is yellow in pH = 2 (pH < 3.8) and blue in pH= 9 (pH > 5.4). The pH of the environment that BCG is present in will change colour depending on its pH when pH gradient is established.

Figure 3.1: The influence of BCG ionisation on its colour and the colour of its environments. Figure 3.1-A was generated using ChemDraw 22.2.0, and figure 3.1-B was created using BioRender.

3.2 Aim and Objectives

This chapter aims to study the use of the pH indicator BCG as a probe to evaluate the ability of different niosomal formulations to establish and maintain a pH gradient across their membranes. BCG will be loaded into different niosomal formulations using pH gradient techniques to validate the efficiency of this probe for studying pH gradients in niosomes.

This chapter will also examine how different niosomal membrane compositions affect pH gradient stability. Span 60 or Span 40 will be the main surfactant in all niosomal formulations. Different co-surfactants (Cremophor RH 40, Cremophor ELP and Solutol HS-15) will be added to the formulations. Various cholesterol-to-surfactant ratios will also be studied to assess the effect of cholesterol on membrane rigidity and, thus, on pH gradient control and drug loading efficiency in niosomes.

Moreover, the effects of various buffers, including Tris, HEPES, citric acid, and hydrochloric acid (HCl), on maintaining the pH gradient will also be studied.

3.3 Results and Discussion

3.3.1 Lambda Max and Calibration Plot

A wavelength scan demonstrated that BCG in its blue form (pH > 5.8) exhibits a maximum absorbance (λmax) at 617 nm (Figure 2.3). In contrast, when BCG is in its yellow form (pH < 3.8), the wavelength scan profile differs significantly, with a λmax observed at 444 nm (Figure 2.4). This is because when a chemical substance changes colour, it interacts differently with visible light. For this reason, when measuring entrapment efficiency and establishing a calibration graph, the colour of BCG should be either entirely yellow or entirely blue. In this study, BCG will always be in its blue form when measuring its concentration. A calibration graph was established for BCG in its blue form, as shown in Figure 3.2 below.

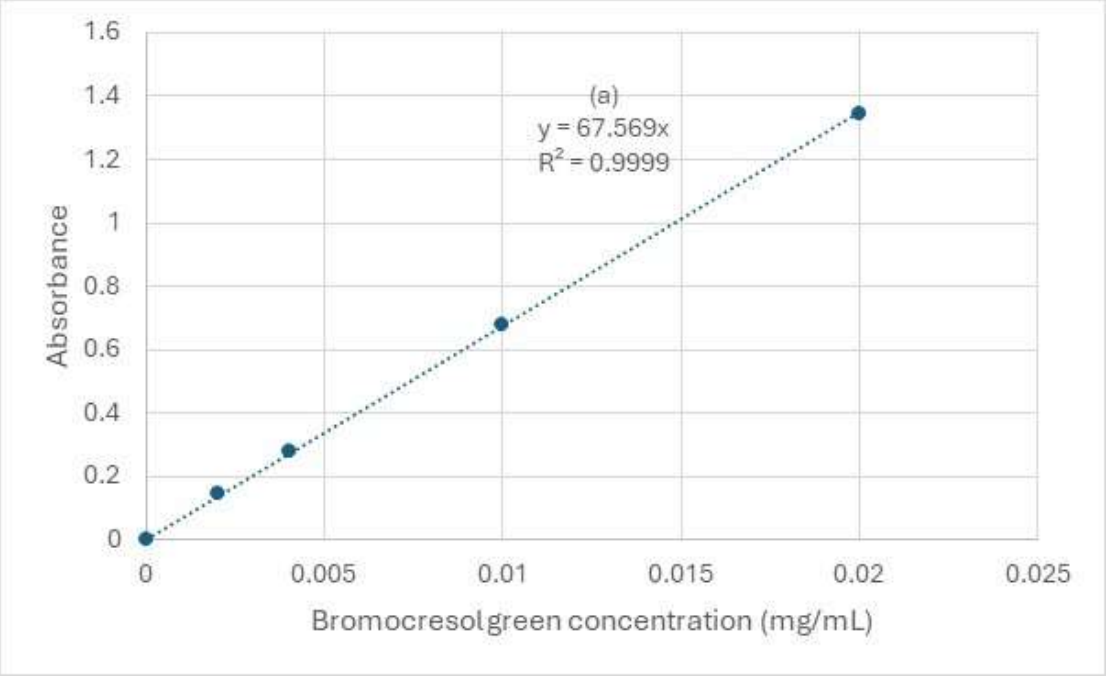

Figure 3.2: Calibration graph for BCG in its blue form at 617 nm wavelength. Similar readings were obtained upon rerunning the results. Measurement was done three times for each concentration and absorbance results were the same for each repeat of each concentration.

3.3.2 Passive Loading of BCG into Niosomes

BCG was passively loaded into three niosomal formulations (F1, F2, and F3) of Span 60 and cholesterol, containing Cremophor RH40, Solutol HS15, or Cremophor ELP. Formulation content (F1 to F3) is summarised in table 2.3.

The size and entrapment efficiency of the three formulations above were studied both before and after bath sonication. Results are summarised in table 3.1 below.

Table 3.1: % Encapsulation Efficiency (EE) (n=3) and size before and after sonication for niosomes with passively loaded BCG in F1-F3 formulations. All formulations formed of Span 60 and cholesterol but contain various co-surfactants: Cremophor RH40 (F1), Cremophor ELP (F2), and Solutol HS-15 (F3).

Formulation	**Before sonication**			**After sonication**		
	%EE (±SD)	**Niosomes Size – d nm** (±SD)	**PDI** (±SD)	**%EE** (±SD)	**Niosomes Size – d nm** (±SD)	**PDI** (±SD)
F1	3.92 (±0.07)	1631 (±191.0)	0.78 (±0.28)	2.37 (± 0.86)	177.9 (±8.28)	0.52 (±0.07)
F2	4.30 (±1.34)	1687 (±493.8)	0.72 (±0.18)	2.55 (± 1.77)	219.1 (±39.38)	0.46 (±0.06)
F3	4.99 (±1.30)	1171 (±119.1)	0.76 (±0.09)	0.00	159.6 (±4.34)	0.53 (±0.03)

As presented in Table 3.1, passive loading resulted in a very low encapsulation efficiency (%EE). This suggests that the incorporation of negatively charged, relatively large, and hydrophilic molecules such as BCG (molar mass = 698.01 g/mol) at a formulation concentration of 12 µmol/mL using Span 60 as the surfactant is limited.

Therefore, BCG is considered an appropriate model compound for investigating how the introduction of a pH gradient (active loading) can improve the encapsulation efficiency of such molecules[1].

Following sonication of the BCG-containing formulations, leakage was observed in all samples. This highlights a limitation of passive loading, where formulation processing and optimisation steps can lead to a reduction in encapsulation efficiency (%EE). The use of probe sonication appears to have a similar impact to bath sonication. For example, Yeo et al. reported a significant decrease in the entrapment efficiency of methylene blue, a hydrophilic compound, after probe sonication at 40%

amplitude for two cycles of 2 minutes with 1-minute intervals. In one formulation, the %EE decreased from 40.1% prior to sonication to 11.6% afterwards[23].

One notable benefit of sonication is its ability to reduce niosomal size. As indicated in Table 3.1, bath sonication led to a significant decrease in particle size and a reduction in the polydispersity index (PDI) across all three formulations ($P < 0.05$).

3.3.3 Investigating Niosomes Ability to Form a pH Gradient Using Bromocresol Green (BCG) and the Consequence of the pH Gradient on the % Encapsulation Efficiency, EE, of BCG

To the best of our knowledge, our publication[1] is the only study to date that has employed active loading of BCG to evaluate the capacity of niosomes to establish and sustain a pH gradient. This approach is feasible because BCG exhibits pH-dependent solubility and ionisation behaviour: it is more water-soluble and exists in a di-anionic form at pH values above 5.4, while at pH values below 3.8 it becomes less soluble and predominantly mono-anionic[125]. When the internal pH of the niosome exceeds 5.4, BCG diffuses into the vesicle and becomes effectively entrapped, as its di-anionic form is unable to permeate back across the hydrophobic bilayer. As a result, this method promotes both the uptake and retention of BCG within the niosomes, as illustrated in Figure 3.3.

In addition, the effect of different co-surfactants on the formation of a pH gradient was examined. Niosomal formulations were prepared using either Span 60 or Span 40 in combination with cholesterol, with or without the inclusion of co-surfactants such as Cremophor RH40, Cremophor ELP, or Solutol HS15.

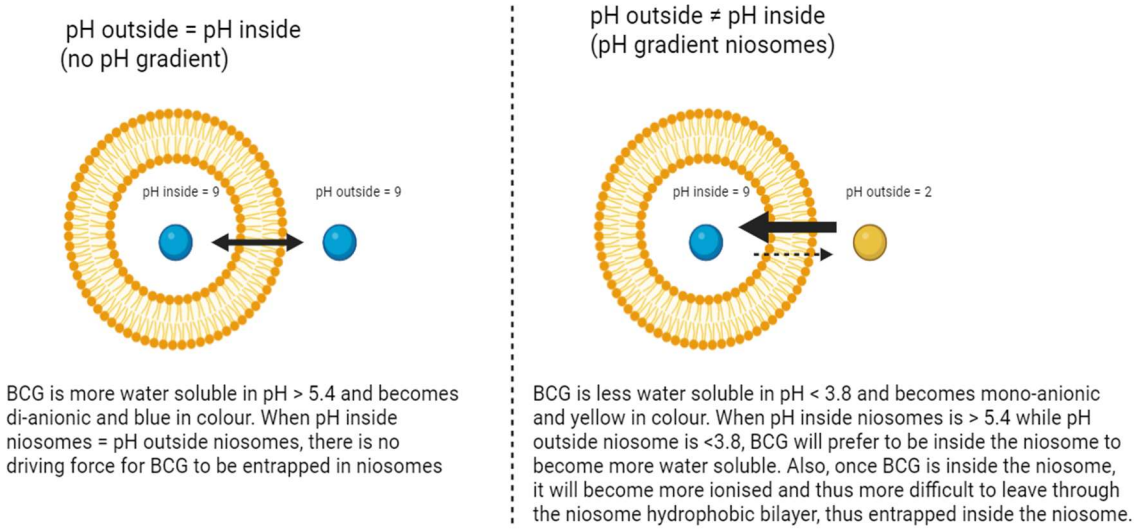

Figure 3.3: Illustrates how a pH gradient can actively load BCG into niosomes.

3.3.3.1 pH Gradient Niosomal Formulations with Span 60 or Span 40 with Cholesterol Only (F4 and F5)

Stable niosomes could not be obtained from formulations containing only Span 60 and cholesterol. Immediately after lowering the pH, the vesicles rapidly aggregated, forming large, visible particles within the suspension (Figure 3.4-A).

A similar outcome was observed with the Span 40–cholesterol formulation (F5), indicating that the aggregation was not specific to Span 60. The issue also persisted when hydrochloric acid was used in place of citric acid, suggesting that the type of acid was not a contributing factor.

To further investigate, the system was tested at a moderately acidic pH of 4.0 in the absence of BCG, to rule out any influence of the indicator or extremely low pH conditions. Aggregation still occurred under these conditions (Figure 3.4-B), confirming that neither BCG nor highly acidic environments were responsible for this behaviour[1].

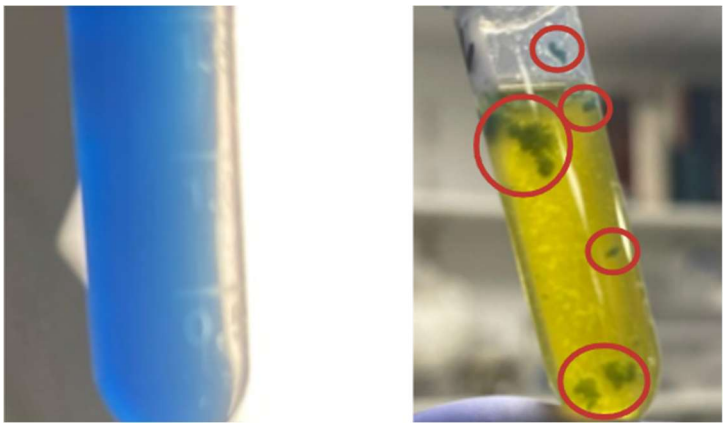

A

B

Figure 3.4: Showing the effect of pH gradient on niosomes without the presence of a co-surfactant. (A)The F4 formulation is produced with Span 60 and cholesterol, without a co-surfactant. F4 was prepared in Trizma buffer (0.1 M, pH 9) containing 0.1 mg/mL BCG (blue suspension - pH 9). The suspension turned yellow after the addition of citric acid (yellow – pH 3.2), where green aggregates (shown in red circles) are clearly visible, indicating that niosomes are not stable without a co-surfactant. (B) On the left, a Span 60-cholesterol niosomal suspension after sonication in trizma buffer (0.1 M, pH 9.0) without BCG. On the right, the same niosomal suspension, after the addition of HCl to reduce the pH to 4.0, showed only aggregates. This indicates that niosomes are unstable under acidic conditions in the absence of co-surfactants, and that this instability is not due to the presence of BCG. The same observation was seen with Span 40-cholesterol niosomes[1].

A comparable finding was reported by Dehaghi et al., who observed that lowering the pH to 6.0 and 5.5 inhibited the formation of niosomes composed of Span 60 and cholesterol[126]. They also highlighted the influence of buffer concentration on niosomal stability. In their study, a diammonium hydrogen phosphate buffer was used to hydrate the surfactant–cholesterol thin film. Niosome formation occurred at pH 6.5

with a buffer concentration of 200 mM; however, increasing the buffer concentration to 250 mM prevented niosome formation at the same pH.

3.3.3.2 Influence of Niosomal Size and Co-surfactant Used on Encapsulation Efficiency Via pH Gradient

The pH gradient loading approach offers several advantages, primarily by improving the encapsulation efficiency (%EE) of nanovesicles[127,128] while avoiding exposure of the drug to potentially degrading conditions, such as elevated temperatures during thin-film hydration or mechanical stress during sonication. Additionally, a higher %EE means that a smaller quantity of niosomes may be required to achieve the desired therapeutic effect. Another benefit is that the drug is introduced after the formation and optimisation of the niosomal system, allowing parameters such as size to be refined beforehand. This helps minimise drug leakage, which can occur during processes like sonication and subsequently reduce %EE[23].

In this study, confirmation of pH gradient formation was based on two key criteria. Firstly, after acidification to a pH below 3.8, the suspension should initially appear yellow, then transition to green or blue. Secondly, an increase in %EE should be observed.

The expected green-blue colour arises from the pH difference between the niosomes' internal and external environments. Specifically, the internal aqueous core maintains a pH above 5.4, while the external medium maintains a pH below 3.8. Under these conditions, BCG appears blue inside the vesicles and yellow in the surrounding solution. The combination of these colours results in a green appearance. At very high encapsulation efficiency, the suspension may appear predominantly blue, reflecting a greater proportion of BCG retained within the niosomes at higher pH.

The inclusion of co-surfactants—such as Cremophor RH40, Cremophor ELP, and Solutol HS-15—improved formulation stability and prevented aggregation following pH reduction. All three co-surfactants supported the formation of niosomes capable of establishing a pH gradient across their membranes. However, their effects on encapsulation efficiency and gradient formation varied. Figure 3.5 illustrates the

observed colour changes after the addition of HCl to formulations F1, F2, and F3 prior to sonication[1].

Figure 3.5: The change that occurred in 3 formulations (from left to right: F1, F2 and F3) after 6 minutes of adding HCl. HCl was added to these formulations before sonication. Note that immediately after adding HCl, the suspension turned yellow; then, it gradually changed in colour to green and blue (from left to right). The %EE reported after 15 minutes of drug loading is F1 = 55.73%, F2 = 41.45%, and F3 = 57.45%[1].

As outlined in the introduction, bromocresol green (BCG) offers two key advantages for studying pH gradients: it provides an immediate visual indication of whether a pH gradient has been established across the niosomal membrane, and changes in solution colour can give an estimate of encapsulation efficiency (%EE).

Following the addition of 0.1 mL of 1 M hydrochloric acid, the suspension is expected to become fully yellow, corresponding to a pH of approximately 1.5. However, as illustrated in Figure 3.5, a pH gradient was successfully established in all three formulations. Formulations F1 and F2 changed to a green colour, whereas F3 appeared blue within 6 minutes of acid addition. Based on this observation, it can be inferred that F3 would exhibit the highest encapsulation efficiency, as indicated by its more intense blue colour. The %EE values are presented in Table 3.2.

Although formulation F3 displayed the most pronounced blue colour in Figure 3.6, its measured encapsulation efficiency was comparable to that of F1 (57.45% versus 55.73%, respectively; p = 0.277; Table 3.2). This outcome may be explained by drug leakage occurring during the centrifugation step used for niosome isolation. The high forces involved in centrifugation, along with the close packing of vesicles during pelleting, can promote vesicle fusion and subsequent drug loss[129,130]. This effect is likely to be more pronounced in F3 due to the higher initial BCG concentration within its niosomes.

This is another advantage of using BCG to study drug loading using the pH gradient technique. The colour change indicated that a significant amount of drug had leaked during the pelleting of formulation F3. The dark blue colour of formulation F3 6 minutes after adding HCl (figure 3.5) suggested that the entrapment efficiency of BCG was almost 100%, whereas only 57.45% was recorded after pelleting.

The relationship between niosomal size and encapsulation efficiency (%EE) was also investigated. Following size reduction by bath sonication, which transformed the vesicles from multilamellar vesicles (MLVs) to large unilamellar vesicles (LUVs), the %EE of the resulting smaller niosomes was evaluated using the pH gradient method. The colour changes observed in the three sonicated formulations after the addition of hydrochloric acid are presented in Figure 3.6. The corresponding data for niosomal size and encapsulation efficiency are summarised in Table 3.2.

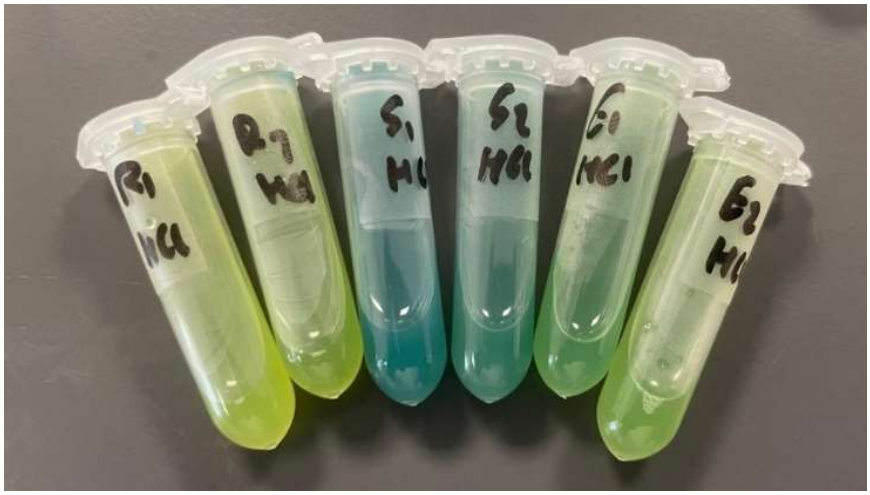

Figure 3.6: The change that occurred in 3 sonicated formulations (from left to right: 2 repeats for F1, two repeats for F3 and two repeats for F2) upon the addition of HCl. HCl was added to these formulations after sonication. The picture was taken 15 minutes after the addition of 0.1 mL of 1 M HCl. %EE reported after sonication after 15minutes of drug loading is F1= 15.57%, F2= 17.81% and F3= 67.86%[1].

As illustrated in Figure 3.6, formulations F1 and F2 appeared more yellow than blue after sonication and 15 minutes of active loading. This suggests that, following size reduction, these formulations may lose the pH gradient more rapidly and show a reduced ability to encapsulate BCG using the pH gradient approach.

Table 3.2: Assessing the effect of niosomes' size on pH-gradient-active drug loading encapsulation efficiency, %EE (n=3). Accordingly, %EE in F1-F3 niosomal formulations was determined before and after sonication.

Formulation	**Before sonication**				**After sonication**			
	Niosomes Size – d nm (±SD)	**PDI** (±SD)	**%EE** 15 min* (±SD)	60 min** (±SD)	**Niosomes Size – d nm** (±SD)	**PDI** (±SD)	**%EE** 15 min* (±SD)	60 min** (±SD)
F1	1631 (±191.0)	0.78 (±0.28)	55.73 (±1.15)	61.80 (±1.53)	177.9 (±8.28)	0.52 (±0.07)	15.57 (±1.72)	15.09 (±2.74)
F2	1687 (±493.8)	0.72 (±0.18)	41.45 (±1.68)	39.83 (±1.74)	219.1 (±39.38)	0.46 (±0.06)	17.81 (±4.48)	13.90 (±2.58)
F3	1171 (±119.1)	0.76 (±0.09)	57.45 (±1.97)	49.47 (±2.52)	159.6 (±4.34)	0.53 (±0.03)	67.86 (±4.26)	42.02 (±4.81)

***%EE measured after 15 minutes of adding HCl**
****%EE measured after 60 minutes of adding HCl**

The data presented in Table 3.2 for the pH gradient following sonication are consistent with the colour changes observed in Figure 3.6. Among the three formulations, F3 exhibited the most intense blue colour after 15 minutes and achieved the highest encapsulation efficiency (%EE) ($p < 0.05$). This finding further highlights the usefulness of BCG as a model indicator, where colour variation can be used as a visual marker of %EE.

It was also observed that, after the addition of hydrochloric acid, larger niosomes (Figure 3.5) appeared more intensely blue compared to smaller niosomes (Figure 3.6). However, the maximum %EE recorded for F3 prior to sonication was lower than that measured after sonication (57.45% versus 67.86%, respectively; $p < 0.05$). This apparent discrepancy can be attributed to the separation method used to distinguish encapsulated from free BCG, namely centrifugation-based pelleting. As discussed earlier, the high forces generated during centrifugation may deform niosomes, leading to drug leakage. Larger vesicles are more susceptible to such damage due to their greater surface area, which increases the likelihood of friction and collision. Consequently, this may have resulted in a lower measured %EE before sonication, despite the stronger blue colour observed in the larger niosomes. This comparison is illustrated in Figure 3.7, where the two size ranges are evaluated directly[1].

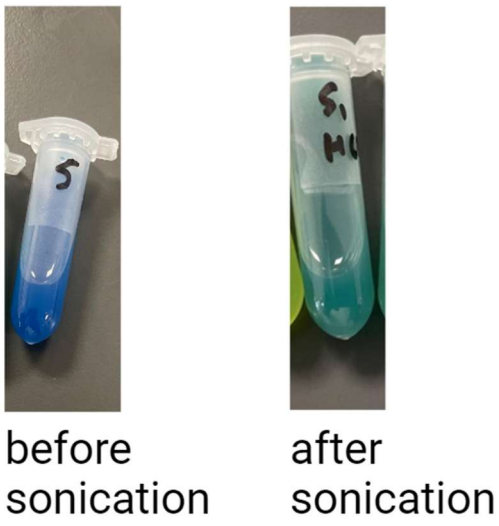

Figure 3.7: Comparison of F3 colour after addition of HCl to the formulation before sonication (left picture) (%EE after 15 minutes of drug loading is 57.45%) and after sonication (right picture) (%EE after 15 minutes of drug loading is 67.86%). The formulation is bluer before sonication but shows lower entrapment efficiency[1].

Based on the observations in Figure 3.7, the greater intensity of the blue colour in formulation F3 before sonication suggests that larger multilamellar vesicles (MLVs) achieved higher encapsulation efficiency (%EE). This can be explained in part by the surface area-to-volume ratio. Similar to liposomes, niosomes can lose their pH gradient, and if this occurs during the active drug-loading phase, the %EE will be reduced[131]. Larger niosomes have a lower surface area-to-volume ratio and a greater internal aqueous volume, which helps them better maintain their internal pH and sustain the pH gradient for a longer period. As a result, the diffusion of hydrogen ions into the vesicles is reduced, allowing more effective maintenance of the gradient and improved drug retention[1].

Another contributing factor relates to the structural differences between niosomes before and after sonication. The thin-film hydration method typically produces multilamellar vesicles, which consist of multiple concentric bilayer structures[132]. This layered arrangement creates additional barriers to the diffusion of hydrogen ions, slowing their movement into the internal compartments. Consequently, the internal pH is better preserved, supporting sustained pH gradients and higher encapsulation efficiency. In addition, the presence of multiple internal compartments provides several regions into which BCG can partition, reducing its exposure to acidic conditions and limiting protonation. The presence of these multilamellar structures was confirmed by light microscopy, as shown in Figure 3.8.

It is also important to note that preliminary findings indicated that sonication of actively loaded MLVs resulted in significant drug loss. For this reason, in the present study, sonication was performed prior to drug loading to convert MLVs into large unilamellar vesicles (LUVs), followed by active loading of BCG. This approach avoids the reduction in encapsulation efficiency that would occur if already loaded MLVs were subjected to sonication.

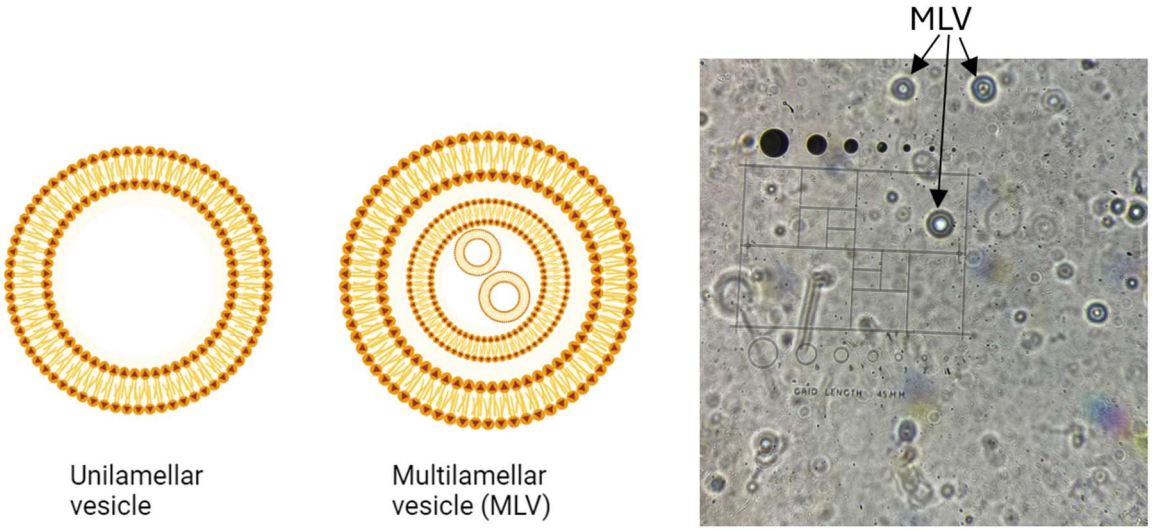

Figure 3.8: Illustrates the structure of and multilamellar vesicles (MLVs) and unilamellar vesicles. Formulation F3 before size reduction using sonication was viewed under the light microscope (100x magnification).

3.3.3.3 Justifying the Influence of Co-surfactants on the Stability of Niosomes During pH Gradient Loading

As discussed earlier, niosomes prepared with only Span 60 or Span 40, in combination with cholesterol, exhibit poor stability under acidic conditions. The surface of these niosomes is rich in hydroxyl (OH) groups, as each Span surfactant molecule contains three hydroxyl groups within its hydrophilic head (Figure 3.9). This results in a surface with a net negative character due to the presence of electronegative oxygen atoms. Under normal conditions, this negative surface charge promotes electrostatic repulsion between vesicles, helping to prevent aggregation and fusion during movement within the suspension.

When the pH of the suspension is reduced, the concentration of hydrogen ions (H^+) increases, which can partially neutralise the negative surface charge of the niosomes. As the surface charge approaches neutrality, the repulsive forces between vesicles diminish. Consequently, when niosomes collide, they are more likely to adhere and merge, leading to aggregation. This explanation is supported by observations that niosomes tend to redisperse when pH is increased, and prolonged exposure to acidic conditions (approximately 1 hour) results in irreversible aggregation.

The inclusion of co-surfactants enhances niosome stability in acidic environments by reducing vesicle fusion and creating a protective surface barrier. As illustrated in Figure 3.9, these co-surfactants insert their hydrophobic tails into the niosomal bilayer alongside the Span surfactants. The hydrophobic chains of Cremophor RH 40, Cremophor ELP, and Solutol HS-15 each contain approximately 17 carbon atoms, which is comparable to the chain length of Span 60. Their hydrophilic head groups extend outward from the niosome surface, forming a hydrated layer that contributes to steric stabilisation. The size of this hydrophilic region varies depending on the co-surfactant. Specifically, Cremophor RH 40 contains around 40 polyethylene glycol units in its head group, Cremophor ELP contains approximately 35, and Solutol HS-15 contains about 15 polyethylene glycol units[1,46].

The data presented in Table 3.2 indicate that the combination of Solutol HS-15 with Span 60 and cholesterol provides superior drug encapsulation using the pH gradient method compared with Cremophor RH40 and Cremophor ELP. This improved performance may be explained by the relatively smaller size of Solutol HS-15 and its structural compatibility with Span 60, as illustrated in Figure 3.9. In particular, Solutol HS-15 possesses a single hydrophobic chain containing 17 carbon atoms, similar to Span 60, which likely facilitates better integration within the niosomal bilayer membrane[1].

Cremophor RH40 and Cremophor ELP each contain three hydrophobic chains, which may disrupt the niosomal bilayer due to limited compatibility with Span surfactants, such as Span 60, which has only a single hydrophobic tail. Furthermore, their relatively large molecular sizes and high molar masses (approximately 2700 g/mol for Cremophor RH40 and 2500 g/mol for Cremophor ELP)[46] are significantly greater than that of Span 60 (430.62 g/mol)[133]. This difference may reduce their ability to integrate effectively within the bilayer, potentially leading to decreased membrane stability.

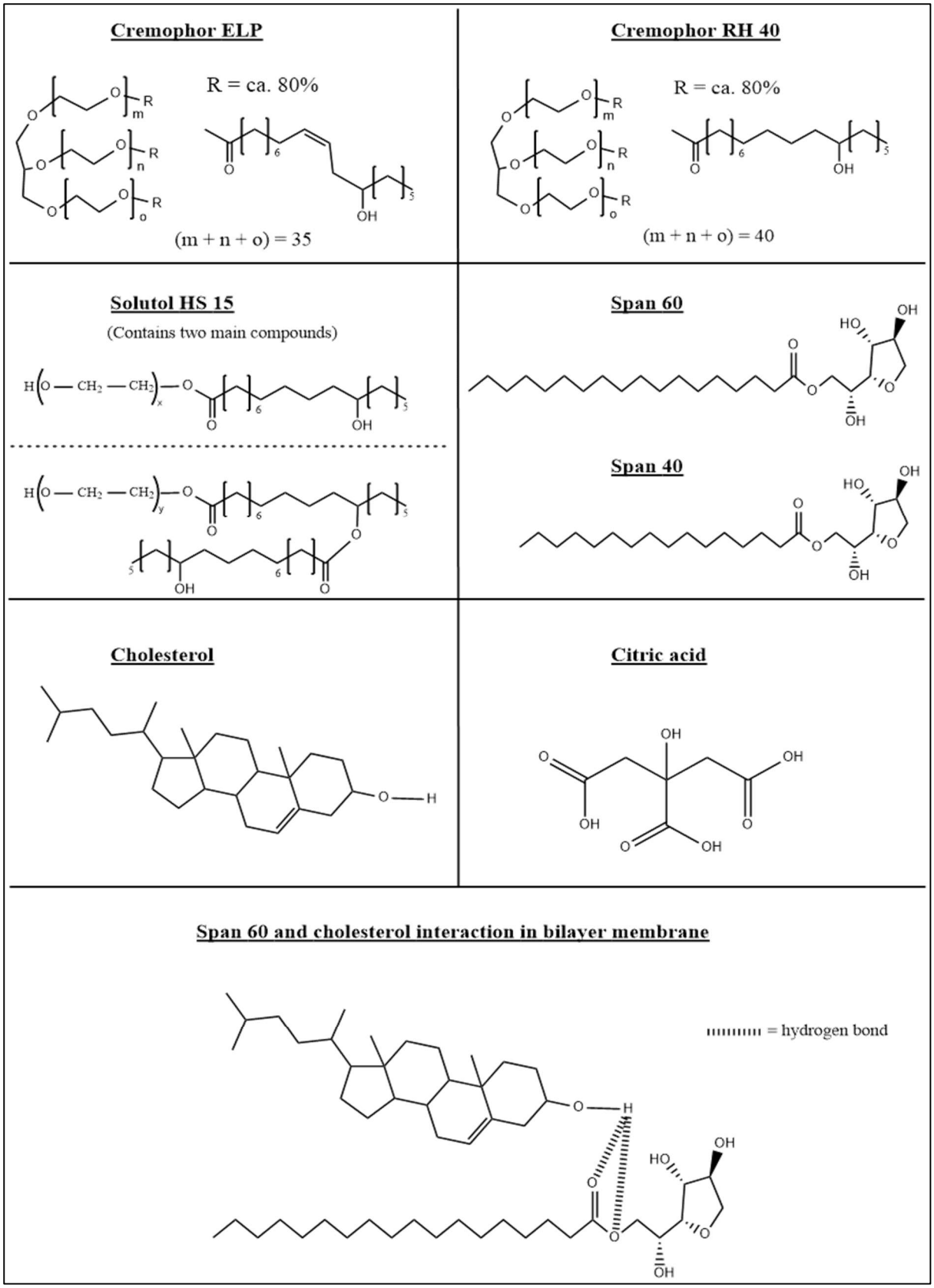

Figure 3.9: Structure of co-surfactants (Cremophor ELP, Cremophor RH40, Solutol HS15), main surfactants (Span 60, Span 40), cholesterol and citric acid. The figure also illustrates the interaction between Span 60 and cholesterol in niosomes[35]. Note

that one hydrogen atom cannot form hydrogen bonds with two oxygen atoms at the same time. However, this figure illustrates that the oxygen atoms with which the hydrogen atom can form hydrogen bonds are one at a time. All structures were generated using ChemDraw 22.2.0.

3.3.3.4 Fourier Transform Infrared Spectroscopy (FT-IR) Analysis of Niosomes

FT-IR can study interactions between ingredients in a mixture by detecting changes in the vibrational spectra of chemical bonds when they absorb infrared (IR) radiation. The purpose of this experiment is to study the interaction between Span 60 and the different co-surfactants (Cremophor RH 40, Cremophor ELP and solutol HS-15) using FT-IR.

Figure 3.10 below shows three graphs. Each graph contains the absorbance of each ingredient used in the formulation of niosomes. It also shows the absorbance of the lyophilised niosomes, which contain all the ingredients combined in niosome form. The purpose is to compare the absorbance of the individual ingredients with that of the combined sample to detect absorbance changes that could indicate interactions.

In conclusion, no noticeable changes were observed in the graphs that could indicate major interactions between Span 60 and Solutol HS-15 over Cremophor RH40 or Cremophor ELP to explain why Span 60 and Solutol HS-15 form better membranes that can maintain a pH gradient. In the absence of such interactions, the rational explanation for why Span 60 forms better membranes for maintaining a pH gradient is related to the structural compatibility between Span 60 and Solutol HS-15 over Cremophor RH40 and Cremophor ELP, as explained in the previous section (section 3.3.3.3). Span 60 and Solutol HS-15 can form a tighter membrane due to structural compatibility, while Span 60 is less compatible with Cremophor co-surfactants, resulting in the presence of pores in the membrane which reduce the membrane ability to maintain pH gradient.

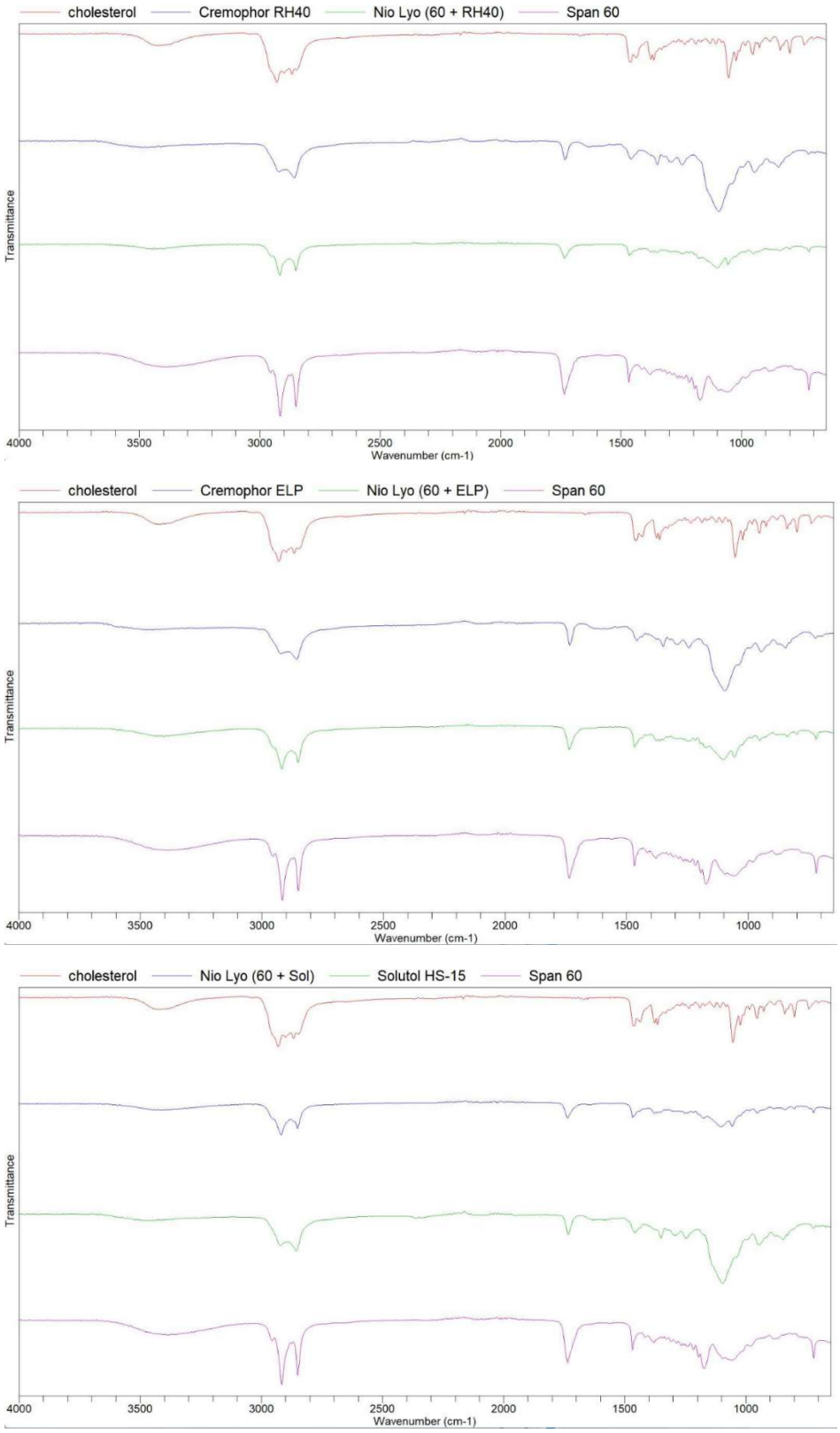

Figure 3.10: FT-IR graphs of surfactants (Span 60) co-surfactant (Cremophor RH 40, Cremophor ELP and Solutol HS-15 and cholesterol with lyophilised form of the niosomal formulations: Nio Lyo (60 + RH40) is the lyophilised F1-IR formulation, Nio Lyo (60 + ELP) is the lyophilised F2-IR formulation, and Nio Lyo (60 + sol) is the lyophilised F3-IR formulation (table 2.9).

3.3.3.5 Maintaining the pH Gradient: Niosomes vs Co-surfactants

To confirm that pH gradient formation is specifically associated with niosome formation, rather than the formation of alternative structures such as micelles from co-surfactants, formulation F3 was prepared by directly dispersing the components in water without using the thin-film hydration method, followed by bath sonication. Upon addition of hydrochloric acid, the suspension turned yellow immediately and did not exhibit the characteristic green colour (Figure 3.11), indicating that a pH gradient was not established under these conditions.

Figure 3.11: Cholesterol, Span 60, Solutol HS15 added to water and sonicated with BCG (0.1mg/mL) after the addition of HCl (0.1 mL of 1 M). The formed suspension changed and stayed yellow.

3.3.3.6 Addition of BCG and Active Loading it into Optimised Niosomes

In many situations, achieving high encapsulation efficiency using passive loading requires elevated concentrations of niosomal components, which may increase the risk of adverse effects upon administration. For instance, pegylated doxorubicin liposomes are known to cause a dose-limiting toxicity, palmar–plantar erythrodysesthesia, which is associated with liposome accumulation in skin capillaries[134]. Therefore, increasing the number of nanovesicles beyond what is necessary may lead to enhanced side effects.

Moreover, niosomes produced using the thin-film hydration method are generally large in size[23,45], making them unsuitable for parenteral administration. Efforts to

reduce their size, such as sonication, can lead to significant drug leakage and a subsequent decrease in encapsulation efficiency[23]. Low encapsulation efficiency poses a significant challenge, as it may limit the formulation's ability to deliver an effective therapeutic dose[1].

Another limitation of passive loading is that the drug may be exposed to harsh conditions that can lead to degradation, particularly for temperature-sensitive compounds. For example, hydration of a thin film composed of Span 60 must be carried out above its gel–fluid transition temperature[16], which is approximately 53 °C[135]. Certain drugs are unstable at elevated temperatures and may degrade when maintained in aqueous environments under such conditions. This is especially relevant for compounds containing ester functional groups, which are susceptible to hydrolysis[1,136].

To address these limitations, the feasibility of introducing BCG after niosome formation and optimisation was explored. This approach helps minimise drug exposure to harsh conditions and reduces the likelihood of degradation. In formulation F6, BCG was added after the sonication step, followed by hydrochloric acid to initiate active loading. The corresponding results are presented in Table 3.3.

Table 3.3: Measuring niosome size, PDI and %EE of BCG in four niosomal formulations (F6-F9), (n=3). BCG was added after the niosomes were formulated and sonicated. Formulations F6 and F8 contain span 60, while formulations F7 and F9 contain span 40. pH gradient was achieved in formulations F6 and F7 by the addition of HCl, while in formulations F8 and F9, it was achieved by adding citric acid[1].

Formulation code	**Niosomes Size – d nm** (±SD)	**PDI** (±SD)	**%EE**	
			15 min* (±SD)	60 min** (±SD)
F6	147.8 (±6.30)	0.39 (±0.04)	68.59 (±0.70)	34.61 (±2.97)
F7	226.9 (±16.08)	0.37 (±0.04)	53.30 (±2.88)	28.53 (±7.91)
F8	147.8 (±6.30)	0.39 (±0.04)	24.18 (±5.56)	29.63 (±3.95)
F9	226.9 (±16.08)	0.37 (±0.04)	14.86 (±0.56)	24.34 (±3.04)

***%EE measured after 15 minutes of adding the acid**
**** %EE measured after 60 minutes of adding the acid**

As shown in Table 3.3, the encapsulation efficiency (%EE) of BCG in formulation F6 was comparable to that of F3 after sonication (68.59% versus 67.86%, respectively, after 15 minutes of loading). This indicates that introducing the drug after formulation optimisation does not adversely affect %EE. Therefore, adding the drug at a later stage should be considered, as it minimises exposure to harsh processing conditions, such as those encountered during thin-film hydration, and reduces the risk of drug degradation.

3.3.3.7 Span 60 vs Span 40 as Main surfactants

Span 40 is a non-ionic surfactant with a structure comparable to that of Span 60, but with a shorter hydrophobic chain (15 carbon atoms compared with 17 in Span 60; Figure 3.9). It also has a lower phase transition temperature (42 °C versus 53 °C)[137] and a smaller molar mass (402.57 g/mol compared with 430.62 g/mol)[133,138].

The influence of the differing physical properties of Span 40 and Span 60 on encapsulation efficiency and niosome size during pH gradient loading of BCG was investigated. In a similar approach to formulation F6, BCG was introduced into formulation F7 after sonication, followed by the addition of hydrochloric acid to initiate active loading. The results are presented in Table 3.3.

Comparison of F7 and F6 indicates that niosomes prepared with Span 60 exhibit a greater capacity to encapsulate BCG via the pH gradient method than those prepared with Span 40. This observation can be interpreted in light of findings from liposomal systems, where lipids with higher phase transition temperatures (Tm) are more effective at maintaining pH gradients[139]. A similar principle appears to apply to surfactant-based niosomes. Additionally, the longer hydrophobic chain of Span 60 contributes to the formation of a thicker, more robust bilayer, providing a stronger barrier and allowing the pH gradient to be sustained for a longer period. Since the pH gradient is the primary driving force for BCG encapsulation, maintaining this gradient for a prolonged period improves encapsulation efficiency. Consistent with behaviour observed in liposomes, the loss of the pH gradient is associated with a marked reduction in %EE[131].

3.3.3.8 Influence of various buffers on BCG encapsulation efficiency

a. Acid Buffer Changing

The use of a weak acid in place of hydrochloric acid was also investigated to determine whether a milder pH reduction could produce a more stable pH gradient and thereby improve encapsulation efficiency. For this purpose, a 0.25 M citric acid solution was evaluated in both Span 40 and Span 60 formulations. Formulations F8 and F9 were prepared in the same manner as F6 and F7, respectively, except that 0.5 mL of 0.25 M citric acid was added instead of 0.1 mL of 1 M hydrochloric acid to adjust the external pH to 3.2. The results are summarised in Table 3.3[1].

The addition of citric acid led to the appearance of a green colour, as shown in Figure 3.12-A, indicating the formation of a pH gradient. However, after 15 minutes, the formulations treated with hydrochloric acid appeared more blue-green than those treated with citric acid, suggesting a higher encapsulation efficiency with hydrochloric acid. This indicates that hydrochloric acid is more effective in rapidly establishing a pH gradient.

Despite this, citric acid demonstrated a greater ability to maintain the pH gradient over time. As illustrated in Figure 3.12-B, after 60 minutes, formulations treated with hydrochloric acid lost the pH gradient and turned completely yellow, whereas those treated with citric acid retained their green colour. This observation is consistent with the encapsulation efficiency data in Table 3.3, where formulations containing hydrochloric acid showed high %EE at 15 minutes but a significant decrease after one hour ($P < 0.05$). In contrast, formulations prepared with citric acid exhibited an increase in %EE over time, with higher values recorded after one hour than after 15 minutes[1].

A B

Figure 3.12: In figure 3.12-A, the F6 formulation after 15 minutes of adding HCl (left Eppendorf) and the F8 formulation after 15 minutes of adding citric acid (right Eppendorf). %EE after 15 minutes for F6 is 68.59% and for F8 is 14.86%. In figure 3.12-B, F6 (left Eppendorf) and F8 (right Eppendorf) formulation after 60 minutes of adding HCl (left Eppendorf) and citric acid (right Eppendorf). %EE after 60 minutes drug loading under pH gradient for F6 is 34.61% and for F8 is 29.63%[1].

This behaviour can be attributed to the buffering capacity of citric acid, which releases hydrogen ions more gradually compared to hydrochloric acid, a strong acid that dissociates completely in aqueous solution[140,141]. In addition, citric acid is highly water-soluble and possesses three dissociation constants (pKa values of 3.15, 4.78, and 6.40) corresponding to its carboxylic acid groups[140]. At an external pH of approximately 3.5, citric acid exists predominantly in its ionised form[140]. Because it remains largely ionised and hydrophilic, citric acid is less able to permeate the niosomal bilayer and therefore remains primarily in the external medium. In contrast, hydrochloric acid establishes a steeper initial pH gradient, promoting a more rapid influx of BCG into the niosomes and resulting in higher encapsulation efficiency after 15 minutes. Based on these findings, 0.25 M citric acid is less effective than hydrochloric acid for loading BCG into niosomes.

A further theoretical consideration in favour of using hydrochloric acid rather than citric acid concerns potential chemical interactions. Citric acid contains three carboxylic acid groups, while Span surfactants possess three secondary alcohol groups (Figure 3.9), creating the possibility of ester formation through esterification reactions[140]. Similarly, cholesterol and Solutol HS-15 also contain alcohol functional groups that could react

with the carboxylic acid groups of citric acid. The impact of such reactions on the stability of pH-gradient niosomes composed of Span 60, cholesterol, and Solutol HS-15 remains unclear, and the safety profile of any resulting esterified products is unknown.

In addition, drugs containing alcohol functional groups may also undergo esterification in the presence of citric acid. Such chemical modification could alter the drug's structure, potentially affecting its encapsulation efficiency and its ability to interact with its intended biological target. Furthermore, the toxicity of any newly formed derivatives would be uncertain, further raising concerns about their use.

b. Alkaline Buffer Changing

The effect of altering the alkaline buffer was also investigated. In formulations F10 and F11, HEPES buffer (0.1 M, pH 8.0) was used in place of Trizma buffer. To establish a pH gradient, 0.1 mL of 1 M hydrochloric acid was added to 1 mL of F10, while 0.5 mL of 0.25 M citric acid was added to 1 mL of F11, reducing the external pH to 2.8 and 3.36, respectively. The results are presented in Table 3.4.

Table 3.4: F10 and F11 size, PDI and %EE using pH gradient (n=3). F10 and F11 were prepared in HEPES buffer (0.1M, pH 8.0) instead of trizma and were sonicated to reduce their size. A pH gradient was created by either adding HCl (F10) or citric acid (F11) to reduce the external pH[1].

Formulation	**Niosomes Size – d nm** (±SD)	**PDI** (±SD)	**%EE (for HCl)**		**%EE (for citric acid)**	
			15 min* (±SD)	60 min** (±SD)	15 min* (±SD)	60 min** (±SD)
F10	283.4 (±34.08)	0.38 (±0.07)	53.19 (±2.90)	72.85 (±2.72)		
F11	283.4 (±34.08)	0.38 (±0.07)			25.92 (±1.29)	31.08 (±1.27)

***%EE measured after 15 minutes of adding HCl/citric acid**
**** %EE measured after 60 minutes of adding HCl/citric acid**

In contrast to Trizma buffer, HEPES buffer demonstrated higher encapsulation efficiency after 1 hour compared to 15 minutes when used with both hydrochloric acid and citric acid. Furthermore, as illustrated in Figure 3.13, HEPES was more effective at sustaining the pH gradient over time. The formulations retained a blue colour after 1 hour, whereas comparable niosomes prepared with Trizma buffer turned yellow, indicating loss of the pH gradient.

Figure 3.13: Right Eppendorf presents F6 (in trizma buffer) after 1 hour of adding HCl. Left Eppendorf indicates F10 (in HEPES buffer) after 1 hour of adding HCl. The % F6 EE after 1 hour of drug loading was 34.61 %, while that of F10 after 1 hour of drug loading was 72.85 %.

To explain this observation, it is important to compare the structural and physicochemical properties of Trizma and HEPES. The molecular structures of both compounds are shown in Figure 3.14, while their key properties are summarised in Table 3.5.

Based on the data in Table 3.5, HEPES appears to be more hydrophilic than Trizma, as indicated by its slightly higher water solubility (70.36 g/100 mL versus 67.8 g/100 mL) and its more negative log Pow value (−3.85 versus −2.31). In addition, HEPES has a significantly larger molar mass (238.30 g/mol compared with 121.14 g/mol), which may reduce its ability to diffuse across the niosomal bilayer.

At the pH conditions used in this study (approximately pH 8–9 inside the niosomes and below 3.5 externally), HEPES is expected to be more ionised within the niosomal core than Trizma (approximately 50% versus 10%) and less ionised in the external medium (approximately 50% versus 100%). This creates a stronger tendency for Trizma to diffuse out of the niosomes into the acidic external environment, where it becomes fully ionised. In contrast, HEPES shows a more balanced degree of ionisation inside and outside the vesicles, resulting in a weaker driving force for its exit from the niosomes.

As buffer molecules diffuse out of the niosomes, the internal environment becomes more vulnerable to pH changes following acid addition, leading to a loss of the pH gradient. Since HEPES is less likely to cross the bilayer and is not strongly driven to leave the vesicles, it is better able to maintain the internal pH and sustain the pH gradient over a longer period.

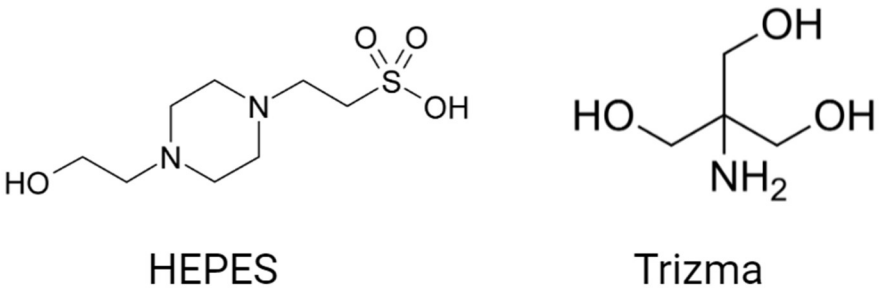

Figure 3.14: Structure of HEPES and trizma compounds

Table 3.5: Comparison between trizma and HEPES physical properties[142–144]

Physical property	HEPES	trizma
Molar mass	238.30 g/mol	121.14 g/mol
Water solubility	70.36 g/100ml	67.80 g/100ml
Number of ionisable functional groups	3	1
pKa of base	7.5 and 3.0	8.1
pKa of acid	Always ionised	N/A
Ionisation state at pH > 5.4	At pH 8 > 50% of HEPES will be negatively charged, and the other 50% will be zwitterionic (neutral)	At pH 9, only ~ 10% will be ionised
Ionisation state at pH < 3.8	At pH 2.8 – 3.36 (i.e. after adding HCl or Citric acid), around 50% of HEPES will be positively charged, and the other 50% will be zwitterionic (neutral)	At pH < 3.8, 100% will be ionised
Partition coefficient Octanol-water (Log Pow)	– 3.85	– 2.31

3.3.3.9 Temperature's Influence on BCG Loading

In liposomal systems, increasing the temperature above the phase transition temperature of the main lipid during pH gradient drug loading has been shown to

enhance encapsulation efficiency by increasing bilayer fluidity[145]. This approach has been widely applied in liposomes, and in the present study, its effect on niosomal membrane properties and the ability to sustain a pH gradient was also investigated.

Formulations F6, F7, F8, and F9 were loaded with BCG using a pH gradient generated by either hydrochloric acid (F6 and F7) or citric acid (F8 and F9) at 40 °C, in order to evaluate the effect of increased temperature on encapsulation efficiency (%EE). Measurements of %EE were taken after 10 and 40 minutes. These time points were selected based on visual observations, as the suspension begins to shift towards a yellow colour after approximately 10 minutes. The results are presented in Table 3.6[1].

Table 3.6: Data of %EE (n=3), size, and PDI of niosomes loaded using pH gradient at 40 °C. This table displays the %EE when drug loading performed at high temperature, 40 °C.

Formulation	**Niosomes size - d nm** (±SD)	**PDI** (±SD)	**%EE (for HCl) at 40 °C**		**%EE (for citric acid) at 40 °C**	
			10 min* (±SD)	40 min** (±SD)	10 min* (±SD)	40 min** (±SD)
F6	147.8 (±6.30)	0.39 (±0.04)	11.19 (±2.49)	2.46 (±1.04)		
F7	226.9 (±16.08)	0.37 (±0.04)	19.59 (±6.77)	4.52 (±5.34)		
F8	147.8 (±6.30)	0.39 (±0.04)			40.44 (±7.79)	23.56 (±1.62)
F9	226.90 (±16.08)	0.37 (±0.04)			26.60 (±1.42)	21.00 (±1.10)

***%EE measured after 10 minutes of adding HCl/citric acid**
**** %EE measured after 40 minutes of adding HCl/citric acid**

It can be concluded from Table 3.6 that increasing the temperature significantly reduces encapsulation efficiency (%EE) during pH gradient loading of niosomes. For formulation F6, the maximum %EE was substantially higher when loading was performed at room temperature (approximately 23 °C) compared to 40 °C (68.59% versus 11.19%, $P < 0.05$). A similar trend was observed for formulation F7 (53.3% versus 19.59%, $P < 0.05$). This reduction in %EE at elevated temperatures can be attributed to increased permeability of the niosomal bilayer, which promotes the loss of the pH gradient. This effect is illustrated in Figure 3.15, where the pH gradient dissipated within 10 minutes following the addition of hydrochloric acid at 40 °C. In contrast, as shown in Figure 3.13-A, the pH gradient was maintained for at least 15

minutes during loading at room temperature (approximately 23 °C). These findings suggest that, unlike many liposomal systems, which require elevated temperatures to enhance drug loading, niosomal formulations composed of Span 60, Solutol HS-15, and cholesterol can achieve effective active loading at room temperature without the need for increased thermal input[1].

Figure 3.15: Figure shows F8 formulation at 40 ºC after 10 minutes of citric acid addition (right Eppendorf) and F6 at 40 ºC after 10 minutes of HCl addition (left Eppendorf). The %EE of F8 after 10 minutes of the drug loading at 40 ºC was 40.44 %, while that of F6 after 10 minutes of the drug loading at 40 ºC was 11.19 %.

Increasing temperature raises the kinetic energy of molecules and enhances the permeability of membrane structures. As a result, elevated temperatures may facilitate the diffusion of Trizma out of the niosomes across the bilayer membrane. This can accelerate the loss of the pH gradient, ultimately leading to a reduction in encapsulation efficiency (%EE)[145].

However, when pH gradient loading was induced using citric acid, a different trend was observed. Increasing the temperature to 40 °C resulted in a higher maximum encapsulation efficiency (%EE) being achieved more quickly than at room temperature (approximately 23 °C). For example, in formulation F8, the %EE reached 40.44% after 10 minutes at 40 °C, whereas at room temperature it reached 29.63% after 60 minutes (Tables 3.3 and 3.6).

Despite this, the pH gradient was more stable at room temperature. Under these conditions, %EE gradually increased from 24.18% at 15 minutes to 29.63% at 60 minutes. In contrast, at 40 °C, %EE decreased over time, from 40.44% at 10 minutes to 23.56% at 40 minutes. These findings suggest that, when using a weak acid, higher temperatures can accelerate drug loading and yield a higher initial %EE, but the pH gradient dissipates more rapidly than at room temperature.

It can also be inferred that, at 40 °C, a weak acid is more effective than a strong acid in maintaining the pH gradient over time, as illustrated in Figure 3.15[1].

3.3.3.10 Cholesterol to Span 60 Different Ratios Effects on Active Loading of BCG and its %EE

Cholesterol plays a key role in regulating the fluidity and permeability of bilayer membranes[145], and its proportion within a formulation can therefore influence encapsulation efficiency (%EE).

In this study, the effect of varying the molar ratio of Span 60 to cholesterol was examined. Formulations F12 and F13 were prepared with different cholesterol-to-Span 60 ratios, as outlined in Table 2.3, and the outcomes of active loading are presented in Table 3.7.

The results indicate that reducing the Span 60-to-cholesterol molar ratio from 45:45 to 35:55 (F12) did not significantly affect the encapsulation efficiency of BCG after 15 minutes (68.59% versus 66.52%). However, this adjustment reduced drug leakage over time. After 60 minutes of exposure to the pH gradient, the %EE of BCG was higher (53.11% compared with 34.61%), suggesting improved retention within the niosomes.

In contrast, increasing the Span 60-to-cholesterol molar ratio from 45:45 to 55:35 (F13) produced the opposite effect. The encapsulation efficiency (%EE) after 15 minutes increased (68.59% compared to 59.77%); however, greater drug leakage was observed over time. After 60 minutes of exposure to the pH gradient, %EE decreased to 34.61% compared with 27.06%, respectively.

Cholesterol is known to play a critical role in modulating membrane rigidity, fluidity, and permeability, all of which influence encapsulation efficiency[16,146]. The findings of this study suggest that reducing cholesterol content to 35% results in a more permeable bilayer, reducing the membrane's ability to retain the drug and maintain the pH gradient over time.

Table 3.7: %EE (n=3), size, and PDI of niosomal formulations with various molar ratios of Span 60 to cholesterol. The molar ratio of Span 60 to cholesterol to solutol HS-15 in F12 formulation was 35:55:10, whereas in F13, it was 55:35:10. The size was measured before and after sonication, however the drug loading was performed on sonicated niosomes.

Formulation	**Before sonication**		**After sonication**		**%EE (for HCl) After sonication**	
	Niosomes size - d nm (±SD)	PDI (±SD)	**Niosomes size - d nm** (±SD)	PDI (±SD)	15 min* (±SD)	60 min** (±SD)
F12	1394 (±68.25)	0.60 (±0.12)	320.9 (±20.64)	0.53 (±0.10)	66.52 (±1.4)	53.11 (±4.86)
F13	1390 (±87.54)	0.45 (±0.16)	148.4 (±9.65)	0.35 (±0.07)	59.77 (±3.46)	27.06 (±6.50)
***%EE measured after 15 minutes of adding HCl ** %EE measured after 60 minutes of adding HCl**						

3.3.3.11 Potential Uses of BCG Niosomes Other Than Studying Active Drug Loading

The use of BCG for pH gradient discovery has proven very successful for studying pH gradients in niosomes and for understanding how different buffers and ingredients affect active drug loading via pH gradients. This discovery can be applied to nanoparticles with an aqueous core surrounded by a membrane, beyond niosomes, such as liposomes, ethosomes, transferosomes, and others.

Moreover, there are potential uses for actively loading BCG into nanovesicles beyond just studying the pH gradient within them. This is based on the following properties of the BCG: it changes colour depending on pH, does not cross the cell membrane in its blue form, is blue at physiological pH, and can be actively loaded into nanovesicles. Below are examples of uses for BCG nanovesicles.

A. Endosomal Trafficking / Intracellular pH Mapping (Proof-of-Concept)

Nanoparticles, such as niosomes and liposomes, can significantly increase the amount of drug that enters the cells. Many drugs, such as nucleic acids like ribonucleic acid (RNA) and deoxyribonucleic acid (DNA), cannot cross cell membranes[147,148]. They rely on the nanocarrier's ability to transport them across the membrane and release them in the cytosol[148,149]. The entry pathway is usually via endocytosis, where the nanocarriers are engulfed by cells and delivered to early endosomes, which mature into late endosomes and eventually lysosomes. The pH of the early endosome is ~6.5, and the pH of the lysosome is ~5.0[149].

In some formulations, endosomal escape must occur before endosomes mature into lysosomes to prevent the degradation of the payload, such as nucleic acids (DNA or RNA). The nanovesicle must be able to break down the endosomal membrane for its payload to escape the endosomes and reach the cytosol intact.

The pH of the cell's cytosol is ~7.2, and the pH of endosomes starts around ~6.5 and decreases to reach ~5.0 when endosomes mature to lysosomes. Also, the pH of the media in which cells are suspended is usually physiological (~7.3–7.4)[149]. In this case, BCG nanovesicles can be used to study their ability to enter cells and escape endosomes.

Given that BCG cannot cross the cell membrane in its ionised blue form, this means that free, unentrapped BCG will not be able to enter cells without the help of a nanocarrier. Based on this, BCG can help study the ability of nanovesicles to cross the membrane and release their payload inside cells. Since a cell's cytosol pH is ~7.2, the presence of blue colour in the cytosol indicates that nanovesicles can successfully cross the cell membrane. Given that BCG can be loaded into niosomes at high concentrations, it should provide a clear blue colour in cells' cytosols, indicating that the nanovesicles have crossed the cells' membranes.

BCG can also be used to determine whether nanovesicles escape from endosomes before reaching lysosomes. The pH inside endosomes is around 6.5, which means BCG will be in its blue form. However, after endosomes become lysosomes, the pH inside lysosomes is around 5.0, meaning that some of the BCG will be di-ionised and in its blue form, while others will be mono-ionised and in its yellow form, producing a green colour. If BCG-loaded nanovesicles produce only blue colour inside cells, this

means that these nanovesicles managed to cross the cell membrane and escape the endosomes. If the nanovesicles produce a green colour inside the cells, it means they could not escape the endosomes and remained there until they reached the lysosome stage.

In addition, this technique can help us study how long endosomes take to mature into lysosomes. For this, a nanovesicle known not to escape endosomes can be loaded with BCG, and colour observation can be used to monitor this. The time it takes for an endosome to mature into a lysosome is from the first appearance of blue colour in the cells until the appearance of green colour. This will provide a valuable, easy method to study the time required for endosomes to develop into lysosomes, and it can also help analyse the effect of nanovesicles on this process.

Different pH indicators can be loaded into endosomes for study. For example, bromocresol purple (BCP), a different pH indicator from BCG, changes colour from yellow to purple over the pH range 5.2 – 6.8[150]. At pH 5.0, which is the pH of lysosomes, BCP will be completely yellow. This can provide a better colour distinction than green when studying endosomes using BCG.

One factor that affects endosomal escape is the lipid used to formulate the liposomes. In liposomes, ionisable lipids, which become ionised at slightly acidic pH, such as pH 5.4 – 6.5, while remaining neutral at physiological pH, can facilitate endosomal escape by becoming ionised inside the endosomes and disrupting the endosome membrane[151]. Actively loading BCG or BCP into liposomes or niosomes with various membrane compositions can potentially help in studying the effect of these membranes on endosomal escape.

B. Studying Factors That Disrupt the Nanovesicles' Membrane and Release the Drug

Targeted drug-delivery nanovesicles are essential for ensuring drug release at a specific site in the body. Several techniques have been studied to encourage drug release in response to external triggers, such as temperature shifts, specific light wavelengths, magnetic fields, or ultrasound waves. This is to ensure that the drug is released at the right place and time to further enhance therapeutic outcomes[26].

Thermosensitive liposomes contain phospholipids with a phase transition temperature (Tm) just above 37 °C, allowing drug release at specific local sites. For example, liposomes rich in DPPC lipid are considered thermosensitive liposomes because the Tm of DPPC is ≈ 41 °C. At temperatures near the phase transition temperatures, the lipid's hydrocarbon chain will become disordered, causing the release of the drug[152]. The site of interest is exposed to focused ultrasound, radiofrequency, or laser photothermal energy to raise its temperature to 40–45 °C for a few minutes. Thermosensitive liposomes, when exposed to elevated temperatures, will release their payload due to membrane disruption[153].

Another technique for raising the temperature of DPPC liposomes is to incorporate superparamagnetic iron oxide nanoparticles (SPIONs) into the aqueous core or to anchor them to the bilayer. An alternating magnetic field can cause the superparamagnetic cores to rotate and spin, generating heat. This will raise the temperature of the nanoparticles' environment to over 42 °C, resulting in rapid drug release[154].

To study the effect of temperature on thermosensitive liposomes, they can be actively loaded with BCG. Then, the liposomes will be exposed to external stimuli that elevate the temperature, and a sufficient amount of excess acid will be added to turn BCG yellow. The membranes of thermosensitive liposomes will become leaky at elevated temperatures near the Tm of the lipid used. The acid will enter the liposomes more quickly than at temperatures below Tm. This will help study the properties of thermosensitive liposomes, such as the amount of DPPC lipid required to form them. It will also examine the effect of other ingredients on the liposomes to ensure drug release does not occur at lower temperatures, such as the addition of specific lipids with a Tm lower than or higher than DPPC and in the case of SPIONs, the effect of their different concentrations and the magnetic field required on membrane leakiness.

3.3.4 Concluding Remarks on the Use of Bromocresol Green in pH Gradient Studies

Using BCG to study pH gradients in niosomes has proven valuable for understanding these gradients. BCG's ability to change colour in response to

different pH environments and its capacity to be actively loaded into niosomes have enabled the study of how various parameters affect the stability of the pH gradient in niosomes and the membrane's ability to actively load drugs.

Through this tool, it was possible to visualise and study how the following factors can influence the stability of pH gradient and active drug loading in niosomes: the type of surfactant used (Span 60 vs. Span 40), the choice of co-surfactant (Solutol HS-15, Cremophor RH 40, or Cremophor ELP), the composition of both alkaline and acidic buffers, the loading temperature and duration, the morphology of the niosomes (MLV vs LUV), and the cholesterol content within the formulation.

These discoveries will aid in understanding how to successfully formulate pH gradient niosomes with therapeutic drugs and how different formulation compositions and buffer choices affect the enhancement of active drug loading into niosomes. In this research, these findings will be applied to improve the entrapment efficiency of the therapeutic agent doxorubicin into niosomes, as discussed in the next chapter. The findings will not be limited to doxorubicin, but they can be applied to enhance the entrapment efficiency of various drugs that can be actively loaded using a pH gradient[1].

Moreover, using BCG in pH-gradient niosomes offers educational advantages. Explaining abstract ideas to students can be challenging. The pH gradient in nanovesicles is an abstract idea that can be made concrete using BCG. The use of BCG to study pH gradients can turn a textbook idea into something students can see, improving their understanding of vesicle behaviour, formulation design, and drug delivery principles in a simple, memorable way. The ingredients used in this experiment are very safe, which means it can be turned into a lab practical with simple steps to help students understand the concept of pH gradients. It will also help students understand that nanovesicles have a membrane separating the aqueous core from the surrounding environment. The same experiment can be conducted on micelles to show how their structure differs from that of bilayered nanovesicles, such as niosomes and liposomes. A famous saying states: “Tell me and I forget, show me and I may remember, involve me and I will understand”. Students can be involved and observe the pH gradient themselves to learn how it works.

Chapter 4: Active Loading of Anticancer Drugs (Doxorubicin and Methotrexate) into Niosomes via pH and Salt Gradient

Part of the data produced form the research and included in this chapter have been open access published[1], cited and referenced in this thesis

Open Access Publication:

Altaee, M.; Faheem, A.M.; Elkordy, A.A. pH Gradient-Driven Loading of Doxorubicin into Niosomes: A Comparative Study Using Bromocresol Green as a Visual Indicator. Pharmaceutics 2025, 17, 862. https://doi.org/10.3390/pharmaceutics17070862

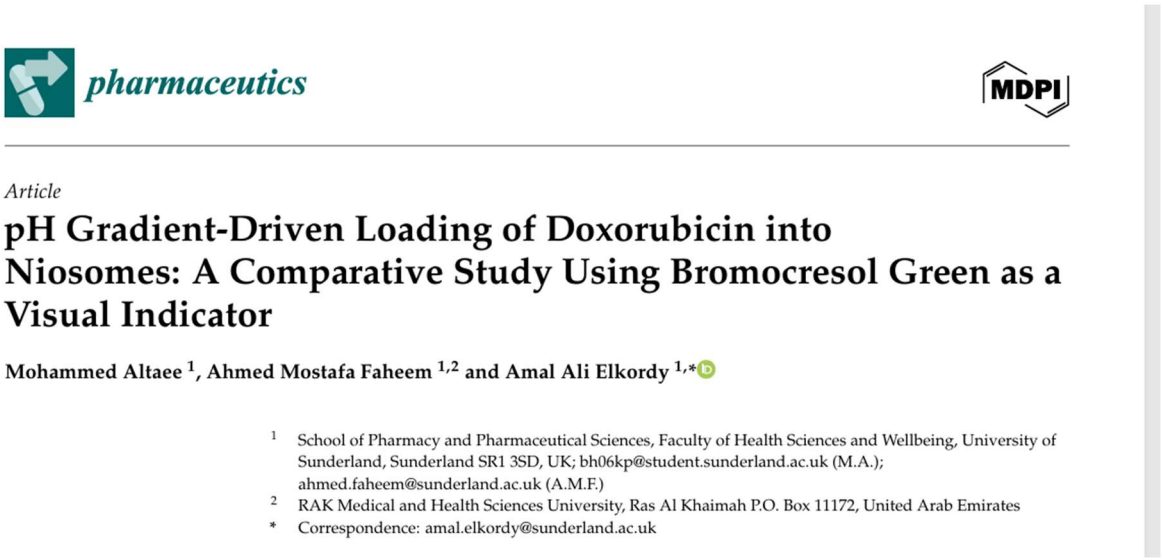

pharmaceutics

MDPI

Article

pH Gradient-Driven Loading of Doxorubicin into Niosomes: A Comparative Study Using Bromocresol Green as a Visual Indicator

Mohammed Altaee [1], Ahmed Mostafa Faheem [1,2] and Amal Ali Elkordy [1,*]

[1] School of Pharmacy and Pharmaceutical Sciences, Faculty of Health Sciences and Wellbeing, University of Sunderland, Sunderland SR1 3SD, UK; bh06kp@student.sunderland.ac.uk (M.A.); ahmed.faheem@sunderland.ac.uk (A.M.F.)
[2] RAK Medical and Health Sciences University, Ras Al Khaimah P.O. Box 11172, United Arab Emirates
* Correspondence: amal.elkordy@sunderland.ac.uk

4.1 Introduction

Given the success of actively loading BCG into niosomes, this chapter will focus on actively loading therapeutic drugs. This chapter will attempt to actively load four therapeutic drugs into niosomes: Doxorubicin, Methotrexate, Ketorolac, and Salicylic acid.

Doxorubicin (figure 1.12) is a cytotoxic drug that belongs to the anthracycline class. Doxorubicin is used in chemotherapy to treat different types of cancers, such as breast cancer, sarcomas, ovarian cancer, and others[155].

One of the drug's mechanisms of action is the generation of reactive oxygen species (ROS) that damage DNA, the cell membrane, and mitochondria. Many healthy cells can deal with ROS through their antioxidant reserves, which help detoxify the cell. However, cardiac cells have a limited antioxidant reserve and are rich in mitochondria. The cardiac cells cannot sufficiently detoxify the ROS generated, leading to mitochondrial damage[156]. For this reason, several measures are taken to protect the heart muscle from doxorubicin, such as limiting the cumulative lifetime dose of anthracyclines. For example, doxorubicin has a cumulative lifetime limit of ~450–550 mg/m², depending on whether the patient has received previous mediastinal radiation[157]. Another solution is to administer dexrazoxane, a prodrug that, upon activation, chelates iron and blunts ROS generated by doxorubicin[158].

A third solution is to encapsulate doxorubicin in liposomes. The capillaries in cancerous tissues are larger and leakier than those in the heart. Doxorubicin-loaded liposomes are around 90 – 150 nm in size (Caelyx® has a size of 90 nm[159] while Myocet® has a size of 150 nm[160]), making them too large to extravasate into heart cells, unlike free doxorubicin (a small molecule), which diffuses readily. Liposomal doxorubicin will reduce the heart's exposure to doxorubicin and concentrate the drug at cancer sites, resulting in markedly reduced myocardial uptake and cardiotoxicity risk versus conventional doxorubicin[161].

The leading challenge researchers faced when incorporating doxorubicin into liposomes was reaching high entrapment efficiency. After research, two main techniques are used by the industry to load doxorubicin into liposomes. The first technique uses a citric acid pH gradient, while the second uses an ammonium sulfate pH and salt gradient (as discussed in section 1.8)[106].

Niosomes are being explored as an alternative nanocarrier for the delivery of doxorubicin in place of liposomal systems. They offer several advantages, including lower manufacturing costs and improved stability. Additionally, unlike lipids used in liposome preparation, which may vary in purity, the components used in niosome formulations are more consistent. For these reasons, niosomes are considered a more attractive option than liposomes for drug delivery applications[16].

Although liposomal systems have been extensively investigated, the application of pH gradient-driven loading in niosomes remains relatively underexplored. Two key knowledge gaps have been identified in this area. First, there is a lack of suitable analytical approaches for evaluating and visualising pH gradients and drug loading within niosomes. To address this, the pH indicator bromocresol green (BCG) was employed in the previous chapter as a model compound for active loading studies. Second, despite ongoing research, no niosomal formulations have yet been translated into marketed medicinal products.

This study, therefore, aims to develop a novel niosomal formulation for doxorubicin delivery, with the objective of enhancing its accumulation in cancer cells by incorporating specific cosurfactants, namely Solutol HS-15 and Cremophor RH 40.

The rationale for choosing these cosurfactants is as follows: Solutol HS-15 and Cremophor RH 40 are known to inhibit P-glycoprotein (P-gp), a glycoprotein that actively pumps cytotoxic drugs out of cancer cells, thereby contributing to multidrug resistance. It reduces intracellular drug accumulation, rendering the cancer more aggressive and challenging to treat[115,116]. Incorporating Solutol HS-15 and Cremophor RH40 can provide the opportunity for a niosomal formulation that reduces side effects by avoiding healthy tissues and is more aggressive against cancer cells expressing P-gp.

Solutol HS-15 is known to exhibit low haemolytic activity, suggesting minimal irritation and toxicity toward healthy cells[115]. In addition, it contains a hydrophilic head group composed of approximately 15 polyethylene glycol (PEG) units, which can help reduce aggregation and enhance the stability of the niosomal membrane.

Cremophor RH 40, which possesses a larger hydrophilic head group containing around 40 PEG units, was selected to investigate the influence of extended PEG chains on the stabilisation of the pH gradient within niosomes. To date, neither of

these co-surfactants has been explored in pH gradient-based niosomal systems, highlighting the novelty of this study.

Methotrexate, ketorolac and salicylic acid are all acidic drugs that have carboxylic acid as functional group, as shown in figures 4.1 A, B and C[162–164]. These three drugs have not been actively loaded before into nanovesicles. This chapter aims to utilise the carboxylic acid functional group and to create pH-gradient niosomes that ionise the carboxylic acid within their cores, while keeping it unionised outside the niosomes. Similar to BCG, the pH outside the niosomes will be acidic, deionising the compounds and allowing them to cross the niosomal membrane. The niosomal core will be alkaline to ionise the compounds and prevent them from leaving the core. This can, in theory, increase their entrapment efficiency within the niosomes.

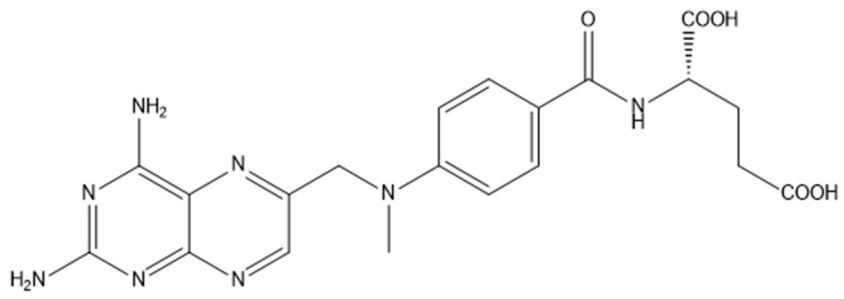

A- Methotrexate

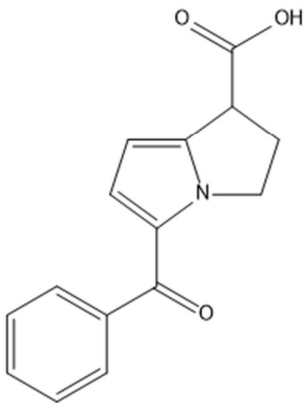

B- Ketorolac

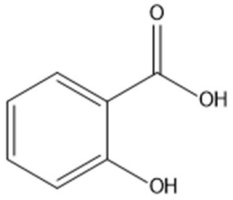

C- Salicylic acid

Figure 4.1: A- Structure of methotrexate. B- Structure of ketorolac. C- Structure of salicylic acid.

In addition to these three drugs having a carboxylic acid functional group, which can, in theory, enhance their entrapment efficiency using active loading, there are other reasons to attempt loading them in niosomes.

Methotrexate is an immunosuppressant and a cytotoxic drug that can be used in inflammatory diseases such as rheumatoid arthritis and malignancies such as breast cancer, ovarian cancer, lung cancer and others. Methotrexate causes side effects by targeting healthy organs, such as immunosuppression, hepatic injury and others[165]. Incorporating chemotherapeutic agents in nanovesicles can reduce side effects. This is because the capillaries in cancerous tissues are larger and leakier than those in healthy tissues. Nanovesicles are usually large (>90 nm), making them too large to extravasate into healthy tissues. However, they can reach malignant tissue due to the nature of their leaky blood vessels. This will accumulate the chemotherapeutic drug in malignant tissues, thereby reducing its side effects[161].

Ketorolac is a non-steroidal anti-inflammatory drug used in postoperative pain[166]. It can also be administered ocularly following an ocular surgery to prevent and reduce inflammation[167]. In the British National Formulary (BNF), a 10mg dose should be administered initially, followed by doses every 4-6 hours. The dose may be increased to every 2 hours, with a maximum dose of 60mg per day[168]. Niosomes are known to have the ability to slow the release of loaded drugs[169,170]. Loading ketorolac into a niosome can slow its release, making it a modified-release formulation that reduces the frequency of administration and controls pain more efficiently. Moreover, ocularly administered niosomes can increase drug retention, sustain drug release, and enhance corneal penetration[53], which can benefit ocular ketorolac formulations.

Salicylic acid can treat various skin conditions, such as acne, and improve the overall skin texture[171]. Niosomes can boost the skin penetration of drugs and sustain the release of drugs in the skin[172]. For this reason, salicylic acid was selected for active loading into niosomes.

4.2 Aim and Objective

This chapter aims to study the active loading of the following therapeutic drugs in niosomes: doxorubicin, methotrexate, ketorolac, and salicylic acid. The formulations will be optimised to obtain a niosomal formulation with the highest entrapment efficiency for each of these drugs. A stability study will also be conducted to ensure that the niosomes are stable after formulation.

Thus, the objective of this chapter is to formulate niosomes to actively load doxorubicin. Different formulations will be tested to achieve good entrapment efficiency and size stability.

4.3 Results and Discussion

4.3.1 Entrapment of Doxorubicin in Niosomes Using a pH Gradient

Doxorubicin has been loaded into liposomal formulations using pH-gradient techniques before. This shows that doxorubicin can be actively loaded into nanovesicles and cross bilayer membranes in its unionised form, reaching the nanovesicle core, where it remains in its ionised form[80].

A commonly used method for loading doxorubicin into nanovesicles involves an ammonium sulfate pH gradient (Figure 1.11)[106]. In this approach, niosomes are initially prepared in an ammonium sulfate buffer, followed by a buffer exchange step to remove ammonium sulfate from the external environment. This process creates a concentration gradient, with a higher concentration of ammonium sulfate inside the niosomal core than in the surrounding medium. Once established, this gradient is expected to be maintained because both ammonium and sulfate ions are unable to readily cross the niosomal bilayer. In this study, the ability of niosomes composed of Span 60, cholesterol, and Solutol HS-15 to generate and sustain an ammonium sulfate gradient was evaluated using doxorubicin as the model drug.

The formulation identified as optimal from the BCG studies consisted of Span 60, cholesterol, and Solutol HS-15 in a molar ratio of 45:45:10 (Table 2.3). Solutol HS-15 was selected as an appropriate component due to its suitability for injectable formulations and its reported ability to inhibit P-glycoprotein (P-gp) in cancer cells.

4.3.1.1 Passive Loading of Doxorubicin into Niosomes

Doxorubicin is a cytotoxic agent administered intravenously, and therefore, the niosomes used for its delivery should be of relatively small size. For this reason, loading during the thin-film hydration stage was not considered, as this method typically produces large vesicles (>1000 nm), as previously shown (Table 3.1). Subsequent size-reduction techniques, such as extrusion or sonication, may result in drug leakage and loss, as discussed earlier. Accordingly, and for comparison, passive loading was evaluated using formulation F1-D (Table 2.4), in which doxorubicin was added to niosomes prepared using Trizma buffer alone, without establishing a pH gradient. Under these conditions, the encapsulation efficiency (%EE) achieved after 1 hour of loading was 36.42% (±1.01).

The reason 36.42% entrapment was achieved could be that, at pH 9.0, doxorubicin is predominantly unionised, given its pKa of 8.4[173]. This will cause doxorubicin to become trapped within the niosomal bilayer membrane. However, the area available for storing hydrophobic drugs in the bilayer is not significant, and for that reason, only 36.42% entrapment occurred.

4.3.1.2 pH Gradient Loading of Doxorubicin into Niosomes

An ammonium sulfate gradient was generated to enable active loading of doxorubicin into niosomes. This was achieved by initially preparing the niosomes in an ammonium sulfate solution, followed by resuspension in either PBS (formulation F2-D) or Trizma buffer (formulation F3-D). Drug loading was then carried out at room temperature (approximately 23 °C) and at an elevated temperature of 60 °C. The results are presented in Table 4.1.

In liposomal systems, ammonium sulfate gradient loading of doxorubicin is typically performed at temperatures above the phase transition temperature of the main lipid. This increases membrane fluidity and permeability, allowing doxorubicin to cross the bilayer more easily and resulting in higher encapsulation efficiency[145].

In niosomal systems, an opposite trend was observed. Increasing the temperature to 60 °C using a water bath resulted in a reduction in encapsulation efficiency when either PBS or Trizma was used as the external buffer. This behaviour is consistent

with the findings in Chapter 3, where elevated temperatures led to disruption of the pH gradient and a corresponding decrease in %EE for BCG-loaded niosomes.

Furthermore, the use of Trizma as the external buffer produced higher encapsulation efficiency than PBS after 1 hour of drug loading (57.14% versus 28.07% at room temperature, approximately 23 °C). This difference may be attributed to the greater ability of Trizma to maintain the pH gradient within niosomes compared with PBS.

4.3.1.3 Effect of Ammonium Sulfate Concentration

“Some literature has used a 120 mM ammonium sulfate buffer in the inner core of liposomes, while other literature has used 250 mM[93,174]. The efficiency of 250 mM ammonium sulfate in niosomes has been tested in formulation F4-D (refer to table 2.4). Drug loading was conducted at RT, ~23 °C, and 60 °C. Results are summarised in table 4.2.

Using 250 mM ammonium sulfate instead of 120 mM did not increase the maximum %EE at either temperature. However, the niosome size increases after 1 hour of drug loading, with niosomes at RT (~23 °C) increasing from 389.1 nm to 543.6 nm. This was not observed at 120 mM ammonium sulfate, as the size did not change significantly after 1 hour of drug loading at room temperature, ~23 °C (360 nm before drug loading vs. 367.3 nm after drug loading). This indicates that using 120 mM ammonium sulfate is preferred over 250 mM, as it reduces the amount needed, improves particle size after loading, and yields a similar maximum %EE.”

Table 4.1: %EE (n=2), Size, and PDI of doxorubicin loaded niosomes at room temperature, RT, ~23 °C, and at 60 °C. The core of niosomes contained 120 mM ammonium sulfate, while the external medium consisted of either PBS (1X, pH 7.4) in formulation F2-D or trizma buffer (0.1 M, pH 9.0) in formulation F3-D[1].

Formulation	**Niosomes' size after sonication and before entrapment** **d nm** (±SD)	**PDI**	**Measuring size and %EE at RT**				**Measuring size and %EE at 60 °C**			
			%EE (after 30min) (±SD)	%EE (after 60min) (±SD)	**Niosomes size - d nm** (±SD) (after 60min)	PDI (after 60min) (±SD)	%EE (after 30min) (±SD)	%EE (after 60min) (±SD)	**Niosomes size - d nm** (±SD) (after 60min)	PDI (after 60min) (±SD)
F2-D	384.6 (± 10.8)	0.45 (± 0.08)	28.07% (± 0.57)	28.07 (± 0.57)	389.2 (± 48.3)	0.35 (± 0.03)	21.55 (± 2.41)	22.33 (± 2.40)	413.0 (± 31.82)	0.36 (± 0.05
F3-D	360.0 (± 2.54)	0.44 (± 0.02)	55.44 (± 2.41)	57.14 (± 3.85)	367.3 (± 18.8)	0.46 (± 0.02)	26.53 (± 3.85)	32.31 (± 4.33)	380.8 (± 10.59)	0.37 (± 0.04)

Table 4.2: Size, PDI and entrapment efficiency (n=2) of niosomal formulation prepared in 250 mM ammonium sulfate buffer, and the drug was loaded at RT, ~23 °C, and 60 °C. The niosomal external buffer consisted of trizma buffer (0.1M, pH 9.0)

Formulation	**Niosomes' size after sonication and before entrapment** **d nm** (±SD)	**PDI**	**Measuring size and %EE at RT**				**Measuring size and %EE at 60 °C**			
			%EE (after 30min) (±SD)	%EE (after 60min) (±SD)	**Niosomes size - d nm** (±SD) (after 60min)	PDI (after 60min) (±SD)	%EE (after 30min) (±SD)	%EE (after 60min) (±SD)	**Niosomes size - d nm** (±SD) (after 60min)	PDI (after 60min) (±SD)
F4-D	389.1 (+/- 30.26)	0.51 (+/- 0.04)	56.76 (± 0.42)	56.47 (± 0)	543.6 (+/- 8.752)	0.44 (+/- 0.06)	25.96 (± 3.44)	27.56 (± 2.98)	693.1 (+/- 29.68)	0.45 (+/- 0.05)

Table 4.3: %EE (n=2), Size, and PDI of niosomal formulation, F5-D formulated with a core containing 120 mM ammonium sulfate and an external buffer of trizma (0.1M, pH 9.0). F5-D prepared with the molar ratio of Span 60 to cholesterol to solutol HS-15 of 55:35:10. Drug loading was taken place with mixing or without mixing as an additional drug loading driving force[1].

Formulation	**Niosomes' size after sonication and before entrapment** **d nm** (±SD)	**PDI**	**Without mixing**				**With mixing**			
			%EE (after 30min) (±SD)	%EE (after 60min) (±SD)	**Niosomes size - d nm** (±SD) (after 60min)	PDI (after 60min) (±SD)	%EE (after 30min) (±SD)	%EE (after 60min) (±SD)	**Niosomes size - d nm** (±SD) (after 60min)	PDI (after 60min) (±SD)
F5-D	473.5 (+/- 37.80)	0.48 (+/- 0.08)	64.93 (± 5.28)	64.93 (± 5.28)	464.8 (+/- 82.76)	0.54 (+/- 0.09)	62.69 (± 2.11)	63.43 (± 3.17)	456.9 (+/- 19.9)	0.50 (+/- 0.03)

4.3.1.4 Effect of Percentage of Cholesterol in the Formulation

As discussed in Chapter 3, the cholesterol content of the formulation plays a key role in determining membrane stability and drug-loading performance. To investigate this further, a modified formulation (F5-D, Table 2.4) was prepared with a reduced cholesterol content of 35%. In addition, the impact of continuous mixing during drug loading, using a magnetic stirrer and stir bar, was evaluated as a potential method to improve encapsulation efficiency (%EE). The resulting data for particle size and %EE following active loading are presented in Table 4.3.

Lowering the cholesterol content to 35% increased encapsulation efficiency compared with formulation F4-D containing 45% cholesterol (64.93% versus 56.47%, respectively; Table 4.2). This change also resulted in a larger niosome size after sonication, measuring 473.5 nm compared with 389.1 nm for F4-D. Despite this increase, the particle size remained stable during drug loading (473.5 nm before loading versus 464.8 nm after 1 hour). These findings indicate that reducing the cholesterol proportion to 35% can enhance %EE without compromising size stability.

Mixing during drug loading did not improve encapsulation efficiency and had no noticeable effect on niosome size. Therefore, incorporating a mixing step during doxorubicin loading does not appear to be necessary (Table 4.3).

Particle size can be controlled through extrusion, as discussed in the following section.

4.3.1.5 Effect of Extrusion on Size and %EE

Extrusion is a common method used to reduce the size of liposomes and niosomes[16,175]. Extrusion is a technique used to control vesicle size by forcing niosomes through a membrane with defined pore dimensions. Under applied pressure, the vesicles pass through small pores (100 nm), resulting in a reduction in their size.

Formulation F5-D (Table 2.4) was selected for this process due to its high encapsulation efficiency. The extruded formulation (F5-D-E) is also detailed in Table 2.4, while the corresponding particle size and encapsulation efficiency (%EE) data are presented in Table 4.4.

Table 4.4: Encapsulation efficiency (n=2), size, PDI of the F5-D-E, which is similar to F5-D in contents, but niosomes were extruded to reduce and unify the size. Drug loading was performed for 1 hour at RT, ~23 °C, and the size was measured after completion of drug loading.

Formulation	**Niosomes' size after extrusion** **d nm** (±SD)	**PDI**	**%EE after 60 min**	**Niosomes size - d nm (±SD) (after 60 min)**	**PDI after 60 min**
F5-D-E	241.1 (+/- 1.65)	0.18 (+/- 0.03)	68.28 (+/- 0.53)	265.8 (+/- 10.05)	0.22 (+/- 0.02)

Sonication is commonly used to reduce niosome size; however, it may not sufficiently improve the polydispersity index (PDI), which can remain relatively high, as observed in Tables 4.1, 4.2, and 4.3. To address this, extrusion was applied, as shown in Table 4.4. This process effectively reduced the particle size to 241.1 nm and improved the formulation's PDI. In addition, encapsulation efficiency (%EE) increased to 68.28%. The particle size remained stable after 1 hour of drug loading, with only a slight increase in PDI (Table 4.4).

The development of doxorubicin-loaded niosomes incorporating Solutol HS-15, a known P-glycoprotein (P-gp) inhibitor, may enhance drug accumulation in cancer cells and represents a potentially cost-effective therapeutic approach.

4.3.2 Comparing the Stability of Span 60 With Span 65 Niosomes

The data in Chapter 3 showed that a stability problem occurred with niosomes during pH gradient formation, indicating that niosomes without a co-surfactant cannot withstand the acidic pH of the environment. The addition of the co-surfactant enhanced niosomal stability and improved pH gradient stability.

The storage stability of niosomes needs to be studied. Span 60 and Span 65 niosomes were prepared in 3 buffers at three different pHs: Trizma (0.1M, pH 9.0), Citric acid (0.1M, pH 4.0) and NaCl (0.9 %w/v, pH 5.5). Stability data were recorded for 1 month or until the niosome size increased significantly. Results are summarised in table 4.5 below.

Table 4.5: Stability study for span 60 and span 65 niosomes with solutol HS-15 prepared in three different buffers: Trizma (0.1M, pH 9.0), NaCl (0.9 %w/v, pH 5.5) and Citric acid (0.1M, pH 4.0). Molar ratio of surfactant to cholesterol to co-surfactant is 45:45:10 in both formulations.

Day of measurement	In trizma				In NaCl				In Citric acid			
	Niosomes Size – d nm (±SD)		**PDI** (±SD)		**Niosomes Size –** d nm (±SD)		**PDI** (±SD)		**Niosomes Size –** d nm (±SD)		**PDI** (±SD)	
	Span 60	**Span 65**	**Span 60**	**Span 65**	**Span 60**	**Span 65**	**Span 60**	**Span 65**	**Span 60**	**Span 65**	**Span 60**	**Span 65**
Day 0	243.0 (±79.50)	246.6 (±37.37)	0.46 (±0.08)	0.35 (±0.04)	413.3 (± 21.65)	252.9 (±1.89)*	0.45 (±0.11)	0.18 (±0.03)	481.4 (±38.14)	339.5 (±26.44)	0.50 (±0.09)	0.30 (±0.07)
Day 1	205.9 (±19.19)	238.0 (±14.26)	0.42 (±0.08)	0.41 (±0.07)	399.1 (±44.36)	275.7 (±5.88)	0.43 (±0.06)	0.26 (±0.04)	496.8 (±27.45)	339.3 (±30.05)	0.43 (±0.14)	0.27 (±0.03)
Day 3	206.1 (±53.75)	237.8 (±23.87)	0.46 (±0.05)	0.50 (±0.09)	691.7 (±45.67)	301.3 (±3.16)	0.53 (±0.12)	0.41 (±0.04)	1121 (±100.8)	382.1 (±14.40)	0.25 (±0.16)	0.52 (±0.15)
Day 7		232.0 (±22.73)		0.47 (±0.07)		330.1 (±7.41)		0.43 (±0.05)		399.4 (±73.32)		0.56 (±0.22)
Day 14		231.3 (±30.36)		0.32 (±0.05)		416.0 (±15.7)		0.36 (±0.02)		744.0 (±174.7)		0.43 (±0.12)
Day 28	216.1 (±25.55)	257.8 (±29.10	0.47 (±0.12)	0.42 (±0.06)								

As can be concluded from table 4.5 above, niosomes prepared with Span 65 produced smaller sizes over time and had better overall stability than niosomes prepared with Span 60, given that the same co-surfactant (Solutol HS-15) is used.

The reason for this is that Span 65 has three hydrophobic tails and an HLB of 2.1, compared to Span 60, which has one hydrophobic tail and an HLB of 4.7 (figure 2.1). The size of niosomes can be affected by the HLB value of the surfactant used. Surfactants with lower HLB form smaller niosomes than surfactants with higher HLB. This is because surfactants with a lower HLB produce niosomes with a lower surface free energy[176]. Surface free energy is the measure of excess energy present on the surface of a material when compared to its bulk. Thus, this is a measure of the energy required to make a new surface. In the case of niosomes, it is governed by the interface between the surfactants forming the niosome membrane and the surrounding aqueous medium. Since surfactants with lower HLB are more hydrophobic, they have less tendency to interact with the aqueous media and thus will produce lower surface free energy. Smaller vesicles have a higher surface area-to-volume ratio, meaning more surfactants are exposed at the interface, thereby increasing the surface free energy. Consequently, small niosomes tend to form larger vesicles to reduce this energy[40]. Niosomes with a lower surface free energy can reduce their size and remain stable because increased hydrophobicity can counteract their tendency to grow, thereby creating smaller niosomes.

The fact that Span 60 niosomes are less stable than Span 65 niosomes does not mean that they are not stable or not suitable for use to entrap doxorubicin. As shown by the stability in Trizma, Span 60 niosomes remained stable for 1 month. This means that with the use of a suitable buffer, Span 60 niosomes can load the drug and stay stable. Moreover, Span 60 niosomes can be lyophilised in future work if suspension stability remains a problem.

Since Span 65 niosomes have proven more stable than Span 60 niosomes (table 4.5), Span 65 niosomes will be further developed to load doxorubicin.

4.3.3 Active Loading of BCG into Span 65 Niosomal Formulations

The ability of Span 65 niosomes to create and maintain a pH gradient has been studied using BCG. Niosomes were formulated using Span 65 and cholesterol with either solutol HS-15 (F14), a mixture of both solutol HS15 and Cremophor RH40 at a

1:1 molar ratio (F15), or Cremophor RH40 (F16) as per table 2.3. HCl was added to the niosomes to establish a pH gradient and initiate active loading of BCG. Results are shown in figure 4.2 below.

(A) (B)

Figure 4.2: Loading of BCG into niosomal formulations containing Span 65 with different co-surfactants (Solutol HS-15 in the formulation on the left, a 1:1 molar mix of Solutol HS-15 and Cremophor RH 40 in the middle formulation and Cremophor RH 40 alone in the formulation on the right). pH gradient was established by adding 0.1 mL of 1M HCl to start active loading of BCG. Figure 4.2 (A) was taken after 15 minutes of active loading, while Figure 4.2 (B) was taken after 1 hour of active loading.

All three Span 65 niosomal formulations successfully created a pH gradient and actively loaded BCG, as shown in figure 4.2, where green colour was produced. However, Span 65 was more compatible with Cremophor RH40 than with solutol HS-15. After 1 hour of pH gradient, niosomes made from Span 65 and Solutol HS-15 lost the pH gradient, and the green colour turned yellow (Figure 4.2-B). In comparison, the presence of Cremophor RH40 in the formulation maintained the pH gradient for 1 hour; after 1 hour, the green colour remained in niosomes containing Cremophor RH40 or Cremophor RH40:Solutol HS-15 (1:1 molar ratio).

Span 65 with Cremophor RH40 was more compatible than Span 60 with Cremophor RH40, yielding a niosomal membrane that maintained a pH gradient for a much longer time. When Span 60 was prepared with Cremophor RH40, the pH gradient was lost within a few minutes (Figure 3.6), and the suspension was ineffective at loading BCG, turning yellow. Moreover, Span 65 with Cremophor RH40 formed a niosomal membrane that more efficiently maintained a pH gradient for a longer

period than Span 60 with Solutol HS-15, where Span 60 and Solutol HS-15 niosomes lost pH gradient within 60 minutes (figure 3.13) while Span 65 and Cremophor RH40 niosomes maintained pH gradient for more than 60 minutes (figure 4.2).

This result supports our theory about the importance of compatibility between the main surfactant (Span 60 or Span 65) and the co-surfactant (Cremophor RH40 vs Solutol HS-15), and its effect on maintaining the pH gradient explained in section 3.3.3.3 of chapter 3. Span 65 was found to be more compatible with Cremophor RH40, while Span 60 was found to be more compatible with Solutol HS-15 to maintain a pH gradient. This concerns the structural compatibility of these ingredients. Span 60 and Solutol HS-15 both have one hydrophobic tail in their structure, while Span 65 and Cremophor RH40 both have three hydrophobic tails in their structure (figure 4.3). This can explain why Cremophor RH40 is more compatible with Span 65 but not with Span 60. Span 65 and Cremophor RH40 can form a niosomal membrane with a denser hydrophobic region, allowing better control of the migration of ions and hydrophilic compounds across the membrane.

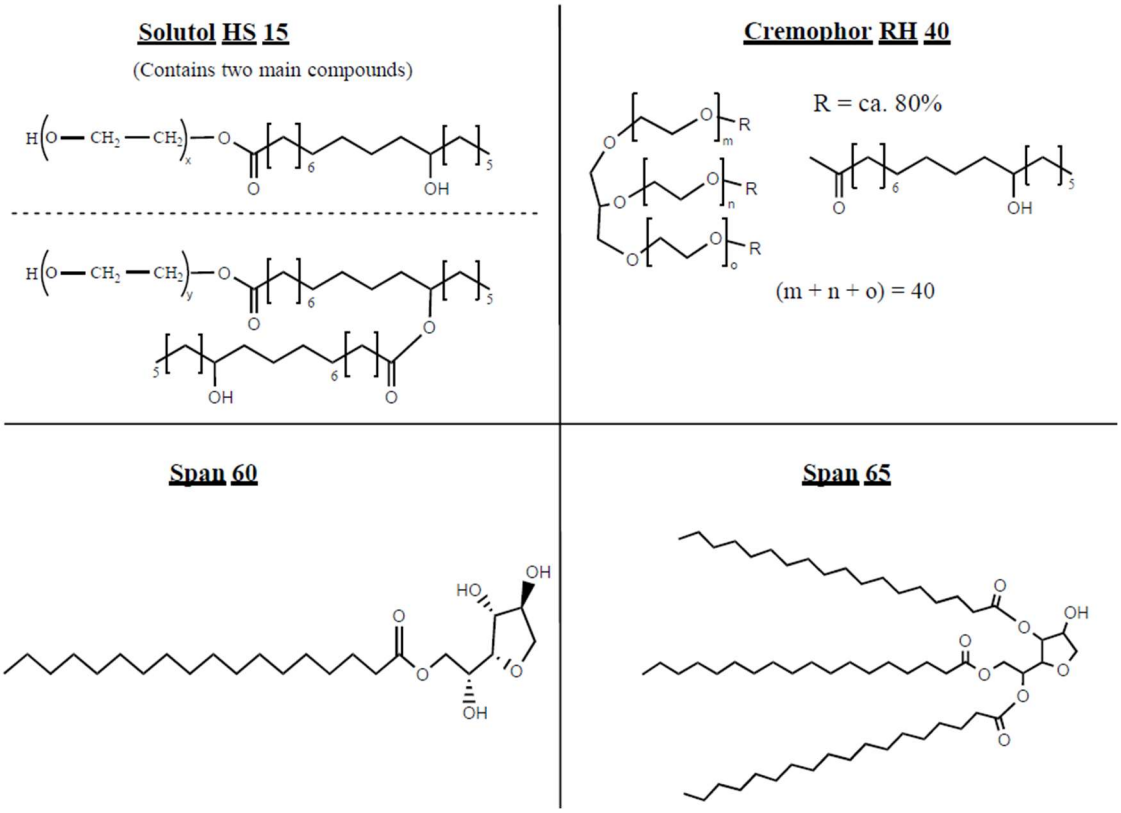

Figure 4.3: Structures of Span 60, Span 65, Solutol HS-15 and Cremophor RH 40.

Another explanation for the compatibility of Cremophor RH40 with Span 65 over Span 60 is that Span 65 can anchor Cremophor RH40 in the niosomal membrane more than Span 60. Span 65 has a bigger molar mass than Span 60 (963.55 g/mol[177] vs 430.6 g/mol) and has three hydrophobic tails compared to one in Span 60. Cremophor RH40 has a very large hydrophilic head (consists of 40 PEG groups) (Figure 4.3). This means it has a strong tendency to partition into aqueous media, which can disrupt the niosomal membrane if it is not firmly anchored within it. Given Span 65 has a bigger molar mass than Span 60 (more than twice) and has three hydrophobic tails, it has a better ability to anchor Cremophor RH 40 in the niosomal membrane than Span 60. Furthermore, the HLB of Cremophor RH40 is 14-16. Span 65 has an HLB of 2.1, while Span 60 has an HLB of 4.7. Cremophor has a high HLB, and Span 65 has a very low HLB. Span 65 has a better ability to balance the HLB of the niosomal membrane system, as very high HLB can disrupt the niosomal membrane without the right additives[24] thereby increasing membrane permeability and preventing the maintenance of the pH gradient.

4.3.4 FTIR Span 65 Formulations

FT-IR has been used to study the interactions between the niosome ingredients to better understand the nature of the interactions between Span 65 and Cremophor RH40, and between Span 65 and Solutol HS-15.

Figure 4.4 below shows the stacked FTIR spectra of the individual ingredients and the spectra of the formulated niosomes. Niosomes were lyophilised to ensure that water peaks did not affect the graph reading.

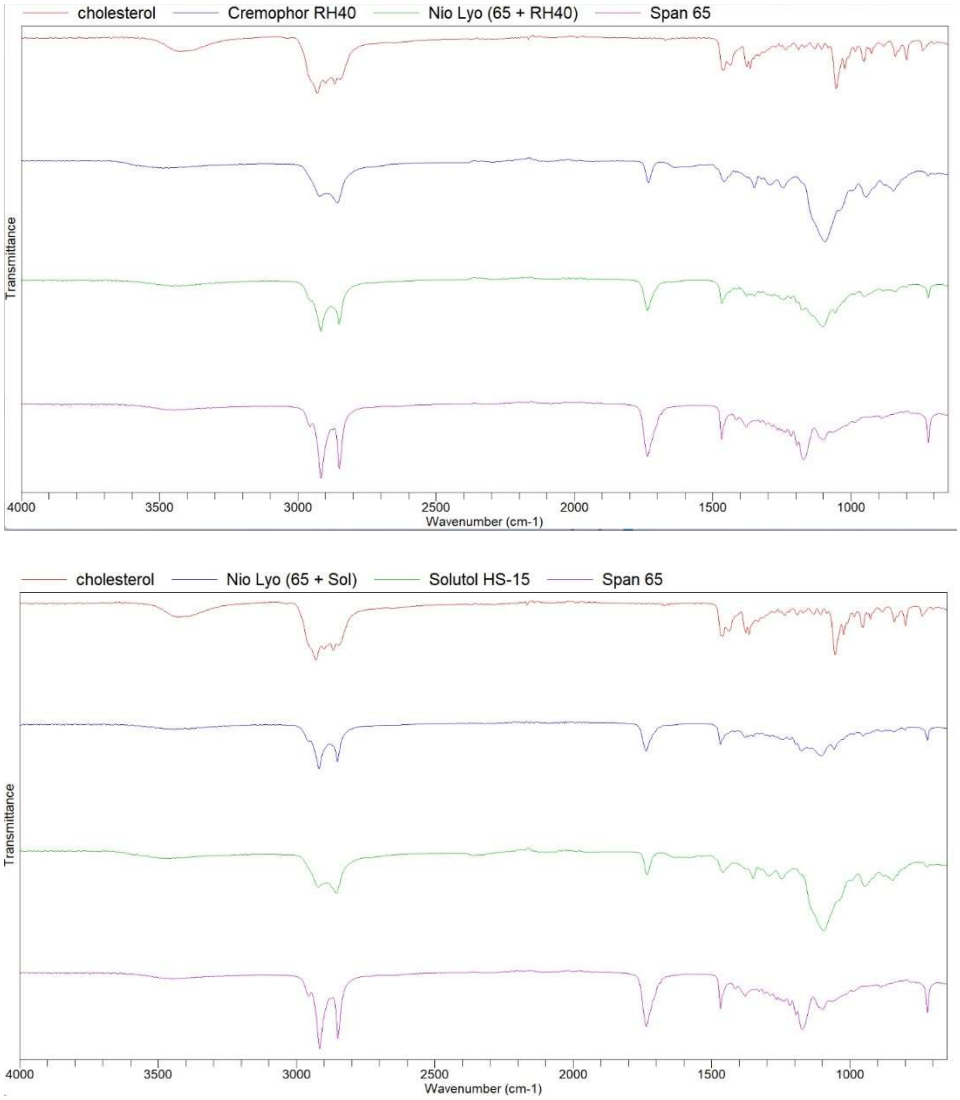

Figure 4.4: FTIR graphs of the individual ingredients and their FTIR spectra after they are formulated into niosomes. Niosomes were lyophilised after formulation. Nio Lyo (65 + RH40) stands for lyophilised niosomes that are composed of Span 65, cholesterol and Cremophor RH40 (molar ratio of 45:45:10, respectively). Nio Lyo (65 + Sol) stands for lyophilised niosomes that are composed of Span 65, cholesterol and Solutol HS-15 (molar ratio of 45:45:10, respectively).

Similar to Span 60 FTIR findings (section 3.3.3.4 and figure 3.10), no significant peak changes were observed in the graphs. This further supports our findings in sections 3.3.3.3 and 3.3.3.4 that Span 65 is compatible with Cremophor RH40 rather than Solutol HS-15 due to shape and size compatibility, rather than a special form of bonding that would have appeared in the FTIR graph. Shape compatibility reduces pore formation in the membrane, thereby prolonging the maintenance of the pH gradient in niosomes.

4.3.5 Zeta Potential of Span 65 Formulations

Malvern, the company that manufactures ZetaSizer instruments, has written a technical note explaining how pH affects the zeta size of nanoparticles[178]. The pH of the environment surrounding the nanoparticles is a significant factor that affects their zeta potential. If the nanoparticle is negatively charged, adding an alkali to the suspension tends to make it more negative by attracting negative ions, such as OH-, to it. Adding an acid to the suspension will neutralise the negative charges by increasing the concentration of H^+ ions around the nanoparticle.

The zeta potential of the four niosomal formulations listed in table 4.6 below has been measured at three pH values (5, 7, and 9). The zeta potential can maintain colloidal stability of the niosomes when it is > 30mv or < -30mv. Table 4.6 below demonstrates that the niosomes' zeta potential is affected by the pH of the media. Neutral and acidic pH values don’t allow the niosomes' zeta potential to reach -30mv. In this case, the colloidal stability will rely on steric stabilisation by the pegylated co-surfactants such as Cremophor RH40 and Solutol HS-15 for both Span 60 and Span 65 niosomes.

Table 4.6: Comparison of zeta potential of Span 60 and Span 65 niosomal formulations with Cremophor RH 40 or Solutol HS-15 at three different pH values (5, 7 and 9)

Niosome formulation	Niosome formulation composition (molar ratio)	Zeta potential (mV)		
		pH 5	pH 7	pH 9
1	Span 60 : solutol HS15 : cholesterol (45:10:45)	-3.13 (±0.39)	-13.31 (±3.51)	-45.17 (±6.02)
2	Span 60 : Cremophor RH 40 : cholesterol (45:10:45)	-2.29 (±0.46)	-7.45 (±1.52)	-35.40 (±2.21)
3	Span 65 : solutol HS15 : cholesterol (45:10:45)	-3.35 (±0.85)	-13.83 (±2.80)	-41.53 (±4.71)
4	Span 65 : Cremophor RH 40 : cholesterol (45:10:45)	-2.89 (±0.51)	-9.09 (±2.00)	-37.80 (±4.62)

4.3.5 Size and Entrapment Efficiency of Span 65 Niosomes

The ability of different combinations of niosomes containing various ratios of Span 65, cholesterol and co-surfactants Solutol HS-15 and/or Cremophor RH40 to entrap doxorubicin using a pH gradient has been studied. Table 2.4 shows four formulations containing Span 65 as the main surfactant (F6-D to F9-D). Moreover, the doxorubicin concentration to be loaded was increased from 0.1mg/mL to 0.5mg/mL (Table 4.7) to study the effect of loading doxorubicin at higher concentrations in more enhanced niosomes.

Table 4.7: Size, PDI and %EE of Span 65 niosomes actively loaded with doxorubicin (0.5 mg/mL). Size was measured after sonication (before the drug was loaded) and after loading the drug.

Formulation	Co-surfactants used (molar percentage of total formulation)	After sonication		After drug loading		%EE
		Niosomes' size d nm (±SD)	PDI (±SD)	Niosomes' size d nm (±SD)	PDI (±SD)	
F6-D	Solutol HS-15 + Cremophor RH40 (10 + 5)	219.6 (± 6.33)	0.25 (±0.05)	275.2 (± 28.01)	0.27 (±0.07)	68.86 (± 1.28)
F7-D	Solutol HS-15 + Cremophor RH40 (5 + 5)	206.8 (± 14.74)	0.24 (±0.07)	242.6 (± 16.81)	0.33 (±0.04)	69.54 (± 2.23)
F8-D	Cremophor RH40 (5)	225.6 (± 3.78)	0.29 (± 0.03)	237.8 (± 10.51)	0.27 (± 0.05)	78.79 (± 2.55)
F9-D	Cremophor RH40 (10)	189.0 (± 17.32)	0.32 (± 0.09)	191.9 (± 12.46)	0.28 (± 0.04)	76.99 (± 5.74)

Formulation F6-D had a size increase during drug loading (275.2 nm vs 219.6 nm). F6-D has solutol HS-15 (10% of formulation) and 5% Cremophor RH40. Removing solutol HS-15 and keeping 5% Cremophor RH40 (as in formulation F8-D) increased entrapment efficiency by ~10% (78.79% vs 68.86%) and reduced the size increase during drug loading (size increase during drug loading was 12.2 nm in F8-D vs 55.6 nm in F6-D). Increasing Cremophor RH40 concentration from 5% to 10% further reduced the niosome size post-production (189 nm vs 225.6 nm) and reduced the size increase during drug loading (2.9 nm vs 12.2 nm). However, it did not improve %EE (76.99% vs 78.79%).

4.3.5.1 Size and Entrapment Efficiency of Span 65 Niosomes vs Span 60 Niosomes

Span 65 produced niosomes with smaller sizes and better PDI values after thin film hydration and sonication than Span 60 niosomes (table 4.7 vs tables 4.1, 4.2 and 4.3). The PDI of Span 60 niosomes was always more than 0.44 after sonication, reaching up to 0.51 for formulation F4-D, while the PDI of Span 65 niosomes was less than 0.33 after sonication.

The niosomes' size was also much smaller in Span 65 niosomes than Span 60, where the Span 60 niosomes always had a size greater than 360 nm after sonication, while Span 65 niosomes had a size less than 226 nm after sonication (table 4.7 vs tables 4.1, 4.2 and 4.3). These results show that Span 65, with or without Solutol HS-15, can produce smaller niosomes with lower PDI than Span 60 niosomes with Solutol HS-15.

4.3.5.2 The Effect of Co-surfactants on Span 65 Niosomes

There were two reasons Solutol HS-15 was included in the niosomal formulation containing Span 65, along with Cremophor RH40 as a co-surfactant. The combination of Solutol HS-15 and Cremophor RH40 did not deteriorate the ability of the niosomes to maintain a pH gradient, as shown from the results of the BCG active loading into these niosomes (figure 4.2). Also, Solutol HS-15 can inhibit P-gp protein. The aim of combining it with Cremophor RH40, which also inhibits P-gp, is to achieve a synergistic effect on inhibiting P-gp.

The results of four formulations were presented in table 4.7. Two formulations were made with Span 65, cholesterol, and only Cremophor RH40 as the co-surfactant, with one containing only 5% Cremophor RH40 (F8-D) and another containing 10% Cremophor RH40 (F9-D). After loading doxorubicin at 0.5 mg/mL, the size of the niosomes did not change, indicating that the niosomes remain stable during drug loading.

When Solutol HS-15 was added to the formulation at a molar percentage of 10% (F6-D) and 5% (F7-D) with Cremophor RH40 being 5% in both formulations, the size of the niosomes after drug loading noticeably increased (Table 4.7), where in formulations F6-D and F7-D, it increased by 55.6 nm and 35.8 nm, respectively. This shows that loading doxorubicin into Span 65 niosomes with Solutol HS-15 can increase niosome size.

Regarding %EE, formulations F8-D and F9-D had higher %EE (78.79% and 76.99%, respectively) than formulations F6-D and F7-D (68.86% and 69.54%, respectively) (Table 4.7). This further indicates that niosomes with Span 65 and Cremophor RH40, without Solutol HS-15, are more efficient at loading doxorubicin and maintain their size after loading.

4.3.6 Factors (Membrane Hydrophobicity and Hydration Buffers) Affecting the Size of Niosomes

In this research, I have established that niosome size is affected by factors such as membrane hydrophobicity and the hydration buffer (Tables 4.1 – 4.5 and 4.7).

The hydrophobicity of the niosomal membrane is affected by the HLB of the surfactant used and the percentage content of cholesterol. In tables 4.2 and 4.3, Formulation F4-D had a total cholesterol concentration of 45% while F5-D had a total cholesterol concentration of 35%. This reduction in cholesterol content has reduced the hydrophobicity of the niosomes and increased their size (389.1nm vs 473.5nm). A similar result was reached by Nowroozi et al., where they changed the percentage content of cholesterol in niosomal formulations containing Span 60 and Brij72 and observed that increasing cholesterol concentration in the formulation from 20 to 40% resulted in decreasing particle size by 27% and 20% of Span 60 and Brij 72 niosomes (578 ± 5.79 *vs.* 466 ± 7.32 and 591 ± 5.08 *vs.* 426 ± 2.18 respectively)[64]. However, they also found that niosomes made with the Tween 60 surfactant did not

exhibit a significant change in particle size when the cholesterol content was increased from 20 to 40%. This is because Tween 60 surfactant has a very high HLB (14.9), and increasing the cholesterol content could not significantly reduce the niosome size.

Agawal et al. have also concluded that the more hydrophobic the niosomal membrane, the smaller the niosomes produced[176]. Niosomes were prepared with Span 20, Span 40, Span 60, Span 80, or Span 85, and they have HLB values of 8.6, 6.7, 4.7, 4.3, and 1.8, respectively. It was found that the niosome size decreased as HLB decreased.

In our study, niosomes made of Span 65, which has an HLB of 2.1, produced smaller niosomes than those made with Span 60. For example, formulation F6-D, which is made with Span 65, had a size of 219.6 nm, while formulation F4-D, which is made with Span 60, had a size of 389.1 nm after sonication. Both formulations were prepared at the same surfactant-to-cholesterol-to-co-surfactant ratio, hydrated with the same buffer, and sonicated for the same duration. A similar finding was reported by Hadjipour et al., who formulated niosomes with Span 60 or Span 65, cholesterol, and Cremophor RH40[29]. Span 65 produced niosomes smaller than those produced by Span 60. For example, a formulation consisting of Span 65, cholesterol, and Cremophor RH 40 at a molar ratio of 45:45:10 produced niosomes with a diameter of 206.7 nm, while the same formulation with Span 60 instead of Span 65 produced niosomes with a diameter of 743.6 nm.

The reason behind this observation is the fact that niosomes with lower HLB and more hydrophobicity have lower surface free energy and tend to produce smaller niosomes, as explained in detail in section 4.3.2 above.

Formulation F9-D produced niosomes with the smallest size after bath sonication (189 nm with PDI of 0.32). However, the ideal formulation should have a size below 150 nm and a PDI below 0.2 to allow sterilisation by filtration through a 220 nm filter[179]. In addition, the niosomes are pegylated with Cremophor RH40, which should reduce opsonisation by white blood cells and increase their half-lives in the blood[180].

To reduce the size of the niosomes to less than 150 nm, the extrusion technique is usually applied. However, in this research, the microfluidic technique will be used in

Chapter 5 to produce niosomes with a small size (<150 nm) and a uniform size distribution (PDI < 0.2). To our knowledge, this technique has not been used before to prepare niosomes for active loading of drugs and, therefore, has not been used to load doxorubicin actively. The microfluidic technique will be explored in the next chapter (Chapter 5).

4.3.7 Attempting Active Loading of Methotrexate in Niosomes

Methotrexate structure comprises three sections: pteridine ring, p-aminobenzoic acid and glutamyl residues (figure 4.5). It also has three ionisable functional groups: two carboxylic acid groups located in the glutamyl residue region and nitrogen 1 situated in the pteridine ring. The ionisation of these functional groups is determined by their pKa and the pH of their surrounding media. The literature does not agree on a specific pKa value for the two carboxylic acid groups because different methods are used to calculate pKa values. Moreover, the pKa of one of the carboxylic acids is higher than that of the second one. However, it is also debatable which of the two carboxylic acids has the higher pKa. Some literatures state it is the one attached to the alpha carbon, while other literature states it is the one attached to the gamma carbon[181].

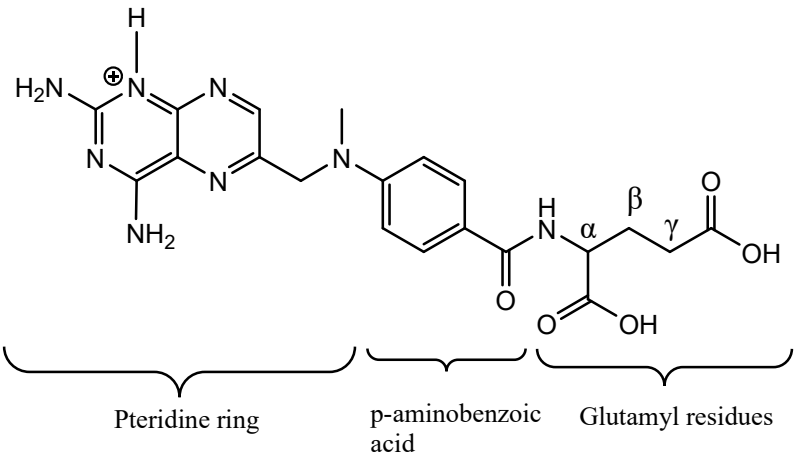

Figure 4.5: Structure of methotrexate

The pKa of the carboxylic acid with a lower pKa is estimated to be between 2.89 and 3.8. The pKa of the second carboxylic acid is estimated at approximately 4.11. The

pKa of the nitrogen in the pteridine ring was reported to be between 5.7 and 6.6. A recent article has reported the pKa value of the two carboxylic acids to be 2.68 for the carboxylic acid attached to the alpha carbon and 4.11 for the carboxylic acid attached to the gamma carbon, while the pKa of the nitrogen is 5.48[181].

Based on this information, methotrexate will be loaded into the niosomes at pH 8.0 (using HEPES) or 9.0 (using Trizma), and the pH outside the niosomes will be reduced to 1.0 and 4.0 as per table 2.5.

4.3.7.1 Behaviour of Methotrexate in Solution at Different pH Values

Methotrexate has different solubilities at different pHs, mainly due to its ionisation state. At pH above 7, methotrexate is di-anionic, with both carboxylic acids ionised and the nitrogen largely neutral, based on their pKa values stated before. As pH decreases, methotrexate becomes less ionised as pH approaches the pKa of the carboxylic acids. For example, at pH 4.0, the nitrogen will be mainly ionised, and the first carboxylic acid with pKa of 2.68 will also be mainly ionised. However, the second carboxylic acid (pKa 4.11) will be mainly unionised. This results in a compound with one positive charge and one negative charge, giving a neutral overall charge. Neutral compounds have poor water solubility and good lipid solubility. At pH 1, both carboxylic acids will be neutral. At the same time, the nitrogen atom in the pteridine ring (pKa 5.48) will be positively charged, giving methotrexate a net positive charge, which can increase the solubility.

It was observed that at pH 8.0 (0.1 M HEPES), methotrexate dissolved completely in the buffer at a concentration of 1 mg/mL. However, when the pH was reduced to 4.0, the buffer became turbid, indicating the precipitation of methotrexate. At pH 1.0 (0.1M HCl), methotrexate, similar to that at pH 8.0, completely dissolved in the solution. This observation supports the pKa values stated for methotrexate. Methotrexate will be loaded into niosomes at pH 4.0, where it will be predominantly in its zwitterionic state. The core of the niosomes will be at pH 8.0 (if HEPES is used) or pH 9.0 (if Trizma is used).

4.3.7.2 Active Loading of Methotrexate into Niosomes

Span 60 niosomes were prepared in Trizma (F1-MKS) or HEPES (F2-MKS) buffer (table 2.5). To initiate active loading, 0.1 mL of a 1 mg/mL methotrexate solution (dissolved in Trizma, pH 9.0) was added to 0.9mL of the niosomal suspension. Then, HCl (1M) solution was added to decrease the pH of the suspension to 1.5 in case of niosomes prepared in Trizma, 2.8 in case of niosomes prepared in HEPES or 4.0 in both cases.

In both niosomes prepared in Trizma and niosomes prepared in HEPES, methotrexate was not actively loaded into the niosomes. Around 99% of the drug remained outside the niosomes. The main reason for this observation was that, when a drug precipitates, it can no longer cross the niosomal membrane. This is because the drug aggregates into a large solid particle that cannot diffuse through the niosomal membrane.

Elevating the temperature of a solution can increase the solubility of a drug. To overcome the solubility problem, the temperature of the niosomal suspension with methotrexate was elevated before the acid was added. Two temperatures have been tested: one (40 °C) below the phase-transition temperature of Span 60, and the other (60 °C) above it.

Increasing the temperature did not seem to improve the entrapment efficiency of methotrexate into the niosomes, where the percentage of unentrapped drug remained around 99%.

A different approach, known as Solvent-Assisted Active Loading Technology (SALT), was tested to actively load methotrexate. Researchers developed this technique to actively load poorly water-soluble compounds into liposomes. The method includes adding a water-miscible solvent at a low %v/v (~5 vol%) to increase the solubility of the poorly water-soluble drug. The researchers have succeeded in actively loading Gambogic Acid (GA), an acidic, poorly water-soluble drug. The technique works by adding a water miscible solvent that can also solubilise the drug of interest. In the case of GA, eight solvents were tested and found to increase solubility and thus the active loading entrapment efficiency. These solvents are Dimethyl sulfoxide (DMSO), dimethylformamide (DMF), ethanol, methanol, acetonitrile, acetone, 1,4-dioxane, and N-Methylpyrrolidone. The researchers found that the solvent plays another vital role,

in addition to enhancing the drug's solubility. It was found that the solvent can also increase liposomal membrane permeability, thereby promoting complete drug loading. However, the solvent concentration added must not exceed the limit that causes membrane instability[182].

DMSO has been used at 5 %v/v to enhance drug loading in the formulations. DMSO was chosen because methotrexate is highly soluble in it, reaching 70 mg/mL[183]. Moreover, the drug loading was tested at room temperature (~23 °C) and at 40 °C.

The solubility of methotrexate improved with the addition of DMSO. However, drug loading remained low, with the percentage of unentrapped drug remaining around 98%.

4.3.7.3 Interpreting Methotrexate Actively Loaded into Niosomes Results

To actively load drugs into the nanovesicles, three conditions must be met. The drug of interest must have an ionisable functional group, there must be a pH or ion gradient that encourages the drug to reside in the nanovesicle core rather than in the surrounding medium, and the drug must be able to cross the nanovesicle bilayer membrane from the medium outside the niosomes to reside inside the niosome and get trapped.

From BCG experiments, it was shown that niosomes can actively load drugs when the inside is alkaline and the outside is acidic. This concludes that the main issue with methotrexate is that it cannot diffuse through the niosomal membrane and thus cannot reach the niosomal core. This could be mainly due to the molecule's polarity, even at low pH. Methotrexate has a high hydrogen-bonding capacity and a high polar surface area. Methotrexate has 6 hydrogen-bond donors and 12 hydrogen-bond acceptors[184]. These can interact with the hydroxyl groups on the surface of the niosomes formed by the Span 60 surfactant and the solutol HS-15 co-surfactant. This results in low drug permeability through bilayer membranes. Moreover, methotrexate, in vivo, enters cells through transporters such as RFC1/SLC19A1 (Reduced Folate Carrier), PCFT/SLC46A1 (Proton-Coupled Folate Transporter), and Folate Receptors (FRα/FRβ), not through passive diffusion[185].

4.3.8 Loading Attempts for Ketorolac and Salicylic Acid

Two other acidic drugs have also been used to load niosomes via a pH gradient: ketorolac and salicylic acid. Both ketorolac and salicylic acid have one carboxylic acid functional group, with pKa values of 3.5[186] and 2.98[187], respectively, and they were attempted to be actively loaded into F1-MKS and F2-MKS formulations.

To start pH gradient loading, 0.1 mL of 1mg/mL of ketorolac and 0.1 mL of 1mg/mL of salicylic acid (both dissolved in trizma buffer with a trizma concentration of 0.1 M and pH 9.0) were individually added to F1-MKS and F2-MKS formulations. Upon pH reduction to 1.5 and 2.8 for formulations F1-MKS and F2-MKS, respectively, using 1 M HCl solution, ketorolac precipitated, while salicylic acid did not precipitate. Entrapment efficiency in both cases was negligible, where 99% of both drugs remained unloaded in their respective formulations.

Like methotrexate, drug loading was also attempted at 40 °C and 60 °C for both drugs, but entrapment efficiency did not improve. Finally, DMSO was added to the solution, as with methotrexate, to enhance the solubility of these two drugs at acidic pH, but this attempt also did not improve entrapment efficiency.

Since, regardless of all attempts to enhance entrapment efficiency and since entrapment efficiency remained near zero, a conclusion has been reached that methotrexate, ketorolac and salicylic acid cannot cross the Span 60, Solutol HS-15 and cholesterol niosomal membrane even in their least ionised states. For this reason, they cannot be actively loaded into the niosomes.

4.4 Concluding Remarks on the Active Loading of Drugs (Doxorubicin, Methotrexate, Ketorolac and Salicylic Acid) into Niosomes

The Span 60 niosomal formulation containing cholesterol and solutol HS-15 was shown to efficiently maintain the pH gradient and actively load doxorubicin. Doxorubicin was loaded at an efficiency of 68.28% at 0.1mg/mL. With the extrusion technique, span 60 niosomes reached a diameter of 241.1 nm.

The effect of the surfactant's HLB on niosome size and stability was also studied. Span 65 with a lower HLB than Span 60 produced smaller and more stable niosomes because they produced niosomes with lower surface free energy.

Span 65 niosomes containing Cremophor RH 40, Solutol HS-15, or a mixture of both were formulated, and pH gradient ability and active drug loading were tested using BCG. Cremophor RH 40 is more compatible with Span 65 than Solutol HS-15, where a pH gradient was maintained for longer with Cremophor RH 40 than with Solutol HS-15. The combination of both Cremophor RH 40 and Solutol HS-15 did not affect the ability of the niosomes to maintain the pH gradient when compared to Cremophor RH 40 alone.

Span 65 niosomes containing cholesterol and Cremophor RH 40 as a co-surfactant have been shown to efficiently load doxorubicin, with entrapment efficiency reaching 78.79% when Cremophor RH40 concentration was 5% and 76.99% when Cremophor RH 40 concentration was 10%. It should be noted that as the concentration of Cremophor RH40 in the formulation increases, the niosome size decreases, where increasing the Cremophor RH 40 content from 5 to 10 molar % decreased the niosome size from 225.6 nm to 189.0 nm.

Span 65 niosomal formulation with Cremophor RH 40 is a promising formulation for actively loading doxorubicin, producing a small size and high entrapment efficiency. For this reason, it will be used in the microfluidic technique in the next chapter to produce niosomes with controlled size, suitable for injection formulations.

Acidic drugs, methotrexate, ketorolac and salicylic acid, were also attempted to be actively loaded using Span 60 niosomal formulation containing cholesterol and Solutol HS-15. However, active loading was not achieved primarily because these drugs were unable to cross the niosomal membrane.

In the next chapter, the data collected from this chapter will be used to formulate niosomes using the microfluidic technique to actively load doxorubicin. The microfluidic technique has not been used to produce pH gradient niosomes. This technique is also promising, as it can reduce the number of steps required to produce a batch and yield niosomes with controlled size and size distribution.

Chapter 5 – Enhancing Niosomal Size and Size Distribution Using Microfluidic Technique for Industrial Scale

5.1 Introduction

Several methods have been developed for the manufacture of niosomes and liposomes. However, for a product to reach the market, the manufacturer must demonstrate that its manufacturing process will produce batches that are identical and exhibit no batch-to-batch variation. As a result, pharmaceutical companies face several challenges in translating research into bedside practice[24,122].

The marketed liposomal formulations of doxorubicin are manufactured using techniques that result in large particle sizes and high PDI values. Manufacturers then use extrusion to reduce and uniform the liposomes' size before loading the drug. This can result in variations in lipid content across formulations and potentially affect the amount of doxorubicin loaded if not carefully monitored[122,188].

The first Food and Drug Administration (FDA) approved nanomedicine was Doxil/Caelyx in 1995. The formulation comprises the fully hydrogenated phosphatidylcholine (HSPC) phospholipid, cholesterol, and a pegylated lipid to maintain liposome stability and stealth within the body, thereby prolonging circulation time and preventing early opsonisation by white blood cells. Despite the success of the Doxil/Caelyx formulation in the market, nanovesicle development in general faces several challenges, including complex regulatory requirements, reproducibility, and practicality for scale-up. As a result, the manufacturing of nanovesicles can be challenging. For example, after 16 years of Doxil's FDA approval, the FDA issued an injunction against the Doxil manufacturer in 2011 for failing to comply with Good Manufacturing Practice (GMP) requirements. As a result, a supply shortage occurred, and in 2013, the FDA approved a generic liposomal doxorubicin (Lipodox) to address it[93].

However, the manufacture of generic liposomes has been considered a time-consuming, multistep process that requires at least 5 days to produce a batch[93]. It involves manufacturing liposomes and then extruding them to obtain a small, uniform size. The liposomes are then buffer-exchanged to generate a pH and ammonium sulfate gradient. The liposomes are then mixed with doxorubicin to initiate loading[80]. Another buffer exchange is then performed to suspend the loaded liposomes in a suitable buffer for long-term storage.

This has become an area of research focused on developing a method to reduce the number of steps required to manufacture nanovesicles while simultaneously producing small, uniform nanovesicles. The microfluidic technique is one answer to this challenge[93]. The microfluidic technique involves mixing two solvents — an organic phase containing lipids/surfactants and an aqueous phase containing the buffer — in a microchannel. This technique can produce small niosomes with low PDI values[189]. As a result, the extrusion step will not be required, as niosomes will be small and uniform. This can reduce the number of steps necessary to make nanovesicles, thereby reducing the time needed to manufacture a batch.

The extrusion step requires the nanovesicles to pass through a membrane filter contained within a stainless-steel container several times, then through tubes until collected. This can increase the risk of product loss. Moreover, extrusion requires raising the temperature of the niosomal/liposomal suspension above the phase transition temperature. This can increase energy consumption and production cost[54].

However, the microfluidic technique controls the amount of lipids and surfactants present in the formulation. This is controlled by adjusting the amount of lipids and surfactants dissolved in the organic phase and the ratio of the organic phase to the aqueous phase, which the instrument accurately measures. In a single step, nanovesicles are produced at a known lipid and surfactant concentration and have a uniform, small size[190].

One challenge in microfluidic formulations is the presence of organic solvents in the final formulation, which require purification[191]. However, in pH-gradient doxorubicin nanovesicles, buffer exchange is necessary to create an ammonium sulfate pH gradient. During buffer exchange, a pH gradient will be generated and the organic solvent removed, yielding pH-gradient nanovesicles free of organic solvent. As a result, nanovesicles produced using the microfluidic technique will not require any extra manufacturing steps. Figure 5.1 below explains the difference between conventional methods for manufacturing liposomes for doxorubicin loading and how the microfluidic technique can save time and reduce the number of steps required.

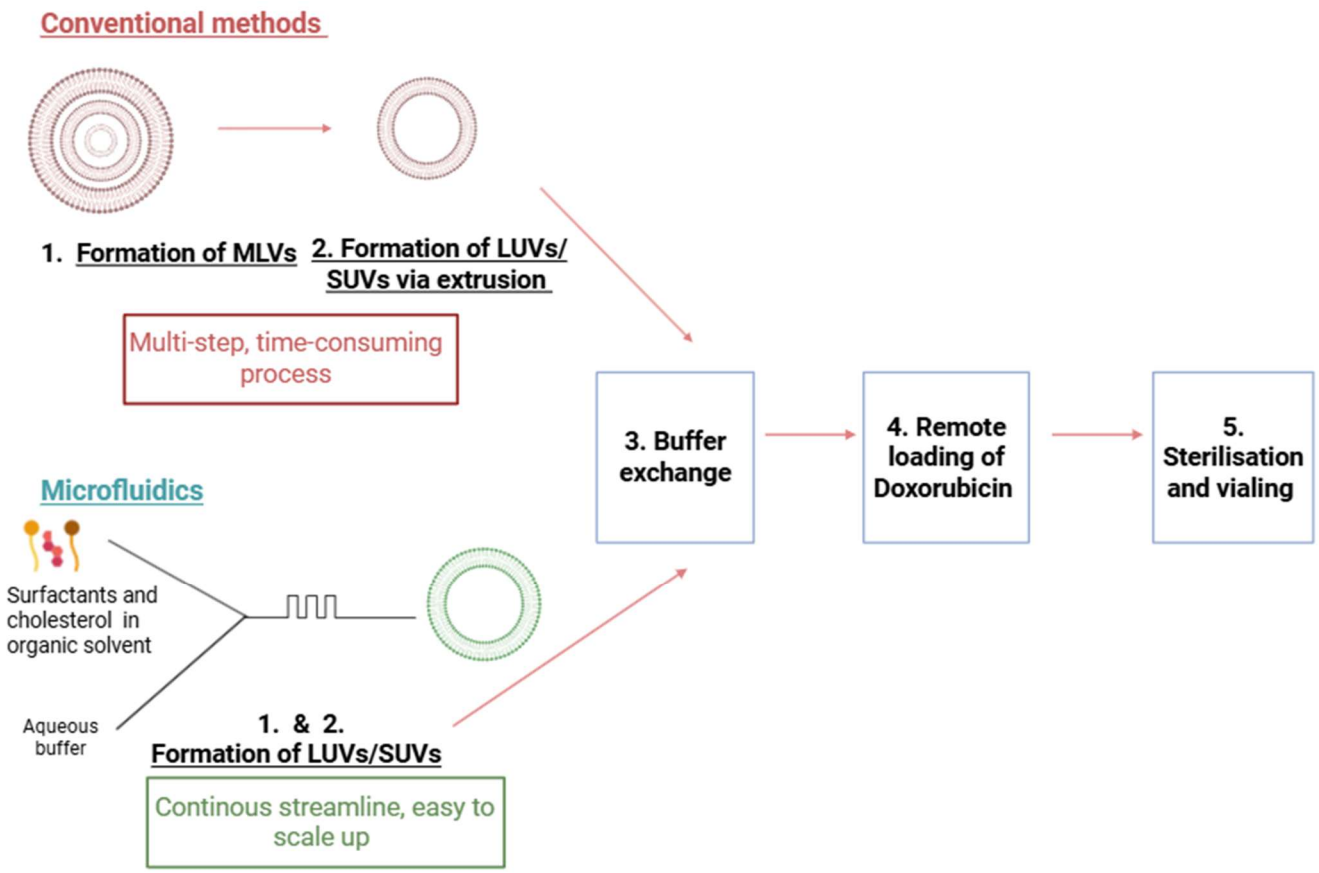

Figure 5.1: Doxorubicin nanovesicle manufactured using a conventional method vs using the microfluidic technique.

The microfluidic technique has been used to manufacture niosomes. However, to our knowledge, no peer-reviewed article has used microfluidics to manufacture niosomes for pH-gradient applications. This work will be the first of its kind, in which I will manufacture niosomes using microfluidic techniques and actively load doxorubicin into the formulation using an ammonium sulfate pH gradient. This will help to avoid many of the challenges that liposomes faced. This technique will also address the size challenges encountered in the previous chapter to achieve small, uniform niosomes (monodisperse).

Several factors need to be considered when manufacturing niosomes using the microfluidic technique. The organic solvent being used to dissolve the lipids and surfactants, the total flow rate, flow rate ratio, the temperature at which the aqueous phase and organic phase mix in the micromixer, the surfactants and lipids used and their ratio, and the nature of the buffer used[56].

Different organic solvents can produce different nanovesicle sizes. Typical organic solvents include ethanol, isopropanol, and methanol. The total flow rate is the rate at which the aqueous and organic phases mix in the micromixer and is measured in mL/min. The flow rate ratio is the ratio of the organic phase to the aqueous phase. The more organic phase is used, the higher the lipid/surfactant concentration in the formulation will be[56]. The temperature can be used for lipids with high phase-transition temperatures. In this chapter, a high temperature was necessary to ensure all ingredients were dissolved. The effect of different co-surfactants on the formulation size and size distribution will also be studied. Also, different concentrations of ammonium sulfate will be tested.

5.2 Aim and Objectives

This chapter aims to study the use of microfluidics to manufacture small, uniform niosomes. The niosomes will be manufactured to actively load doxorubicin. To our knowledge, no published peer-reviewed article has used Span 65, solutol HS 15, and Cremophor RH 40 in combination to manufacture niosomes using microfluidic techniques. For this reason, this chapter will examine how the following parameters affect niosome size and size distribution: different combinations of surfactant and co-surfactants, total flow rates and flow rate ratios, buffer concentration, and organic solvent.

The chapter will also study the doxorubicin loading into the most optimised formulation using active drug loading. The loaded formulations will be analysed for their entrapment efficiency and stability. They will also be studied for their ability to be filtered through a 0.2 micrometre filter for sterilisation and the effect of this on drug retention.

5.3 Results and Discussion

5.3.1 Preliminary Data

There are no peer-reviewed journal articles reporting the formulation of niosomes using microfluidic techniques to actively load drugs via pH- and salt-gradients. Given the novelty of this work, no studies have reported the formulation of niosomes using a microfluidic technique with an aqueous buffer containing ammonium sulfate (0.12 M)

For this reason, a preliminary study was conducted to assess the effects of various parameters on the size and size distribution of various niosomal formulations. The following factors will be explored: the type of co-surfactant used, the concentrations of ingredients in the organic solvent, the total flow rate, and the flow-rate ratio of the aqueous solvent to the organic solvent.

5.3.1.1 The Effect of Changing Co-surfactants

The compatibility study conducted in Chapter 4 on Span 65 with Cremophor RH40 and Solutol HS-15 has shown that different co-surfactants interact differently with Span 65. Cremophor RH 40 was proven to be more compatible with Span 65 than Solutol HS-15. Cremophor RH 40 with Span 65 formulation maintained the pH gradient when tested with BCG for a longer time than the Span 65 with Solutol HS-15 formulation.

Table 2.6 shows the different formulations of niosomes with varying co-surfactant compositions used to synthesise niosomes via the microfluidic technique. Table 5.1 below shows the effects of different co-surfactant formulations on niosome size and PDI.

Table 5.1: Size and PDI of different niosomal formulations prepared using the microfluidic technique at TFF of 12mL/min and FRR of 5:1, 3:1 and 2:1 at 60 °C.

Niosome formulation	FRR 5:1		FRR 3:1		FRR 2:1	
	Niosomes Size – d nm (±SD)	**PDI** (±SD)	**Niosomes Size –** d nm (±SD)	**PDI** (±SD)	**Niosomes Size –** d nm (±SD)	**PDI** (±SD)
F1-1	79.61 (±1.27)	0.12 (±0.02)	118.7 (±2.70)	0.12 (±0.04)	162.7 (±2.58)	0.12 (±0.02)
F2-1	98.86 (±1.74)	0.08 (±0.02)	120.9 (±1.04)	0.06 (±0.02)	181.4 (±8.21)	0.12 (±0.03)
F3-1	64.96 (±3.13)	0.14 (±0.04)	75.38 (±2.50)	0.08 (±0.04)	112.1 (±1.96)	0.11 (±0.02)
F4-1	103.1 (±1.96)	0.06 (±0.02)	116.4 (±1.32)	0.05 (±0.02)	154.6 (±1.94)	0.07 (±0.02)
F5-1	58.42 (±0.46)	0.12 (±0.03)	71.31 (±0.74)	0.08 (±0.02)	112.9 (±3.60)	0.10 (±0.02)
F6-1	52.89 (±1.78)	0.09 (±0.03)	58.76 (±2.03)	0.10 (±0.03)	92.61 (±0.66)	0.13 (±0.03)
F7-1	231.4 (±2.04)	0.10 (±0.05)	365.1 (±21.47)	0.51 (±0.08)	769.2 (±69.86)	0.80 (±0.17)

The results in table 5.1 are illustrated in figure 5.2 below for better presentation.

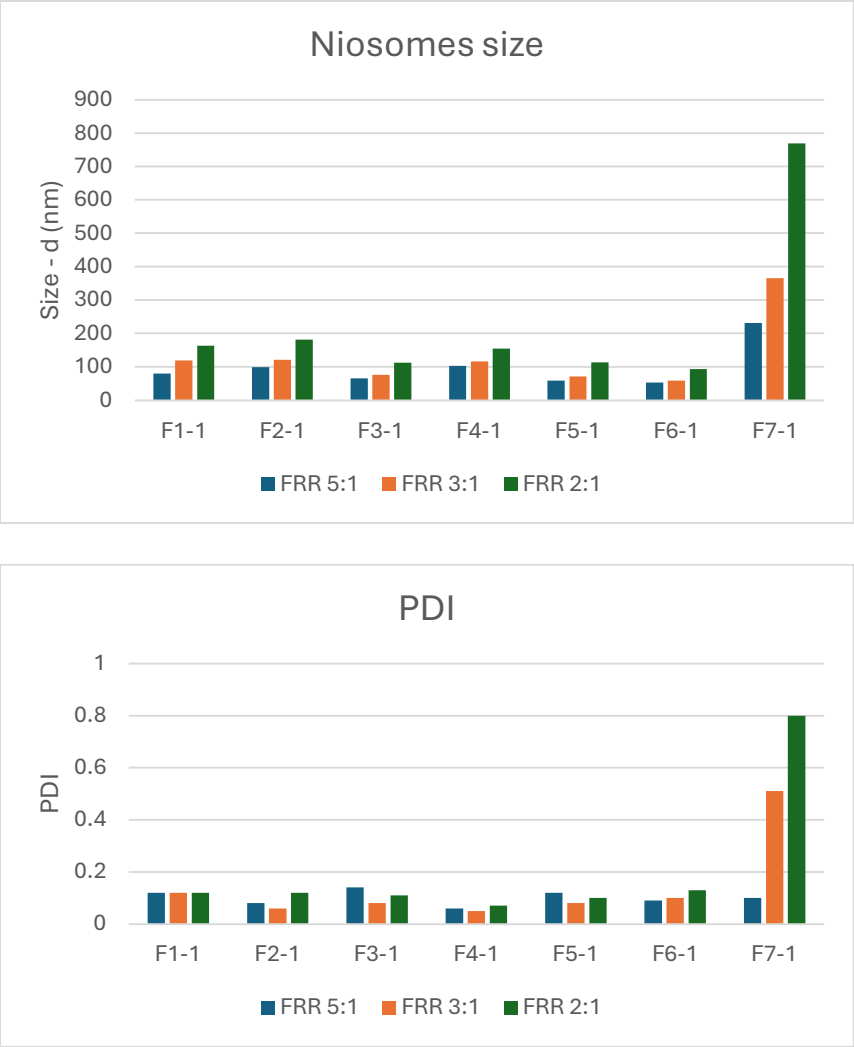

Figure 5.2: Two graphs showing the size and PDI of the different niosomal formulations prepared at different FRR as per table 2.6.

Given the fact that Cremophor RH40 is more compatible with Span 65 than solutol HS-15, figure 5.2 above shows that the niosome size of formulations containing only Solutol HS-15 (F7-1) is much larger than the other formulations, which contain either 5% or 10% Cremophor RH 40 with or without Solutol HS-15.

The formulation containing only 5% co-surfactant is formulation F4-1, which is composed of 50% Span 65, 45% cholesterol, and 5 molar% Cremophor RH40. The size of the F4-1 formulation increased from 103.1 nm to 154.6 nm as the FRR was reduced from 5:1 to 2:1. The FRR was reduced to make more concentrated niosomes because the ratio of the organic phase containing the surfactants and co-surfactants would be higher than the aqueous phase containing the buffer. This means that 5% of Cremophor RH40 co-surfactant is insufficient to control niosome size as the FRR decreases.

The microfluidic technique formulates niosomes by rapidly mixing the organic phase with the aqueous phase in a microchannel (figure 1.6). During this process, niosomes self-assemble, and the presence of co-surfactants appears to help pegylate their surface and prevent collision and aggregation during mixing. The presence of only 5% co-surfactant appears insufficient to control the size of Span 65 niosomes when the FRR is reduced. However, formulation F3-1 contains 10% of Cremophor RH40. Compared to F4-1, F3-1 always produced much smaller niosomes (64.96 nm vs 103.1 nm at FRR 5:1, 75.38 nm vs 116.4 nm at FRR 3:1, and 112.1 nm vs 154.6 nm at FRR 2:1).

Moreover, F1-1 and F2-1 contain 10% and 5% of Solutol HS-15, respectively, and both contain 5% Cremophor RH40. As FRR decreased from 5:1 to 2:1, F1-1 size increased from 79.61 nm to 162.7 nm, and F2-1 size increased from 98.86 nm to 181.4 nm.

The addition of Solutol HS-15 on top of the 10% Cremophor RH 40 content did not worsen the formulation size. F5-1 and F6-1 contain 5% and 10% of Solutol HS-15, respectively, and both contain 10% Cremophor RH 40. As FRR decreased from 5:1 to 2:1, the sizes of F5-1 and F6-1 remained below 150 nm (112.9 nm and 92.61 nm, respectively), and close to that of F3-1 (112.1 nm).

This shows that to produce niosomes with a size less than 150 nm at a low FRR and thus higher niosome concentration, a minimum of 10% Cremophor RH 40 needs to be present in the Span 65 formulation.

It should be noted that the microfluidic technique produced niosomes with a narrow size distribution, except for formulations F7-1 at FRRs of 3:1 and 2:1, for which the PDI exceeded 0.2 (0.51 and 0.8, respectively). All other formulations had a PDI < 0.2. This is one of the main advantages of using the microfluidic technique to produce niosomes, as it allows control of niosome size and size distribution without extrusion. The literature also shows that a low PDI and small particle size can be achieved using the microfluidic technique if the right ingredients, FRR, organic solvent and aqueous phase are chosen correctly. Seleci et al. formulated niosomes containing Span 60, cholesterol, and DSPE-PEG (2000) maleimide, and, at an FRR of 1:1, produced niosomes using chloroform as the organic solvent, with a size of 128.5 nm and a PDI of 0.13[189]. However, they did not obtain the same size pattern as I did. They found that FRRs of 2:1, 3:1, and 5:1 could not produce monodispersed niosomes, as the size distribution graphs for each of these FRRs showed two peaks rather than one. This could be due to them using a different organic phase (chloroform vs ethanol), a different surfactant (Span 60 vs Span 65), and a different co-surfactant (DSPE-PEG (2000) maleimide vs Cremophor RH 40 and Solutol HS-15) than what I used.

Obeid et al. formulated niosomes consisting only of surfactants and cholesterol at either a 50:50 or 70:30 molar ratio and dissolved them in ethanol. Surfactants were Span 20, Span 80, Span 85 and Tween 85. Size was measured before and after atenolol drug loading. FRR for all formulations was 3:1, and TFR was 12 mL/min. All niosomes produced had a size less than 120 nm, and all empty formulations had a PDI less than 0.2[190]. This further demonstrates the microfluidic technique's ability to make small, monodispersed niosomes. Moreover, Obeid et al. obtained monodispersed niosomes with an FRR of 3:1, whereas Seleci et al. were unable to obtain them. This may be due to other factors, such as the ingredients used and the organic solvent used to dissolve them. In our research, an FRR of 3:1 produced monodispersed niosomes in all formulations (PDI < 0.2) with niosome size ranging between 58 and 121 nm, except for F7-1, where PDI was 0.51 and niosome size was 365.1 nm. This occurred because F7-1 contained only Solutol HS-15, not

Cremophor RH 40. Consistent with the literature, this demonstrates the importance of using compatible ingredients to obtain monodisperse, small niosomes via microfluidic techniques.

Table 5.1 showed that the FRR has an important effect on the niosomes' size, where in all formulations, there was an increase in the niosomes' size as the FRR decreased from 5:1 to 2:1. This can be because, as the FRR decreases, more niosomes will be formed. More collisions can occur between the niosomes as they form in the mixing microchannels. This collision can merge niosomes, forming larger niosomes. Machado et al. reached the same conclusion when formulating cholesterol-free niosomes using microfluidic techniques with Span 80 and Tween 80 surfactants[192]. They concluded that as FRR increases, the average niosome diameter decreases. Obeid et al., in another study from the one referenced above, also concluded that increasing FRR from 1:1 to 3:1 reduced particle size, with niosomes made from Span 80 or Tween 80 and cholesterol showing decreases from 142.3 nm to 70.51 nm and 228.33 nm to 71.31 nm, respectively[57].

The zeta potential for the formulations above was measured at three different pHs, as summarised in table 5.2. The zeta potential was measured at an FRR of 2:1 to obtain more concentrated niosomes, thereby improving its measurability. However, as shown in table 5.1, formulation F7-1 is very large at FRRs of 2:1 and 3:1. Therefore, the zeta potential was measured for niosomes produced at an FRR of 5:1.

Table 5.2: Zeta potential of niosomal formulations prepared using the microfluidic technique at TFR of 12mL/min and FRR 2:1 (except 5:1 for F7-1) at 60 °C. Zeta potential was measured at three pH values (5, 7, and 9).

Niosome formulation	Zeta potential (mV)		
	pH 5	pH 7	pH 9
F1-1	-6.36 (±0.78)	-9.20 (±0.97)	-30.5 (±2.15)
F2-1	-2.43 (±0.64)	-10.8 (±2.08)	-33.1 (±1.10)
F3-1	-2.38 (±0.39)	-7.44 (±1.76)	-25.7 (±2.07)
F4-1	-3.15 (±0.37)	-8.96 (±0.50)	-29.5 (±1.35)
F5-1	-1.75 (±1.67)	-6.78 (±0.63)	-24.9 (±1.70)
F6-1	-2.04 (±0.42)	-6.88 (±0.41)	-26.8 (±1.18)
F7-1	-4.09 (±0.84)	-15.7 (±0.83)	-45.0 (±2.66)

The niosomes' zeta potential was affected by the pH of the environment in which the niosomes are suspended. The zeta potential decreased by approximately 25–30 mV (towards the negative) as the pH increased from 5 to 9. Increasing pH increases the concentration of OH^- ions in the suspension. This can deprotonate hydroxyl groups in the niosome membrane, resulting in a negative zeta potential. It can be concluded from table 5.2 that at neutral pH (around 7.0), the niosomes' zeta potential is not sufficient to create repulsive forces strong enough to prevent niosome aggregation because a zeta potential less than -30 mV is needed for this to happen[178]. However, the stability of the niosomes will rely in this case mainly on two things: the pegylation effect of Cremophor RH 40 (steric stabilisation) and the reduced surface free energy of niosomes containing Span 65. Cremophor RH 40 has 40 PEG molecules extending in front of the niosomes, acting as a physical barrier that prevents aggregation and merging.

5.3.1.2 The Effect of Different TFR

The TFR is the speed at which the organic and aqueous phases flow through and mix in the microchannels to form niosomes. Increasing the TFR can reduce the size of niosomes in some formulations but may not affect the size in others. The effect of changing TFR on the F3-1 and F6-1 formulation sizes is documented in table 5.3 below.

Table 5.3: Size and PDI of two niosomal formulations (F3-1 and F6-1) made with different TFR at FRR of 2:1.

TFR (mL/min)	F3-1		F6-1	
	Niosomes Size – d nm (±SD)	**PDI** (±SD)	**Niosomes Size –** d nm (±SD)	**PDI** (±SD)
4	114.5 (±0.13)	0.13 (±0.02)	90.04 (±2.34)	0.14 (±0.02)
8	95.65 (±1.49)	0.10 (±0.02)	92.81 (±4.22)	0.09 (±0.02)
16	92.94 (±0.66)	0.11 (±0.01)	96.50 (±1.49)	0.12 (±0.02)
20	87.52 (±3.01)	0.14 (±0.04)	101.0 (±6.30)	0.10 (±0.02)

For formulation F3-1, increasing the TFR from 4 mL/min to 20 mL/min reduced the size from 114.5 nm to 87.52 nm. A similar observation was reported by Obeid et al., who found that increasing the TFR reduced niosome size[193]. As TFR increased from

0.5 ml/min to 9 ml/min, the niosome size decreased in three different FRR (1:1, 3:1 and 5:1). However, no effect on niosome size was observed with TFR between 9 ml/min and 12 ml/min. Their niosomes are composed of monopalmitin glycerol, cholesterol, and dicetyl phosphate.

Roces et al. formulated two liposomal formulations using a microfluidic technique (one composed of HSPC, cholesterol and DSPE-PEG2000 and the other is made of DSPC, cholesterol and DSPE-PEG2000)[93]. Upon increasing the TFR from 10 ml/min to 20 ml/min, no change in niosome size was observed. This could further support the finding of Obeid et al., who reported that increasing TFR above 9 ml/min does not affect the size of nanovesicles (niosomes/liposomes).

However, in formulation F6-1, the average niosome size increased with TFR, but the change was small. Some studies have also found that increasing the TFR did not significantly affect nanovesicle size. The literature provides no definitive conclusion regarding the effect of TFR on niosome size[193].

It can be concluded that the effect of TFR on the niosome size depends on the formulation ingredients. F3-1 contains 10% Cremophor RH 40, while F6-1 contains 10% Cremophor RH 40 and 10% Solutol HS-15 as co-surfactants. However, TFR is an important factor to consider, as it can increase batch manufacturing speed and determine nanovesicle size. The higher the TFR, the less time it takes to make a batch.

5.3.1.3 The Effect of Different Concentrations of Surfactants and Cholesterol in Ethanol

Increasing the concentration of niosomes in the final product can be achieved by reducing FRR, which increases the amount of ethanol added to the formulation and thus the surfactant concentration in the final product. However, I have established that reducing FRR can increase niosome size. The second way to increase the concentration of niosomes without reducing FRR is to increase the surfactant concentration in the organic phase. Each formulation in table 5.1 was prepared with a higher surfactant and cholesterol concentration in the organic phase, as explained in table 2.8. The niosomes' size and PDI were measured by formulating niosomes at three different FRRs (5:1, 3:1, and 2:1), and the results are summarised in table 5.4.

Table 5.4: Size and PDI of niosomes formulated at different total concentrations of surfactants and cholesterol in ethanol and at TFR of 12mL/min and at 60 °C. Each niosomal formulation was formed at three different FRRs (5:1, 3:1 and 2:1). Refer to tables 2.6 and 2.8 for formulation composition.

Niosome formulation	FRR 5:1		FRR 3:1		FRR 2:1	
	Niosomes Size – d nm (±SD)	**PDI** (±SD)	**Niosomes Size –** d nm (±SD)	**PDI** (±SD)	**Niosomes Size –** d nm (±SD)	**PDI** (±SD)
F1-1	79.61 (±1.27)	0.12 (±0.02)	118.7 (±2.70)	0.12 (±0.04)	162.7 (±2.58)	0.12 (±0.02)
F1-2	87.19 (±0.33)	0.08 (±0.02)	125.7 (±2.36)	0.09 (±0.03)	171.8 (±2.29)	0.12 (±0.02)
F1-3	97.91 (±1.64)	0.10 (±0.03)	128.2 (±4.18)	0.11 (±0.03)	187.4 (±20.75)	0.19 (±0.03)
F2-1	98.86 (±1.74)	0.08 (±0.02)	120.9 (±1.04)	0.06 (±0.02)	181.4 (±8.21)	0.12 (±0.03)
F2-2	97.65 (±2.05)	0.12 (±0.05)	118.2 (±3.63)	0.06 (±0.02)	190.1 (±6.23)	0.14 (±0.04)
F2-3	111.6 (±2.45)	0.11 (±0.03)	130.8 (±1.85)	0.07 (±0.02)	187.1 (±8.92)	0.11 (±0.04)
F3-1	64.96 (±3.13)	0.14 (±0.04)	75.38 (±2.50)	0.08 (±0.04)	112.1 (±1.96)	0.11 (±0.02)
F3-2	70.07 (±0.96)	0.10 (±0.01)	82.36 (±2.61)	0.11 (±0.03)	108.2 (±1.36)	0.12 (±0.03)
F3-3	84.15 (±1.78)	0.12 (±0.03)	90.75 (±0.76)	0.12 (±0.02)	115.4 (±1.28)	0.14 (±0.01)
F4-1	103.1 (±1.96)	0.06 (±0.02)	116.4 (±1.32)	0.05 (±0.02)	154.6 (±1.94)	0.07 (±0.02)
F4-2	108.5 (±1.23)	0.08 (±0.02)	122.5 (±0.74)	0.06 (±0.02)	163.4 (±2.02)	0.10 (±0.02)
F4-3	120.4 (±2.36)	0.12 (±0.04)	130.6 (±2.47)	0.11 (±0.03)	171.7 (±2.12)	0.10 (±0.02)
F5-1	58.42 (±0.46)	0.12 (±0.03)	71.31 (±0.74)	0.08 (±0.02)	112.9 (±3.60)	0.10 (±0.02)
F5-2	63.78 (±2.30)	0.09 (±0.03)	73.66 (±4.49)	0.11 (±0.03)	122.0 (±4.46)	0.10 (±0.01)
F5-3	76.82 (±2.60)	0.13 (±0.01)	85.39 (±3.48)	0.17 (±0.03)	117.8 (±1.73)	0.15 (±0.02)
F6-1	52.89 (±1.78)	0.09 (±0.03)	58.76 (±2.03)	0.10 (±0.03)	92.61 (±0.66)	0.13 (±0.03)
F6-2	60.69 (±3.95)	0.12 (±0.05)	66.58 (±0.83)	0.14 (±0.02)	105.9 (±0.98)	0.13 (±0.01)
F6-3	73.07 (±3.26)	0.13 (±0.03)	75.07 (±3.53)	0.15 (±0.03)	114.9 (±1.75)	0.11 (±0.03)

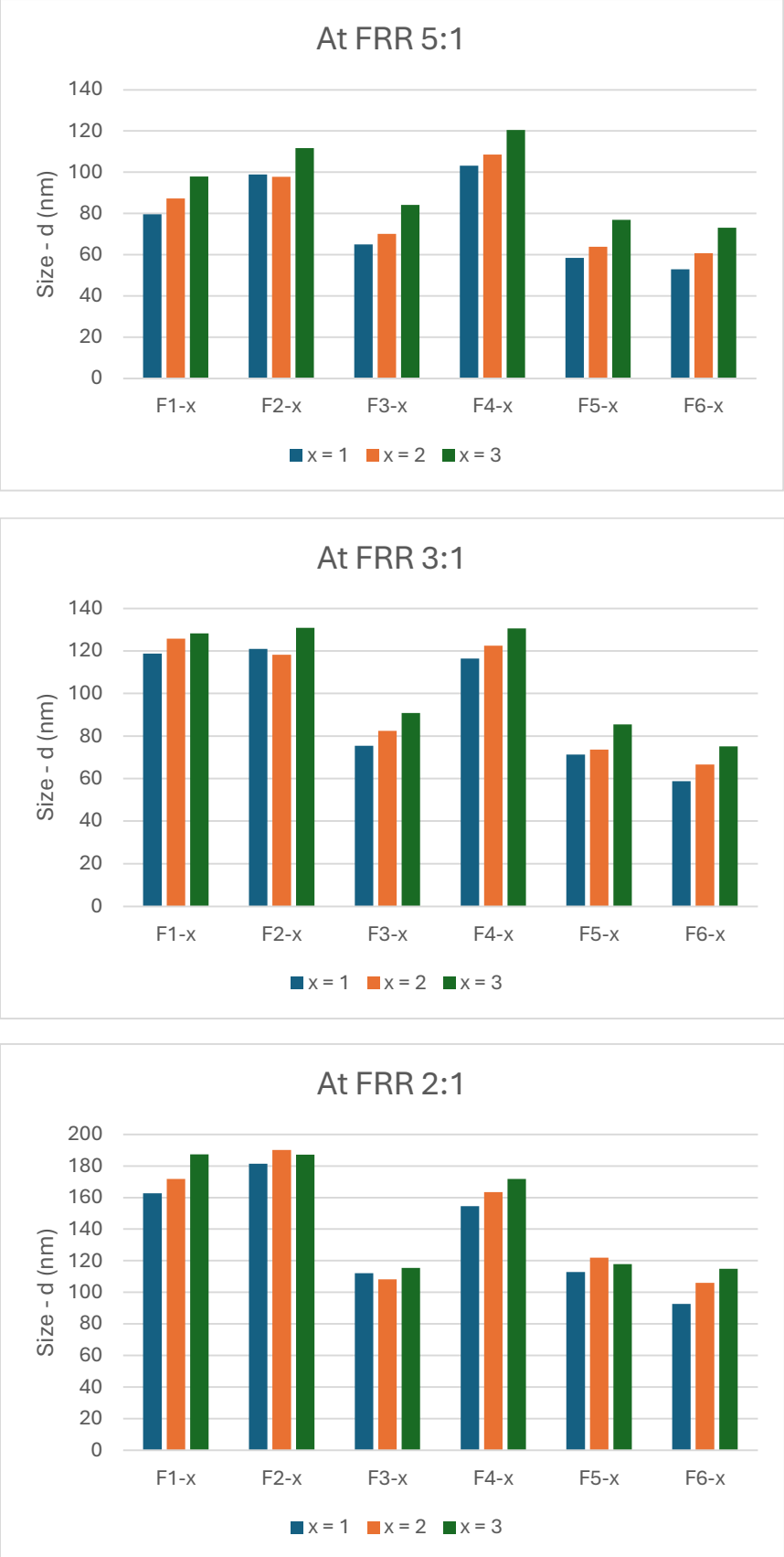

Figure 5.3: Size of different niosomes formulations prepared at different concentrations at three different FRRs. “X” stands for the formulation number.

Table 5.4 and figure 5.3 show that increasing the concentration of surfactants and cholesterol in the organic phase can increase the size of the niosomes, but not in all formulations and not at all FRRs. It can be concluded that reducing the FRR can have a more significant effect on the niosome size than increasing the concentration of ingredients in the organic phase.

For example, reducing the FRR from 5:1 to 2:1 should double the niosome concentration, as the surfactant concentration in the final product will be doubled. Formulation F1-1 at FRR 5:1 had an average size of 79.61 nm. In formulation F1-2, which has twice the amount of ingredients dissolved in the organic phase compared to F1-1, niosomes were produced with a size of 87.19 nm, 7.58 nm larger than in F1-1. However, when the FRR for formulation F1-1 was reduced from 5:1 to 2:1, which should also produce double the concentration of niosomes, the niosome size increased from 79.61 to 162.7 nm, an 83.09 nm increase in size.

Machado et al. found that increasing the niosome concentration increased their size in one formulation but not in the other[192]. For example, for niosomes composed of Span 80 and Tween 80, when FRR was 5:1, increasing the niosome ingredients concentration from 5 mM to 10 mM increased the niosome size from 186 nm to 224 nm. The same outcome was observed at FRRs of 15:1 (83.5 nm vs 108.8 nm), 25:1 (78 nm vs 93.1 nm), and 50:1 (65 nm vs 77.7 nm), but no significant change was observed at an FRR of 35:1 (69 nm vs 71 nm). However, for niosomes composed of Span 80, Tween 80 and 1-dodecanol, increasing the concentration of the ingredients from 5 mM to 10 mM resulted in the opposite where the niosomes size was reduced from 309 nm to 191.4 nm when FRR was 5:1. This shows that the effect of the concentration of the niosomes on the particle size is dependent on the ingredients composition of the niosomes. The presence of 1-dodecanol in the formulation could have stabilised the niosomes and controlled particle size as the concentration increased.

Moreover, Roces et al. have shown that increasing the lipid concentration can have different effects on liposome size[93]. For example, in a liposomal formulation comprising HSPC, cholesterol, and DSPE-PEG2000, increasing the lipid concentration from 2.5 mg/mL to 5.0 mg/mL reduced the liposome size from around

110 nm to around 90 nm. However, increasing the lipid concentration from 5.0 mg/mL to 40 mg/mL did not result in a significant change in size.

These results show that two methods can be used to increase niosome concentration, but they have different effects on niosome size. FRR has a more significant impact on niosome size than surfactant concentration in the organic phase. In conclusion, the target niosome size and concentration can be reached by balancing the amount of ingredients dissolved in the organic solvent and the FRR.

From the preliminary analyses of the effect of different parameters of the microfluidic process of niosomes synthesis, it can be concluded that the two parameters that have the most significant effect on niosome size and size distribution (PDI) are the surfactants and co-surfactants used along with their ratios, and the FRR. This is consistent with other literature.

5.3.2 Doxorubicin Loading and its effect on Niosomes' Size

Doxorubicin was actively loaded into the niosomes using an ammonium sulfate gradient. The main advantage of actively loading doxorubicin into niosomes is the enhanced entrapment efficiency, as passive loading typically achieves entrapment efficiency below 40%. In contrast, active loading achieves much higher EE and allows doxorubicin to be precipitated inside the nanovesicle. Inside the nanovesicle, doxorubicin will bind to sulfate ions and precipitate, allowing it to be loaded at concentrations much higher than its solubility limits[93,106].

The aqueous phase contained 0.12 M ammonium sulfate, while the organic phase (ethanol) contained the surfactants and cholesterol. There are organic solvents other than ethanol that can serve as the organic phase in the microfluidic technique. However, ethanol was chosen because it has been shown to be more efficient for loading doxorubicin into liposomes than methanol and isopropanol[93].

After niosomes formation, 1 mL of the freshly made niosomal suspension was passed through a Sephadex G50 column preequilibrated with trizma buffer. Then, 0.15 mL of 2 mg/mL doxorubicin solution was added to 0.85 mL of the buffer-exchanged niosomes to achieve a final concentration of 0.3 mg/mL, and 0.25 mL of 2 mg/mL was added to 0.75 mL of the buffer-exchanged niosomes to achieve a final

concentration of 0.5 mg/mL. After 1 hour of drug loading, 1 mL of niosomes was passed through another Sephadex column pre-equilibrated with a sucrose-histidine buffer (10% w/v sucrose, 10 mM histidine, pH 6.5) to measure entrapment efficiency and size. Size, PDI and entrapment efficiency are summarised in table 5.5 below.

Table 5.5: Drug loading of doxorubicin into F3-3 niosomal formulation prepared at TFR 12 mL/min and FRR of 2:1.

Niosome formulation	After Trizma buffer exchange		After 1 hour of loading with 0.3mg/mL			After 1 hour of loading with 0.5mg/mL		
	Niosomes Size – d nm (±SD)	**PDI** (±SD)	**Niosomes Size –** d nm (±SD)	**PDI** (±SD)	**%EE** (±SD)	**Niosomes Size –** d nm (±SD)	**PDI** (±SD)	**%EE** (±SD)
F3-3	109.1 (±1.98)	0.14 (±0.02)	124.1 (±2.82)	0.22 (±0.02)	69.92 (±2.55)	165.5 (±3.63)	0.16 (±0.01)	70.21 (±2.81)

Drug loading of doxorubicin in formulation F3-3 has been shown to affect niosome size, with the effect being concentration-dependent. Loading with 0.5 mg/mL had a greater effect on increasing the niosomes' size than loading with 0.3 mg/mL (+56.4 nm vs +15 nm, respectively, compared to niosomes' size before drug loading, Table 5.5).

Table 5.5 also shows that the entrapment efficiency for loading 0.3 mg/mL is similar to that for 0.5mg/mL (~70%). This means that more doxorubicin has entered the niosomes at the 0.5 mg/mL than at the 0.3 mg/mL. The ammonium sulfate pH gradient technique can explain this. As doxorubicin enters the niosomes, ammonium ions leave the niosomes (figure 1.11). This reduces the pH inside the niosomes, thereby driving more doxorubicin into them. A higher concentration of doxorubicin means more ammonium ions will leave the niosomes, and more doxorubicin will enter. Thus, as the doxorubicin concentration increases, this process becomes more efficient at loading doxorubicin. In addition, it seems from Table 5.5 that the niosome size has also increased more when drug loading occurred at 0.5 mg/mL than at 0.3 mg/mL. This could also explain why more drug entered the niosomes at the higher concentration than at 0.3 mg/mL, where the increase in niosome size allowed more drug to enter.

Passive drug loading of doxorubicin into niosomes using the microfluidic technique has also been studied. The aqueous phase contained doxorubicin dissolved in sucrose-histidine buffer, while the organic phase contained Span 65, Cremophor RH

40 and cholesterol dissolved in ethanol. The concentration of doxorubicin in the final niosomal product was 0.5 mg/mL. The average niosome size was 157.7 nm (PDI = 0.17), and the average doxorubicin EE was 41.88%. The low entrapment efficiency is consistent with literature reports[93], as passive drug loading does not yield high entrapment efficiency and indicates the need for active drug loading.

Roces et al. have shown that liposomes can actively load doxorubicin using an ammonium sulfate pH gradient[93]. However, they could achieve efficient active loading only by using an elevated temperature above the phase transition temperature of the main lipid during drug loading. In this study, however, I managed to load the drug using a pH gradient at room temperature, ~23 °C. This is an advantage to loading doxorubicin into niosomes when compared to liposomes, as it requires less energy.

5.3.3 Stability Study

Given that the niosomal formulation is in suspension, an important parameter to measure is niosomal size stability. The niosomes' size and size distribution (PDI) were measured over three months, and the results are summarised in tables 5.6 and 5.7 below. After niosomes synthesis using a microfluidic technique, the niosomes were passed through a Sephadex column pre-equilibrated with trizma buffer to remove the ethanol and create a pH gradient. Then, doxorubicin was added to either make the concentration 0.3 mg/mL or 0.5mg/mL. Then, another buffer exchange process took place to remove the unentrapped drug and suspend the niosomes in a buffer of choice that can stabilise them. Two buffers were studied: a normal saline made of 0.9% w/v NaCl (table 5.6) or a Histidine-Sucrose buffer (10% w/v sucrose, 10 mM histidine) (table 5.7).

Table 5.6: Stability study (size and PDI) of niosomes after NaCl buffer exchange that followed doxorubicin loading at 0.3 mg/mL and 0.5 mg/mL. After the niosome size exceeded 200 nm, size measurement was stopped as visible aggregation began to appear.

Day of measurement	NaCl (0.3 mg/mL)		NaCl (0.5 mg/mL)	
	Niosomes Size – d nm (±SD)	**PDI** (±SD)	**Niosomes Size –** d nm (±SD)	**PDI** (±SD)
Day 1	113.0 (±1.69)	0.13 (±0.01)	132.3 (±1.76)	0.12 (±0.03)
Day 4	116.9 (±1.42)	0.13 (±0.03)	351.5 (±155.8)	0.42 (±0.15)
Day 6	124.7 (±2.49)	0.16 (±0.02)		
Day 11	141.9 (±4.16)	0.21 (±0.02)		
Day 19	201.0 (±15.02)	0.38 (±0.06)		

As shown in table 5.6, NaCl was not a good choice of buffer. Even though doxorubicin is known to be stable in NaCl, some manufacturers prepare doxorubicin injections in NaCl solution[194], niosomes were not stable in it. The reason why niosomes were not stable in NaCl solution is due to the ionic effect of the sodium and chloride ions on the niosome membrane. Na^+ and Cl^- ions shield the surface charges on niosomes, reducing electrostatic repulsion and potentially promoting fusion and aggregation. Moreover, ions interact with the surfactant headgroups, altering bilayer packing and reducing bilayer integrity. It is clearly visible in figure 5.4 that the niosomes aggregated in the NaCl solution.

Figure 5.4: Aggregation of niosomes in NaCl solution for formulation loaded at doxorubicin concentration of 0.3 mg/mL (two runs)

An alternative approach for suspending niosomes to maintain their stability is to use a low-ionic-strength buffer, such as a histidine-sucrose buffer (10% w/v sucrose, 10 mM histidine, pH 6.5). As shown in table 5.7 below, after niosomes were loaded with 0.3 mg/mL or 0.5 mg/mL doxorubicin, the niosomes remained stable for 3 months. After loading, the size of niosomes loaded with 0.5 mg/mL doxorubicin is bigger than that of those loaded with 0.3 mg/mL, as explained before. However, the niosome size remained stable after the initial loading throughout the stability study. For reference purposes and to study the stability of niosomes in trizma buffer, the size of niosomes after trizma buffer exchange and before drug loading, or histidine-sucrose buffer exchange, was monitored over 3 months as well. As shown in table 5.7, the niosomes demonstrated great stability in trizma buffer, further illustrating that using a buffer different to NaCl can stabilise the niosomes and prevent their aggregation. Caelyx liposomal formulation (doxorubicin liposomes) is prepared in Histidine-sucrose buffer as well, and has a 2-year shelf-life[195].

Table 5.7: Size and PDI of niosomes after trizma buffer exchange, and after Sucrose-histidine buffer exchange that followed doxorubicin loading at 0.3 mg/mL and 0.5 mg/mL.

Day of measurement	After trizma		Sucrose-histidine buffer (0.3mg/mL doxorubicin)		Sucrose-histidine buffer (0.5mg/mL doxorubicin)	
	Niosomes Size – d nm (±SD)	**PDI** (±SD)	**Niosomes Size –** d nm (±SD)	**PDI** (±SD)	**Niosomes Size –** d nm (±SD)	**PDI** (±SD)
Day 1	108.5 (±1.58)	0.12 (±0.02)	109.9 (±1.74)	0.17 (±0.01)	140.6 (±2.84)	0.11 (±0.02)
Day 4	108.8 (±1.48)	0.13 (±0.02)	106.5 (±2.29)	0.16 (±0.01)	140.9 (±0.55)	0.10 (±0.01)
Day 7	108.6 (±0.60)	0.14 (±0.00)	105.4 (±0.65)	0.16 (±0.01)	139.0 (±2.69)	0.14 (±0.01)
Day 14	108.5 (±1.50)	0.14 (±0.02)	108.9 (±2.10)	0.18 (±0.03)	140.9 (±2.17)	0.10 (±0.02)
Day 21	109.9 (±1.90)	0.13 (±0.01)	109.5 (±1.71)	0.16 (±0.02)	140.0 (±1.75)	0.10 (±0.03)
Day 28	112.2 (±3.55)	0.16 (±0.01)	111.4 (±0.92)	0.17 (±0.03)	143.1 (±1.53)	0.13 (±0.04)
Day 56	109.1 (±1.71)	0.13 (±0.03)	108.7 (±1.17)	0.13 (±0.05)	137.3 (±0.63)	0.09 (±0.02)
Day 84	109.7 (±1.11)	0.16 (±0.02)	108.6 (±1.43)	0.15 (±0.02)	138.4 (±1.69)	0.08 (±0.01)

5.3.3 Drug Recovery After Sterilisation

One important step in preparing nanovesicles for patient administration is sterilising the final product. The gold standard approach for sterilising liposomes before they are released to the market is membrane filtration, in which liposomes are passed through a 0.22 μm filter[122]; liposomes below 220 nm can pass through, while microorganisms and contaminants are retained behind the filter. Similar to liposomes, it is recommended that a similar procedure be used to sterilise the niosomes[196], given the success of this technique in sterilising liposomes and the structural similarity between niosomes and liposomes. Also, other techniques such as autoclaving or dry heating are not suitable for niosomes and liposomes because these nanocarriers are heat-sensitive, and high temperatures can destroy them. Irradiation is also not suitable, as it can compromise nanovesicle stability and denature the drug.

The niosomal formulation containing doxorubicin was passed through a 0.2 μm filter to assess drug recovery after sterilisation. Drug recovery is calculated using the following equation:

$$\text{Drug recovery} = \frac{concentration\ of\ drug\ after\ filtration}{concentration\ of\ drug\ before\ filtration}\ x\ 100$$

Drug recovery is important to ensure that the drug is not lost during the filtration process. It also helps to determine whether the filtration process has retained some niosomes and prevented them from passing through due to size or filter-niosome

compatibility issues. In this case, the niosome size may need to be further reduced to allow sterilisation by filtration without losing niosomes/drug, or the filter type may need to be changed to one more compatible with the niosomes.

PES-type sterile filters with 0.2 μm pore size were used to sterilise the niosomes. No change was observed in drug content or niosome size after sterilisation. Recovered drug content was ~ 100%, and there was no significant change in size for both loading doxorubicin concentrations (0.3 mg/mL and 0.5 mg/mL).

5.4 Conclusion

The microfluidic technique is an efficient method to form niosomes with controlled size and size distribution. It can reduce the number of steps and the time required compared to conventional nanoparticle manufacturing methods that require an extrusion step. Several factors can affect the size of niosomes produced using the microfluidic technique, but the most significant ones are the ingredients used and the FRR of the aqueous phase to the organic phase. A 70% EE was achieved, indicating the success of this technique in actively loading doxorubicin into niosomes. The niosomal formulation suspended in histidine-sucrose buffer remained stable for a minimum of 3 months, where the niosome size did not change.

Chapter 6 – Conclusion and Future Work

6.1 General Conclusion

In conclusion, this study highlights the significant yet underexplored potential of pH gradient–based approaches in niosomal drug delivery systems. While this area remains relatively under reviewed, the findings presented here demonstrate that it holds considerable promise as a cost-effective alternative to liposomal technologies, particularly in applications requiring efficient drug encapsulation and controlled release.

The use of bromocresol green (BCG) as a pH-sensitive probe proved to be a simple yet powerful tool for investigating the formation and maintenance of transmembrane pH gradients in niosomes. Its distinct colour changes across different pH environments enabled clear visual and analytical confirmation of gradient establishment, offering valuable insight into the behaviour of niosomal membranes. Importantly, these observations emphasised that the compatibility between surfactants and co-surfactants is a critical determinant in achieving stable pH gradients. Specifically, Span 60 demonstrated optimal compatibility with Solutol HS-15, whereas Span 65 showed better compatibility with Cremophor RH 40, likely due to their favourable molecular sizes and structural alignment. Other important factors that affect the pH gradient in niosomes are the composition of both alkaline and acidic buffers, the loading temperature and duration, the niosome morphology (MLV vs LUV), and the cholesterol content in the formulation. These discoveries have aided in understanding how to successfully formulate pH gradient niosomes with doxorubicin and how different formulation compositions and buffer choices affect the enhancement of active drug loading into niosomes.

The successful active loading of doxorubicin into both Span 60/Solutol HS-15 and Span 65/Cremophor RH 40 niosomal systems further validates the practical applicability of pH gradient techniques. However, notable differences in performance were observed. Span 65-based niosomes exhibited superior stability compared to those formulated with Span 60. Additionally, the use of Cremophor RH 40 with Span 65 resulted in smaller vesicle sizes and more controlled size increases following drug loading, indicating a more robust and predictable formulation profile than systems incorporating Solutol HS-15. Span 60 niosomes achieved a doxorubicin entrapment efficiency of 68.28% at 0.1 mg/mL. With the extrusion technique, span 60 niosomes reached a diameter of 241.1 nm. Span 65 niosomes containing cholesterol and

Cremophor RH 40 as a co-surfactant have been shown to efficiently load doxorubicin, with entrapment efficiency reaching 78.79% when Cremophor RH 40 concentration was 5% and 76.99% when Cremophor RH 40 concentration was 10%. It should be noted that as the concentration of Cremophor RH 40 in the formulation increases, the niosome size decreases, where increasing the Cremophor RH 40 content from 5 to 10 molar % decreased the niosome size from 225.6 nm to 189.0 nm.

Acidic drugs, methotrexate, ketorolac and salicylic acid, were also attempted to be actively loaded using Span 60 niosomal formulation containing cholesterol and Solutol HS-15. However, active loading was not achieved primarily because these drugs were unable to cross the niosomal membrane.

Furthermore, the application of microfluidic techniques for niosome preparation emerged as a highly promising strategy for achieving precise control over vesicle size and distribution. Active loading of doxorubicin into microfluidically prepared niosomes was successfully achieved, and key formulation parameters—particularly the flow rate ratio (FRR) and the concentration of components in the organic phase—were identified as critical factors influencing vesicle characteristics. Stability studies over a three-month period confirmed the robustness of the optimised formulations, while also underscoring the importance of the dispersion medium. Notably, niosomes suspended in NaCl solution exhibited aggregation and precipitation, whereas those in a low ionic strength buffer containing sucrose and histidine (pH 6.5) maintained their stability, highlighting the role of external media in preserving system integrity. The doxorubicin-loaded formulation achieved an EE of 70% at a 0.5 mg/mL doxorubicin concentration, demonstrating the success of this technique in actively loading doxorubicin into niosomes.

Overall, this work not only reinforces the feasibility of pH gradient–driven active loading in niosomes but also provides practical insights into formulation design, component compatibility, and processing techniques. These findings lay a strong foundation for future research aimed at optimising niosomal systems and advancing their potential as efficient, scalable, and economically viable drug delivery platforms.

6.2 Future Work and Optimisation of Formulation for Industrial Use

The work presented in this thesis is promising, as it offers a cost-effective alternative to liposomes. Moreover, the use of BCG was proven to be successful in studying pH gradient in niosomes. These findings urge further research into this topic.

The use of BCG can be further developed into a practical that students can use to understand how the pH gradient works in niosomes and liposomes. New techniques can also be developed using BCG to study endosomal trafficking of nanovesicles such as niosomes and liposomes. Further research is also needed to investigate how BGC can be used to analyse factors affecting drug release from nanovesicles, such as temperature and pH.

The methods and techniques used in this thesis are suitable for research at this scale. However, for industrial-scale applications, different techniques must be employed. For example, to create a pH gradient, I used a Sephadex G50 column pre-equilibrated with trizma buffer. However, this process is slow and can lead to contamination with Sephadex beads. An alternative, more suitable method to the niosomal suspension buffer is tangential flow filtration.

Tangential flow filtration (TFF) is a cross-flow filtration technique in which a niosomal suspension flows parallel to a semipermeable membrane, allowing small molecules, such as buffer components, to pass through while larger structures, such as niosomes, are retained[197]. When used to create a pH gradient in niosomes, the niosomes are first formed in an acidic internal buffer (such as ammonium sulfate buffer), so their aqueous core has a low pH. TFF is then used for diafiltration, in which the external medium is continuously exchanged with a neutral or basic buffer while the membrane retains the niosomes. Because only the outer buffer is replaced and the niosomes' bilayer is largely impermeable to protons on the short timescale, the internal acidic environment remains unchanged, maintaining a stable transmembrane pH gradient.

Moreover, using TFF is a novel technique that has not been tested before on niosomes to create a pH gradient and to load doxorubicin. This can be further discovered in future work.

Another advantage of using TFF is that the niosomal formulation can be concentrated[93]. When using a 0.5 mg/mL drug loading , EE was around 70%. This means the drug concentration in the niosomes is 0.35 mg/mL. TFF can be used to filter out any unentrapped drug and to concentrate the niosomal suspension to a 2 mg/mL loaded doxorubicin concentration. Once the optimal niosomal formulation with a suitable drug concentration is reached, a stability study must also be assessed, and drug leakage will then be evaluated for the concentrated formulation.

The formulation has been proven to be sterilisable. In this case, in vitro cytotoxicity should be tested on cancerous cells, and in vivo animal trials can then follow to assess the formulation's safety and efficacy in living animals.

The microfluidic instrument used is for lab-scale. Larger microfluidic instruments are available for the manufacturing of large batches. For example, Precision Nanosystems offers microfluidic instruments that can manufacture larger batches of nanovesicles and are suitable for commercial-scale production. For example, their commercial formulation systems can produce between 12 and 48 litres per hour[198].

A stability study was conducted over 3 months on niosomes prepared using the microfluidic technique. The stability study should continue for a longer period to establish the stability of the niosomal formulations, ensuring a suitable market shelf life.

Cremophor RH40 and Solutol HS-15 co-surfactants have been shown to be effective at maintaining pH gradients when combined with Span 65 and Span 60, respectively. More co-surfactants can be tested to examine the effects of different co-surfactants on niosome stability and active drug loading capacity. Moreover, new co-surfactants and surfactants can be synthesised with different structures and thus properties to study their effect on pH gradient active loading of drugs into niosomes.

Lyophilisation can also be tested for niosomes to allow formulation storage at room temperature. A niosomal formulation in its solid form is usually more stable than in its liquid form.

Once the optimal niosomal formulation is obtained, the safety and efficiency of these nanovesicles will be compared to those of liposomes, the current nanovesicles on

the market. Overall, the cost-effectiveness of these niosomal formulations can then be compared with that of liposomes.

Moreover, there are other drugs that were proven to be actively loadable into liposomes, such as lidocaine and daunorubicin. The ability of niosomes to actively load these drugs can also be tested in the future. The clinical benefit of these niosomal formulations can also be tested once they are successfully formulated.

Chapter 7: References

1. Altaee M, Faheem AM, Elkordy AA. pH Gradient-Driven Loading of Doxorubicin into Niosomes: A Comparative Study Using Bromocresol Green as a Visual Indicator. Pharmaceutics. 2025;17(7). doi:10.3390/pharmaceutics17070862

2. Nammas M. The Impact of Drug Delivery Systems on Pharmacokinetics and Drug-Drug Interactions in Neuropsychiatric Treatment. Cureus. 2025. doi:10.7759/cureus.85563

3. Alagga AA, Pellegrini MV, Gupta V. Drug Absorption. In: StatPearls [Internet]. Treasure Island (FL): StatPearls Publishing; 2025 [cited 2026 Mar 2]. Available from: http://www.ncbi.nlm.nih.gov/books/NBK557405/ PubMed PMID: 32491337.

4. Stielow M, Witczyńska A, Kubryń N, Fijałkowski Ł, Nowaczyk J, Nowaczyk A. The Bioavailability of Drugs—The Current State of Knowledge. Molecules. 2023;28(24):8038. doi:10.3390/molecules28248038 PubMed PMID: 38138529; PubMed Central PMCID: PMC10745386.

5. Bhalani DV, Nutan B, Kumar A, Singh Chandel AK. Bioavailability Enhancement Techniques for Poorly Aqueous Soluble Drugs and Therapeutics. Biomedicines. 2022;10(9):2055. doi:10.3390/biomedicines10092055 PubMed PMID: 36140156; PubMed Central PMCID: PMC9495787.

6. Kumari N, Siddhanta K, Panja S, Joshi V, Jogdeo C, Kapoor E, et al. Oral Delivery of Nucleic Acid Therapies for Local and Systemic Action. Pharm Res. 2023;40(1):107–22. doi:10.1007/s11095-022-03415-7

7. Zhang L, Lou W, Wang J. Advances in nucleic acid therapeutics: structures, delivery systems, and future perspectives in cancer treatment. Clin Exp Med. 2024;24(1):200. doi:10.1007/s10238-024-01463-4

8. Sarhan OM. Recent Trends in Drug Delivery Systems. ASSAY and Drug Development Technologies. 2026;24(1):2–29. doi:10.1089/adt.2025.031

9. Andrade C. The Practical Importance of Half-Life in Psychopharmacology. Psychiatrist.com [Internet]. 2022 [cited 2026 Mar 2]. Available from: https://www.psychiatrist.com/jcp/importance-of-half-life-in-psychopharmacology/

10. Masjedi M, Montahaei T. An illustrated review on nonionic surfactant vesicles (niosomes) as an approach in modern drug delivery: Fabrication, characterization, pharmaceutical, and cosmetic applications. Journal of Drug Delivery Science and Technology. 2021;61:102234. doi:10.1016/j.jddst.2020.102234

11. Mitchell MJ, Billingsley MM, Haley RM, Wechsler ME, Peppas NA, Langer R. Engineering precision nanoparticles for drug delivery. Nat Rev Drug Discov. 2021;20(2):101–24. doi:10.1038/s41573-020-0090-8

12. Ricci A, Stefanuto L, Gasperi T, Bruni F, Tofani D. Lipid Nanovesicles for Antioxidant Delivery in Skin: Liposomes, Ufasomes, Ethosomes, and Niosomes. Antioxidants. 2024;13(12). doi:10.3390/antiox13121516

13. Opatha SAT, Titapiwatanakun V, Chutoprapat R. Transfersomes: A Promising Nanoencapsulation Technique for Transdermal Drug Delivery. Pharmaceutics. 2020;12(9). doi:10.3390/pharmaceutics12090855

14. Sivadasan D, Sultan MH, Alqahtani SS, Javed S. Cubosomes in Drug Delivery—A Comprehensive Review on Its Structural Components, Preparation Techniques and Therapeutic Applications. Biomedicines. 2023;11(4):1114. doi:10.3390/biomedicines11041114 PubMed PMID: 37189732; PubMed Central PMCID: PMC10135881.

15. Athulya KR, Varughese T, Kumar AC. Polymersomes: Beyond Basics-Synthesis, Stimuli Response and Biomedical Applications. ChemistrySelect. 2024;9(36):e202402040. doi:10.1002/slct.202402040

16. Liga S, Paul C, Moacă EA, Péter F. Niosomes: Composition, Formulation Techniques, and Recent Progress as Delivery Systems in Cancer Therapy. Pharmaceutics. 2024;16(2):223. doi:10.3390/pharmaceutics16020223 PubMed PMID: 38399277; PubMed Central PMCID: PMC10892933.

17. Salem EM, Dawaba HM, Elbaset MA, Gad S, Hassan TH. Optimizing bioavailability and antihypertensive activity of Carvedilol cubosomes using D-optimal design: Comparative analysis of Cremophor RH 40 and Polyvinyl alcohol as secondary stabilizers. Journal of Drug Delivery Science and Technology. 2024;97:105817. doi:10.1016/j.jddst.2024.105817

18. Chaw CS, Kim KYA. Effect of formulation compositions on niosomal preparations. Pharm Dev Technol. 2013;18(3):667–72. doi:10.3109/10837450.2012.672988 PubMed PMID: 22468904.

19. Bulbake U, Doppalapudi S, Kommineni N, Khan W. Liposomal Formulations in Clinical Use: An Updated Review. Pharmaceutics. 2017;9(2):12. doi:10.3390/pharmaceutics9020012 PubMed PMID: 28346375; PubMed Central PMCID: PMC5489929.

20. Gao S, Sui Z, Jiang Q, Jiang Y. Functional Evaluation of Niosomes Utilizing Surfactants in Nanomedicine Applications. Int J Nanomedicine. 2024;19:10283–305. doi:10.2147/IJN.S480639 PubMed PMID: 39403709; PubMed Central PMCID: PMC11472738.

21. Bautista-Solano AA, Dávila-Ortiz G, Perea-Flores M de J, Martínez-Ayala AL. A Comprehensive Review of Niosomes: Composition, Structure, Formation,

Characterization, and Applications in Bioactive Molecule Delivery Systems. Molecules. 2025;30(17). doi:10.3390/molecules30173467

22. Sharma B, Attri S, Syal J, Sharma U, Sharma B, Attri S, et al. Liposomal Nanoparticles: A Viable Nanoscale Drug Carriers for the Treatment of Cancer. In: Liposomes - Recent Advances, New Perspectives and Applications [Internet]. IntechOpen; 2023 [cited 2026 Mar 2]. Available from: https://www.intechopen.com/chapters/85673 doi:10.5772/intechopen.109581

23. Yeo LK, Chaw CS, Elkordy AA. The Effects of Hydration Parameters and Co-Surfactants on Methylene Blue-Loaded Niosomes Prepared by the Thin Film Hydration Method. Pharmaceuticals (Basel). 2019;12(2):46. doi:10.3390/ph12020046 PubMed PMID: 30934834; PubMed Central PMCID: PMC6631696.

24. Mawazi SM, Ge Y, Widodo RT. Niosome Preparation Techniques and Structure—An Illustrated Review. Pharmaceutics. 2025;17(1):67. doi:10.3390/pharmaceutics17010067 PubMed PMID: 39861715; PubMed Central PMCID: PMC11768252.

25. Bhardwaj P, Tripathi P, Gupta R, Pandey S. Niosomes: A review on niosomal research in the last decade. Journal of Drug Delivery Science and Technology. 2020;56:101581. doi:10.1016/j.jddst.2020.101581

26. Ababei-Bobu A, Profire B Ștefania, Iacob AT, Chirliu OM, Lupașcu FG, Profire L. Niosomes as Vesicular Carriers: From Formulation Strategies to Stimuli-Responsive Innovative Modulations for Targeted Drug Delivery. Pharmaceutics. 2025;17(11). doi:10.3390/pharmaceutics17111473

27. Liu Y, Binks BP. Fabrication of Stable Oleofoams with Sorbitan Ester Surfactants. Langmuir. 2022;38(48):14779–88. doi:10.1021/acs.langmuir.2c02413 PubMed PMID: 36410861; PubMed Central PMCID: PMC9730906.

28. Okorafor EA, Gordon EA, Sahu ID, Shah MZ, Konkolewicz D, Lorigan GA. Influence of Lipid Saturation on the Structural Properties of Styrene Maleic Acid Lipid Nanoparticles (SMALPs). Biochim Biophys Acta Biomembr. 2025;1867(5–6):184424. doi:10.1016/j.bbamem.2025.184424 PubMed PMID: 40412742; PubMed Central PMCID: PMC12490428.

29. Hadjipour A, Essa EA, Elkordy AA. A glance into factors affecting the possible combined entrapment of curcumin and methylene blue into niosomal formulations as a potential anticancer therapy. Journal of Drug Delivery Science and Technology. 2024;100:106120. doi:10.1016/j.jddst.2024.106120

30. Shafiepour M, Razavi SH, Khanniri E, Jahan FM, Nouri M, Afraei M. Nanocarriers for foods: A review of niosomes and proniosomes in bioactive compounds. Food and Humanity. 2025;4:100623. doi:10.1016/j.foohum.2025.100623

31. Das A, Parta A, Mitra RK. Modulation of anionic reverse micellar interface with non-ionic surfactants can regulate enzyme activity within the micellar waterpool. Colloid Polym Sci. 2016;294(4):715–26. doi:10.1007/s00396-016-3829-3

32. Yasamineh S, Yasamineh P, Ghafouri Kalajahi H, Gholizadeh O, Yekanipour Z, Afkhami H, et al. A state-of-the-art review on the recent advances of niosomes as a targeted drug delivery system. International Journal of Pharmaceutics. 2022;624:121878. doi:10.1016/j.ijpharm.2022.121878

33. Nollet M, Boulghobra H, Calligaro E, Rodier JD. An efficient method to determine the Hydrophile-Lipophile Balance of surfactants using the phase inversion temperature deviation of CiEj/n-octane/water emulsions. International Journal of Cosmetic Science. 2019;41(2):99–108. doi:10.1111/ics.12516

34. Thakare M, Israel B, Garner J Solomon, Ahmed H, Elder D, Capomacchia A. Nonionic surfactant structure on the drug release, formulation and physical properties of ethylcellulose microspheres. Pharmaceutical Development and Technology. 2016;22:1–27. doi:10.1080/10837450.2016.1221431

35. Kumar GP, Rajeshwarrao P. Nonionic surfactant vesicular systems for effective drug delivery—an overview. Acta Pharmaceutica Sinica B. 2011;1(4):208–19. doi:10.1016/j.apsb.2011.09.002

36. Chen S, Hanning S, Falconer J, Locke M, Wen J. Recent advances in non-ionic surfactant vesicles (niosomes): Fabrication, characterization, pharmaceutical and cosmetic applications. European Journal of Pharmaceutics and Biopharmaceutics. 2019;144:18–39. doi:10.1016/j.ejpb.2019.08.015

37. Kobierski J, Wnętrzak A, Chachaj-Brekiesz A, Dynarowicz-Latka P. Predicting the packing parameter for lipids in monolayers with the use of molecular dynamics. Colloids and Surfaces B: Biointerfaces. 2022;211:112298. doi:10.1016/j.colsurfb.2021.112298

38. Khodadadi E, Khodadadi E, Chaturvedi P, Moradi M. Comprehensive Insights into the Cholesterol-Mediated Modulation of Membrane Function Through Molecular Dynamics Simulations. Membranes (Basel). 2025;15(6):173. doi:10.3390/membranes15060173 PubMed PMID: 40559352; PubMed Central PMCID: PMC12195132.

39. Alberts B, Johnson A, Lewis J, Raff M, Roberts K, Walter P. The Lipid Bilayer. In: Molecular Biology of the Cell. 4th edition [Internet]. Garland Science; 2002 [cited 2026 Mar 4]. Available from: https://www.ncbi.nlm.nih.gov/books/NBK26871/

40. Abdelkader H, Alani AWG, Alany RG. Recent advances in non-ionic surfactant vesicles (niosomes): self-assembly, fabrication, characterization, drug delivery applications and limitations. Drug Delivery. 2014;21(2):87–100. doi:10.3109/10717544.2013.838077 PubMed PMID: 24156390.

41. Fadaei MS, Fadaei MR, Kheirieh AE, Rahmanian-Devin P, Dabbaghi MM, Nazari Tavallaei K, et al. Niosome as a promising tool for increasing the effectiveness of anti-inflammatory compounds. EXCLI J. 2024;23:212–63. doi:10.17179/excli2023-6868 PubMed PMID: 38487088; PubMed Central PMCID: PMC10938253.

42. Poustforoosh A. The impact of cationic/anionic ratio on the physicochemical aspects of catanionic niosomes as a promising carrier for anticancer drugs. Journal of Molecular Liquids. 2024;408:125338. doi:10.1016/j.molliq.2024.125338

43. Han X, Zhang H, Butowska K, Swingle KL, Alameh MG, Weissman D, et al. An ionizable lipid toolbox for RNA delivery. Nat Commun. 2021;12:7233. doi:10.1038/s41467-021-27493-0 PubMed PMID: 34903741; PubMed Central PMCID: PMC8668901.

44. Weerapol Y, Limmatvapirat S, Nunthanid J, Sriamornsak P. Self-Nanoemulsifying Drug Delivery System of Nifedipine: Impact of Hydrophilic–Lipophilic Balance and Molecular Structure of Mixed Surfactants. AAPS PharmSciTech. 2014;15. doi:10.1208/s12249-014-0078-y

45. Elkordy AA, Chaw CS, Yeo LK. Effects of preparation methods on the characteristics of niosomes. British Journal of Pharmacy. 2019;4(1):1. doi:10.5920/bjpharm.616

46. Downloads [Internet]. [cited 2025 Apr 5]. Available from: https://products.basf.com/basf/products/global/en/downloads

47. Hemati M, Haghiralsadat F, Yazdian F, Jafari F, Moradi A, Malekpour-Dehkordi Z. Development and characterization of a novel cationic PEGylated niosome-encapsulated forms of doxorubicin, quercetin and siRNA for the treatment of cancer by using combination therapy. Artificial Cells, Nanomedicine, and Biotechnology. 2019;47(1):1295–311. doi:10.1080/21691401.2018.1489271 PubMed PMID: 30033768.

48. Afereydoon S, Haghiralsadat F, Hamzian N, Shams A, Hemati M, Naghib SM, et al. Multifunctional PEGylated Niosomal Nanoparticle-Loaded Herbal Drugs as a Novel Nano-Radiosensitizer and Stimuli-Sensitive Nanocarrier for Synergistic Cancer Therapy. Front Bioeng Biotechnol. 2022;10:917368. doi:10.3389/fbioe.2022.917368 PubMed PMID: 36046674; PubMed Central PMCID: PMC9421251.

49. DSPE PEG2k-OH | 3056014-08-2 | Avanti Research [Internet]. [cited 2026 Mar 4]. Available from: https://www.avantiresearch.com/en-gb/products/product/880172-dspe-peg2k-oh

50. Sun D, Lu ZR. Structure and Function of Cationic and Ionizable Lipids for Nucleic Acid Delivery. Pharm Res. 2023;40(1):27–46. doi:10.1007/s11095-022-03460-2 PubMed PMID: 36600047; PubMed Central PMCID: PMC9812548.

51. Jung HN, Lee SY, Lee S, Youn H, Im HJ. Lipid nanoparticles for delivery of RNA therapeutics: Current status and the role of in vivo imaging. Theranostics. 2022;12(17):7509–31. doi:10.7150/thno.77259 PubMed PMID: 36438494; PubMed Central PMCID: PMC9691360.

52. Bangham AD, Standish MM, Watkins JC. Diffusion of univalent ions across the lamellae of swollen phospholipids. J Mol Biol. 1965;13(1):238–52. doi:10.1016/s0022-2836(65)80093-6 PubMed PMID: 5859039.

53. Durak S, Esmaeili Rad M, Alp Yetisgin A, Eda Sutova H, Kutlu O, Cetinel S, et al. Niosomal Drug Delivery Systems for Ocular Disease—Recent Advances and Future Prospects. Nanomaterials (Basel). 2020;10(6):1191. doi:10.3390/nano10061191 PubMed PMID: 32570885; PubMed Central PMCID: PMC7353242.

54. Lombardo D, Kiselev MA. Methods of Liposomes Preparation: Formation and Control Factors of Versatile Nanocarriers for Biomedical and Nanomedicine Application. Pharmaceutics. 2022;14(3):3. doi:10.3390/pharmaceutics14030543

55. Yeo LK, Olusanya TOB, Chaw CS, Elkordy AA. Brief Effect of a Small Hydrophobic Drug (Cinnarizine) on the Physicochemical Characterisation of Niosomes Produced by Thin-Film Hydration and Microfluidic Methods. Pharmaceutics. 2018;10(4):185. doi:10.3390/pharmaceutics10040185 PubMed PMID: 30322124; PubMed Central PMCID: PMC6321096.

56. Naderi M, Saidi S, Barani M. Advancements in microfluidic-based synthesis of niosomes for cancer and infection therapy: A comprehensive review. Journal of Molecular Liquids. 2025;434:128048. doi:10.1016/j.molliq.2025.128048

57. Obeid MA, Khadra I, Albaloushi A, Mullin M, Alyamani H, Ferro VA. Microfluidic manufacturing of different niosomes nanoparticles for curcumin encapsulation: Physical characteristics, encapsulation efficacy, and drug release. Beilstein J Nanotechnol. 2019;10(1):1826–32. doi:10.3762/bjnano.10.177

58. Khan DH, Bashir S, Khan MI, Figueiredo P, Santos HA, Peltonen L. Formulation optimization and *in vitro* characterization of rifampicin and ceftriaxone dual drug loaded niosomes with high energy probe sonication technique. Journal of Drug Delivery Science and Technology. 2020;58:101763. doi:10.1016/j.jddst.2020.101763

59. Khan MI, Madni A, Hirvonen J, Peltonen L. Ultrasonic Processing Technique as a Green Preparation Approach for Diacerein-Loaded Niosomes. AAPS PharmSciTech. 2017;18(5):1554–63. doi:10.1208/s12249-016-0622-z

60. Ly PD, Ly KN, Phan HL, Nguyen HHT, Duong VA, Nguyen HV. Recent advances in surface decoration of nanoparticles in drug delivery. Front Nanotechnol. 2024;6. doi:10.3389/fnano.2024.1456939

61. Khalil IA, Faheem A, El-Tanani M. Targeted Drug Delivery to the Spleen and Its Implications for the Prevention and Treatment of Cancer. Pharmaceutics. 2025;17(5). doi:10.3390/pharmaceutics17050651

62. Moammeri A, Chegeni MM, Sahrayi H, Ghafelehbashi R, Memarzadeh F, Mansouri A, et al. Current advances in niosomes applications for drug delivery and cancer treatment. Materials Today Bio. 2023;23:100837. doi:10.1016/j.mtbio.2023.100837

63. What is the Polydispersity Index (PDI) in Dynamic Light Scattering (DLS)? [Internet]. [cited 2026 Mar 6]. Available from: https://www.malvernpanalytical.com/en/learn/knowledge-center/insights/dynamic-mine-column-in-dls-what-is-polyvariance-index-pdi

64. Nowroozi F, Almasi A, Javidi J, Haeri A, Dadashzadeh S. Effect of Surfactant Type, Cholesterol Content and Various Downsizing Methods on the Particle Size of Niosomes. Iran J Pharm Res. 2018;17(Suppl2):1–11. PubMed PMID: 31011337; PubMed Central PMCID: PMC6447874.

65. Extruder Kits & More | Avanti Research [Internet]. [cited 2026 Mar 6]. Available from: https://www.avantiresearch.com/en-gb/services/equipment-products

66. LIPEX® LIPOSOME EXTRUDERS [Internet]. [cited 2026 Mar 6]. Available from: https://healthcare.evonik.com/en/drugdelivery/parenteral-drug-delivery/lipex-liposome-extruders

67. Klisch S, Gilbert D, Breaux E, Dalier A, Gupta S, Jakobi B, et al. Building a Simplistic Automatic Extruder: Instrument Development Opportunities for the Laboratory. J Chem Educ. 2024;101(8):3292–300. doi:10.1021/acs.jchemed.4c00287

68. Weiss VU, Urey C, Gondikas A, Golesne M, Friedbacher G, Von Der Kammer F, et al. Nano electrospray gas-phase electrophoretic mobility molecular analysis (nES GEMMA) of liposomes: applicability of the technique for nano vesicle batch control. Analyst. 2016;141(21):6042–50. doi:10.1039/C6AN00687F

69. Constant Pressure-controlled Extrusion Method for the Preparation of Nano-sized Lipid Vesicles - PMC [Internet]. [cited 2026 Mar 6]. Available from: https://pmc.ncbi.nlm.nih.gov/articles/PMC3471306/

70. Preparation of VC nanoliposomes by high pressure homogenization: Process optimization and evaluation of efficacy, transdermal absorption, and stability: Heliyon [Internet]. [cited 2026 Mar 6]. Available from: https://www.cell.com/heliyon/fulltext/S2405-8440%2824%2905547-6

71. Liposome Processing: High-Pressure Homogenizer or Liposome Extruder? [Internet]. [cited 2026 Mar 6]. Available from: https://www.genizer.com/info/liposome-processing-high-pressure-homogenizer-or-liposome-extruder_i0042.html?srsltid=AfmBOoq4ilUpDpJs-OsfehB9CsqWn8VfK5lDNj0ab0FpwlPqc0sM-AbS

72. Mineart KP, Kelley EG. Size reduction, purification, sterilization and storage/packaging of liposomes. In: Liposomes in Drug Delivery [Internet]. Elsevier; 2024 [cited 2026 Mar 6]. p. 489–515. Available from: https://linkinghub.elsevier.com/retrieve/pii/B978044315491100016X doi:10.1016/B978-0-443-15491-1.00016-X

73. Owodeha-Ashaka K, Ilomuanya MO, Iyire A. Evaluation of sonication on stability-indicating properties of optimized pilocarpine hydrochloride-loaded niosomes in ocular drug delivery. Prog Biomater. 2021;10:207–20. doi:10.1007/s40204-021-00164-5 PubMed PMID: 34549376; PubMed Central PMCID: PMC8511210.

74. EP3354260A1 - Methods for coacervation induced liposomal encapsulation and formulations thereof - Google Patents [Internet]. [cited 2026 Mar 7]. Available from: https://patents.google.com/patent/EP3354260A1/en

75. Odeh F, Nsairat H, Alshaer W, Alsotari S, Buqaien R, Ismail S, et al. Remote loading of curcumin-in-modified β-cyclodextrins into liposomes using a transmembrane pH gradient. RSC Adv. 2019;9(64):37148–61. doi:10.1039/C9RA07560G

76. Zhigaltsev IV, Maurer N, Akhong QF, Leone R, Leng E, Wang J, et al. Liposome-encapsulated vincristine, vinblastine and vinorelbine: A comparative study of drug loading and retention. Journal of Controlled Release. 2005;104(1):103–11. doi:10.1016/j.jconrel.2005.01.010

77. Acid-Base Concepts [Internet]. [cited 2026 Mar 7]. Available from: https://www.sciencedirect.com/science/chapter/monograph/abs/pii/B9780323034104500079 doi:10.1016/B978-0-323-03410-4.50007-9

78. Lemke TL, Williams DA. Foye's Principles of Medicinal Chemistry. Lippincott Williams & Wilkins; 2008. 1406 p.

79. myocet-liposomal-epar-product-information_en.pdf [Internet]. [cited 2026 Mar 7]. Available from: https://www.ema.europa.eu/en/documents/product-information/myocet-liposomal-epar-product-information_en.pdf

80. Alyane M, Barratt G, Lahouel M. Remote loading of doxorubicin into liposomes by transmembrane pH gradient to reduce toxicity toward H9c2 cells. Saudi Pharmaceutical Journal. 2016;24(2):165–75. doi:10.1016/j.jsps.2015.02.014

81. digi-14230-pdf.pdf [Internet]. [cited 2026 Mar 7]. Available from: https://cdn.cytivalifesciences.com/api/public/content/digi-14230-pdf

82. Guide to Gel Filtration or Size Exclusion Chromatography.

83. Engudar G, Schaarup-Jensen H, Fliedner FP, Hansen AE, Kempen P, Jølck RI, et al. Remote loading of liposomes with a ^{124}I-radioiodinated compound and their *in vivo* evaluation by PET/CT in a murine tumor model. Theranostics. 2018;8(21):5828–41. doi:10.7150/thno.26706

84. Mihaila R, Chang S, Wei AT, Hu ZY, Ruhela D, Shadel TR, et al. Lipid nanoparticle purification by Spin Centrifugation–Dialysis (SCD): A facile and high-throughput approach for small scale preparation of siRNA–lipid complexes. International Journal of Pharmaceutics. 2011;420(1):118–21. doi:10.1016/j.ijpharm.2011.08.017

85. Trémouille L, Charcosset C. Preparation of liposomes, lipid nanoparticles, or polymer nanoparticles by nanoprecipitation and their purification: Where are membrane processes? Current Opinion in Colloid & Interface Science. 2026;82:101989. doi:10.1016/j.cocis.2025.101989

86. Cave G, Kee R, Harvey M, Wu Z. pH Gradient Liposomes Extract Protein Bound Amitriptyline in Peritoneal Dialysis—Exploratory Work. International Journal of Molecular Sciences. 2022;23(19). doi:10.3390/ijms231911577

87. Forster V, Luciani P, Leroux JC. Treatment of calcium channel blocker-induced cardiovascular toxicity with drug scavenging liposomes. Biomaterials. 2012;33(13):3578–85. doi:10.1016/j.biomaterials.2012.01.042

88. Forster V, Signorell RD, Roveri M, Leroux JC. Liposome-supported peritoneal dialysis for detoxification of drugs and endogenous metabolites. Science Translational Medicine. 2014;6(258):258ra141-258ra141. doi:10.1126/scitranslmed.3009135

89. De Silva L, Fu JY, Htar TT, Muniyandy S, Kasbollah A, Wan Kamal WHB, et al. Characterization, optimization, and in vitro evaluation of Technetium-99m-labeled niosomes. Int J Nanomedicine. 2019;14:1101–17. doi:10.2147/IJN.S184912 PubMed PMID: 30863048; PubMed Central PMCID: PMC6391155.

90. Dynamic light scattering common terms defined.pdf [Internet]. [cited 2026 Mar 7]. Available from: https://facilities.bioc.cam.ac.uk/files/media/dls_terms_defined_malvern.pdf.

91. Zainol N, Siew Chin C, Rashidah Ahmed N, Zainol N, Abdul Aziz A, Sabtu R, et al. Optimization study on Niosome Loaded Ficus Deltodia Extract. Hamontree C, editor. MATEC Web Conf. 2018;192:03025. doi:10.1051/matecconf/201819203025

92. Ugorji OL, Umeh ONC, Agubata CO, Adah D, Obitte NC, Chukwu A. The effect of noisome preparation methods in encapsulating 5-fluorouracil and real time cell assay against HCT-116 colon cancer cell line. Heliyon. 2022;8(12):e12369. doi:10.1016/j.heliyon.2022.e12369 PubMed PMID: 36582708; PubMed Central PMCID: PMC9793284.

93. Roces CB, Port EC, Daskalakis NN, Watts JA, Aylott JW, Halbert GW, et al. Rapid scale-up and production of active-loaded PEGylated liposomes. International Journal of Pharmaceutics. 2020;586:119566. doi:10.1016/j.ijpharm.2020.119566

94. Zeta Potential - Overview [Internet]. [cited 2026 Mar 7]. Available from: https://www.malvernpanalytical.com/en/products/measurement-type/zeta-potential

95. Understanding the zeta potential of nanomaterials through predictive nanoinformatics. Nano Today. 2025;64:102783. doi:10.1016/j.nantod.2025.102783

96. Izumi K, Ji J, Koiwai K, Kawano R. Long-Term Stable Liposome Modified by PEG-Lipid in Natural Seawater. ACS Omega. 2024;9(9):10958–66. doi:10.1021/acsomega.3c10346 PubMed PMID: 38463291; PubMed Central PMCID: PMC10918668.

97. Shiri S, Gharanjig K, Tahghighi A, Hosseinnezhad M, Etezad M. Formulation and characterization of BBR loaded niosomes using saponin as a nonionic biosurfactant investigating synergistic effects to enhance antibacterial activity. Sci Rep. 2025;15(1):5231. doi:10.1038/s41598-025-87950-4

98. Aldawsari MF, Khafagy ES, Moglad EH, Selim Abu Lila A. Formulation optimization, *in vitro* and *in vivo* evaluation of niosomal nanocarriers for enhanced topical delivery of cetirizine. Saudi Pharmaceutical Journal. 2023;31(9):101734. doi:10.1016/j.jsps.2023.101734

99. Hermida LG, Sabés-Xamaní M, Barnadas-Rodríguez R. Combined strategies for liposome characterization during in vitro digestion. Journal of Liposome Research. 2009;19(3):207–19. doi:10.1080/08982100902740847 PubMed PMID: 19548842.

100. Joguparthi V, Feng S, Anderson BD. Determination of Intraliposomal pH and its Effect on Membrane Partitioning and Passive Loading of a Hydrophobic Camptothecin, DB-67. Int J Pharm. 2008;352(1–2):17–28. doi:10.1016/j.ijpharm.2007.10.003 PubMed PMID: 18065174; PubMed Central PMCID: PMC2277365.

101. Horie M, Yanagisawa H, Sugawara M. Fluorometric immunoassay based on pH-sensitive dye-encapsulating liposomes and gramicidin channels. Anal Biochem. 2007;369(2):192–201. doi:10.1016/j.ab.2007.07.007 PubMed PMID: 17718997.

102. Christine Kemmer G, Ammitzbøll Bogh S, Urban M, G. Palmgren M, Vosch T, Schiller J, et al. Lipid-conjugated fluorescent pH sensors for monitoring pH changes in reconstituted membrane systems. Analyst. 2015;140(18):6313–20. doi:10.1039/C5AN01180A

103. Leiding T, Górecki K, Kjellman T, Vinogradov SA, Hägerhäll C, Årsköld SP. Precise detection of pH inside large unilamellar vesicles using membrane-impermeable dendritic porphyrin-based nanoprobes. Anal Biochem. 2009;388(2):296–305. doi:10.1016/j.ab.2009.02.023 PubMed PMID: 19248752; PubMed Central PMCID: PMC2804896.

104. Bhowmick SB, Namdeo AB, Natarajan J, Jain P. Process for the preparation of doxorubicin liposomes [Internet]. WO2010092590A2, 2010 [cited 2026 Mar 7]. Available from: https://patents.google.com/patent/WO2010092590A2/en

105. Zhu Y, Wang F, Zhao Y, Zheng X. Pegylated liposomal doxorubicin-related palmar-plantar erythrodysesthesia: a literature review of pharmaceutical and clinical

aspects. Eur J Hosp Pharm. 2021;28(3):124–8. doi:10.1136/ejhpharm-2020-002311 PubMed PMID: 32591480; PubMed Central PMCID: PMC8077615.

106. Barenholz Y. Doxil®--the first FDA-approved nano-drug: lessons learned. J Control Release. 2012;160(2):117–34. doi:10.1016/j.jconrel.2012.03.020 PubMed PMID: 22484195.

107. d'Avanzo N, Sidorenko V, Simón-Gracia L, Rocchi A, Ottonelli I, Ruozi B, et al. C-end rule peptide-guided niosomes for prostate cancer cell targeting. Journal of Drug Delivery Science and Technology. 2024;91:105162. doi:10.1016/j.jddst.2023.105162

108. ResearchGate [Internet]. [cited 2025 Apr 3]. (PDF) Doxorubicin: An Overview of the Anti-Cancer and Chemoresistance Mechanisms OPEN ACCESS. Available from: https://www.researchgate.net/publication/346969867_Doxorubicin_An_Overview_of_the_Anti-Cancer_and_Chemoresistance_Mechanisms_OPEN_ACCESS

109. Drake P, Amalina I, Sari R, Ruiz A, Ramazan S, Hope G, et al. Magnetically induced drug release from niosome-based nanocarriers loaded with doxorubicin. Soft Matter. 2025;21(31):6197–206. doi:10.1039/D5SM00411J

110. Bragagni M, Mennini N, Ghelardini C, Mura P. Development and characterization of niosomal formulations of doxorubicin aimed at brain targeting. J Pharm Pharm Sci. 2012;15(1):184–96. doi:10.18433/j3230m PubMed PMID: 22365096.

111. Yamada Y. Dimerization of Doxorubicin Causes Its Precipitation. ACS Omega. 2020;5(51):33235–41. doi:10.1021/acsomega.0c04925 PubMed PMID: 33403285; PubMed Central PMCID: PMC7774281.

112. Zaer M, Moeinzadeh A, Abolhassani H, Rostami N, Tavakkoli Yaraki M, Seyedi SA, et al. Doxorubicin-loaded Niosomes functionalized with gelatine and alginate as pH-responsive drug delivery system: A 3D printing approach. International Journal of Biological Macromolecules. 2023;253:126808. doi:10.1016/j.ijbiomac.2023.126808

113. Doxorubicin decomposition on storage. Effect of pH, type of buffer and liposome encapsulation - ScienceDirect [Internet]. [cited 2026 Mar 9]. Available from: https://www.sciencedirect.com/science/article/abs/pii/0378517385902170

114. Kolliphor® HS 15 - An Enabler for Parenteral and Oral Formulations [Internet]. [cited 2025 Apr 4]. Available from: https://www.americanpharmaceuticalreview.com/Featured-Articles/358749-Kolliphor-HS-15-An-Enabler-for-Parenteral-and-Oral-Formulations

115. Yan H, Zhang Z, Jia X, Song J. d-α-Tocopheryl polyethylene glycol succinate/Solutol HS 15 mixed micelles for the delivery of baohuoside I against non-small-cell lung cancer: optimization and in vitro, in vivo evaluation. Int J Nanomedicine. 2016;11:4563–71. doi:10.2147/IJN.S112204 PubMed PMID: 27660448; PubMed Central PMCID: PMC5019457.

116. Katrajkar K, Darji L, Kethavath D, Thakkar S, Kshirsagar B, Misra M. Shedding light on interaction of so called inactive ingredients (excipients) with permeability-glycoprotein. Journal of Drug Delivery Science and Technology. 2019;52:531–52. doi:10.1016/j.jddst.2019.05.022

117. Strickley RG. Solubilizing excipients in oral and injectable formulations. Pharm Res. 2004;21(2):201–30. doi:10.1023/b:pham.0000016235.32639.23 PubMed PMID: 15032302.

118. UV-Visible Spectroscopy [Internet]. [cited 2025 Apr 3]. Available from: https://www2.chemistry.msu.edu/faculty/reusch/virttxtjml/spectrpy/uv-vis/spectrum.htm

119. Pratiwi RA, Nandiyanto ABD. How to Read and Interpret UV-VIS Spectrophotometric Results in Determining the Structure of Chemical Compounds. Indonesian Journal of Educational Research and Technology. 2022;2(1):1–20. doi:10.17509/ijert.v2i1.35171

120. Seleci D, Seleci M, Walter JG, Stahl F, Scheper T. Niosomes as Nanoparticular Drug Carriers: Fundamentals and Recent Applications. Journal of Nanomaterials. 2016;2016(1):7372306. doi:10.1155/2016/7372306

121. Somjid S, Krongsuk S, Johns JR. Cholesterol concentration effect on the bilayer properties and phase formation of niosome bilayers: A molecular dynamics simulation study. Journal of Molecular Liquids. 2018;256:591–8. doi:10.1016/j.molliq.2018.02.077

122. Basak S, Das TK. Liposome-Based Drug Delivery Systems: From Laboratory Research to Industrial Production—Instruments and Challenges. ChemEngineering. 2025;9(3). doi:10.3390/chemengineering9030056

123. Nikitina NA, Reshetnyak EA, Svetlova NV, Mchedlov-Petrossyan NO. Protolytic properties of dyes embedded in gelatin films. J Braz Chem Soc. 2011;22:857–66. doi:https://doi.org/10.1590/S0103-50532011000500007

124. Bromocresol green - Bromocresol green [Internet]. [cited 2025 Apr 3]. Available from: https://www.sigmaaldrich.com/FR/en/substance/bromocresolgreen6980176608

125. Shokrollahi A, Firoozbakht. F. Determination of the acidity constants of neutral red and bromocresol green by solution scanometric method and comparison with spectrophotometric results. Beni-Suef University Journal of Basic and Applied Sciences. 2016;5(1):13–20. doi:10.1016/j.bjbas.2016.02.003

126. Hashemi Dehaghi M, Haeri A, Keshvari H, Abbasian Z, Dadashzadeh S. Dorzolamide Loaded Niosomal Vesicles: Comparison of Passive and Remote Loading Methods. Iran J Pharm Res. 2017;16(2):413–22. PubMed PMID: 28979296; PubMed Central PMCID: PMC5603850.

127. Shi NQ, Qi XR, Xiang B. Preparation and Characterization of Drug Liposomes by pH-Gradient Method. In: Lu WL, Qi XR, editors. Liposome-Based Drug Delivery Systems [Internet]. Berlin, Heidelberg: Springer; 2021 [cited 2025 Apr 2]. p. 47–58. Available from: https://doi.org/10.1007/978-3-662-49320-5_18 doi:10.1007/978-3-662-49320-5_18

128. Gabizon AA, Gabizon-Peretz S, Modaresahmadi S, La-Beck NM. Thirty years from FDA approval of pegylated liposomal doxorubicin (Doxil/Caelyx): an updated analysis and future perspective. bmjonc. 2025;4(1). doi:10.1136/bmjonc-2024-000573 PubMed PMID: 10.1136/bmjonc-2024-000573.

129. Yang K, Tran K, Salvati A. Tuning Liposome Stability in Biological Environments and Intracellular Drug Release Kinetics. Biomolecules. 2022;13(1):59. doi:10.3390/biom13010059 PubMed PMID: 36671444; PubMed Central PMCID: PMC9855369.

130. Arslanov VV, Krylov DI. Reassembly of the vesicular structure of niosomes after their destruction in a mechanical field. Journal of Colloid and Interface Science. 2024;662:342–56. doi:10.1016/j.jcis.2024.02.035

131. Dos Santos N, Cox KA, McKenzie CA, van Baarda F, Gallagher RC, Karlsson G, et al. pH gradient loading of anthracyclines into cholesterol-free liposomes: enhancing drug loading rates through use of ethanol. Biochimica et Biophysica Acta (BBA) - Biomembranes. 2004;1661(1):47–60. doi:10.1016/j.bbamem.2003.11.016

132. Thabet Y, Elsabahy M, Eissa NG. Methods for preparation of niosomes: A focus on thin-film hydration method. Methods. 2022;Methods for Preparation of Nanoconstructs199:9–15. doi:10.1016/j.ymeth.2021.05.004

133. Span® 60 CAS 1338-41-6 | 840121 [Internet]. [cited 2025 Apr 26]. Available from: https://www.merckmillipore.com/GB/en/product/Span-60,MDA_CHEM-840121

134. Aloss K, Hamar P. Recent Preclinical and Clinical Progress in Liposomal Doxorubicin. Pharmaceutics. 2023;15(3):893. doi:10.3390/pharmaceutics15030893 PubMed PMID: 36986754; PubMed Central PMCID: PMC10054554.

135. Annisa R. Spanlastic as a Transdermal Drug Delivery System: A Systematic Review. Biomedical and Pharmacology Journal. 2025;18(1):447–57.

136. de Souza HMR, Guedes JS, Freitas RHCN, Gelves LGV, Fokoue HH, Sant'Anna CMR, et al. Comparative chemical and biological hydrolytic stability of homologous esters and isosteres. J Enzyme Inhib Med Chem. 37(1):718–27. doi:10.1080/14756366.2022.2027933 PubMed PMID: 35156494; PubMed Central PMCID: PMC8856110.

137. Mohsen AM, Wagdi MA, Salama A. Rutin loaded bilosomes for enhancing the oral activity and nephroprotective effects of rutin in potassium dichromate induced

acute nephrotoxicity in rats. Scientific Reports. 2024;14:23799. doi:10.1038/s41598-024-73567-6 PubMed PMID: 39394242.

138. Sorbitan monopalmitate - Span® 40 [Internet]. [cited 2025 Apr 26]. Available from: https://www.sigmaaldrich.com/FR/en/substance/sorbitanmonopalmitate4025726266579

139. Fatima MT, Islam Z, Ahmad E, Barreto GE, Md Ashraf G. Ionic gradient liposomes: Recent advances in the stable entrapment and prolonged released of local anesthetics and anticancer drugs. Biomedicine & Pharmacotherapy. 2018;107:34–43. doi:10.1016/j.biopha.2018.07.138

140. Lambros M, Tran T (Henry), Fei Q, Nicolaou M. Citric Acid: A Multifunctional Pharmaceutical Excipient. Pharmaceutics. 2022;14(5):972. doi:10.3390/pharmaceutics14050972 PubMed PMID: 35631557; PubMed Central PMCID: PMC9148065.

141. RLO: Acids Alkalis and Bases: Further application [Internet]. [cited 2025 Apr 11]. Available from: https://www.nottingham.ac.uk/helmopen/rlos/biological-sciences/acid_base_further_app/page_two.html

142. HEPES Buffer, 7365-45-9, High-Purity, H3375, Sigma-Aldrich [Internet]. [cited 2025 Apr 11]. Available from: https://www.sigmaaldrich.com/FR/en/product/sigma/h3375

143. Trizma base, 77-86-1, High-Purity, T1503, Sigma-Aldrich [Internet]. [cited 2025 Apr 11]. Available from: https://www.sigmaaldrich.com/FR/en/product/sigma/t1503

144. Electrophoretic behavior of charge regulated zwitter ionic buffers in covalently and dynamically coated fused silica capillaries. Bulletin of Faculty of Pharmacy, Cairo University. 2014;52(1):71–8. doi:10.1016/j.bfopcu.2014.03.001

145. Bi H, Xue J, Jiang H, Gao S, Yang D, Fang Y, et al. Current developments in drug delivery with thermosensitive liposomes. Asian J Pharm Sci. 2019;14(4):365–79. doi:10.1016/j.ajps.2018.07.006 PubMed PMID: 32104466; PubMed Central PMCID: PMC7032122.

146. Somjid S, Shinsuphan N, Temprom L, Krongsuk S. Effects of cholesterol and temperature on structural properties and dynamic behavior of niosome bilayers with melatonin Inclusion: A Coarse-Grained simulation study. Journal of Molecular Liquids. 2022;368:120686. doi:10.1016/j.molliq.2022.120686

147. Pei D. How Do Biomolecules Cross the Cell Membrane? Acc Chem Res. 2022;55(3):309–18. doi:10.1021/acs.accounts.1c00560 PubMed PMID: 35015508; PubMed Central PMCID: PMC9175464.

148. Cheung TH, Shoichet MS. The Interplay of Endosomal Escape and RNA Release from Polymeric Nanoparticles. Langmuir. 2025;41(11):7174–90. doi:10.1021/acs.langmuir.4c05176

149. Smith SA, Selby LI, Johnston APR, Such GK. The Endosomal Escape of Nanoparticles: Toward More Efficient Cellular Delivery. Bioconjugate Chem. 2019;30(2):263–72. doi:10.1021/acs.bioconjchem.8b00732

150. Funnekotter B, Mancera RL, Bunn E. A Simple but Effective Combination of pH Indicators for Plant Tissue Culture. Plants (Basel). 2023;12(4):740. doi:10.3390/plants12040740 PubMed PMID: 36840088; PubMed Central PMCID: PMC9959788.

151. Lu ZR, Sun D. Mechanism of pH-sensitive Amphiphilic Endosomal Escape of Ionizable Lipid Nanoparticles for Cytosolic Nucleic Acid Delivery. Pharm Res. 2025;42(7):1065–77. doi:10.1007/s11095-025-03890-8

152. Gomes IP, Duarte JA, Maia ALC, Rubello D, Townsend DM, Barros ALB de, et al. Thermosensitive Nanosystems Associated with Hyperthermia for Cancer Treatment. Pharmaceuticals. 2019;12(4). doi:10.3390/ph12040171

153. Haemmerich D, Ramajayam KK, Newton DA. Review of the Delivery Kinetics of Thermosensitive Liposomes. Cancers (Basel). 2023;15(2):398. doi:10.3390/cancers15020398 PubMed PMID: 36672347; PubMed Central PMCID: PMC9856714.

154. Luiz MT, Dutra JAP, Viegas JSR, Araújo JTC de, Junior AGT, Chorilli M. Hybrid Magnetic Lipid-Based Nanoparticles for Cancer Therapy. Pharmaceutics. 2023;15(3). doi:10.3390/pharmaceutics15030751

155. Johnson-Arbor K, Dubey R. Doxorubicin. In: StatPearls [Internet]. Treasure Island (FL): StatPearls Publishing; 2025 [cited 2026 Jan 22]. Available from: http://www.ncbi.nlm.nih.gov/books/NBK459232/ PubMed PMID: 29083582.

156. Rawat PS, Jaiswal A, Khurana A, Bhatti JS, Navik U. Doxorubicin-induced cardiotoxicity: An update on the molecular mechanism and novel therapeutic strategies for effective management. Biomedicine & Pharmacotherapy. 2021;139:111708. doi:10.1016/j.biopha.2021.111708

157. Venkatesh P, Kasi A. Anthracyclines. In: StatPearls [Internet]. Treasure Island (FL): StatPearls Publishing; 2025 [cited 2026 Jan 22]. Available from: http://www.ncbi.nlm.nih.gov/books/NBK538187/ PubMed PMID: 30844214.

158. van der Geest JSA, Kelters IR, Arends B, van Ham WB, Benavente ED, Lapré TA, et al. Dexrazoxane protects against doxorubicin-induced cardiotoxicity in susceptible human living myocardial slices: A proof-of-concept study. British Journal of Pharmacology. 2025;182(18):4262–80. doi:10.1111/bph.70085

159. Dadpour S, Mehrabian A, Arabsalmani M, Mirhadi E, Askarizadeh A, Mashreghi M, et al. The role of size in PEGylated liposomal doxorubicin biodistribution and anti-tumour activity. IET Nanobiotechnol. 2022;16(7–8):259–72. doi:10.1049/nbt2.12094 PubMed PMID: 35983586; PubMed Central PMCID: PMC9469787.

160. Lee J, Choi MK, Song IS. Recent Advances in Doxorubicin Formulation to Enhance Pharmacokinetics and Tumor Targeting. Pharmaceuticals. 2023;16(6). doi:10.3390/ph16060802

161. Fulton MD, Najahi-Missaoui W. Liposomes in Cancer Therapy: How Did We Start and Where Are We Now. International Journal of Molecular Sciences. 2023;24(7). doi:10.3390/ijms24076615

162. Uzzaman M, Uddin MN. Optimization of structures, biochemical properties of ketorolac and its degradation products based on computational studies. Daru. 2019;27(1):71–82. doi:10.1007/s40199-019-00243-w PubMed PMID: 30784007; PubMed Central PMCID: PMC6593035.

163. Ruszkowski M, Sekula B, Ruszkowska A, Contestabile R, Nogues I, Angelaccio S, et al. Structural basis of methotrexate and pemetrexed action on serine hydroxymethyltransferases revealed using plant models. Sci Rep. 2019;9(1):19614. doi:10.1038/s41598-019-56043-4

164. Macario A, López JC, Blanco S. Molecular Structure of Salicylic Acid and Its Hydrates: A Rotational Spectroscopy Study. International Journal of Molecular Sciences. 2024;25(7). doi:10.3390/ijms25074074

165. Hanoodi M, Mittal M. Methotrexate. In: StatPearls [Internet]. Treasure Island (FL): StatPearls Publishing; 2025 [cited 2026 Jan 24]. Available from: http://www.ncbi.nlm.nih.gov/books/NBK556114/ PubMed PMID: 32310574.

166. Mahmoodi AN, Patel P, Kim PY. Ketorolac. In: StatPearls [Internet]. Treasure Island (FL): StatPearls Publishing; 2025 [cited 2026 Jan 24]. Available from: http://www.ncbi.nlm.nih.gov/books/NBK545172/ PubMed PMID: 31424756.

167. Sandoval HP, Fernández de Castro LE, Vroman DT, Solomon KD. A review of the use of ketorolac tromethamine 0.4% in the treatment of post-surgical inflammation following cataract and refractive surgery. Clin Ophthalmol. 2007;1(4):367–71. PubMed PMID: 19668513; PubMed Central PMCID: PMC2704525.

168. Ketorolac trometamol | Drugs | BNF content published by NICE [Internet]. [cited 2026 Jan 24]. Available from: https://bnf.nice.org.uk/drugs/ketorolac-trometamol/

169. Çalışkan EE, Aydın YÇ, Ozbek EN, Alcın I, Kilinc E, Yetik Anacak G, et al. In Vitro Drug Release Kinetics and Antioxidant Activity of Metformin-Loaded Niosomes. ACS Omega. 2025;10(48):58225–37. doi:10.1021/acsomega.5c03679

170. Agbaje KO, Adesina SK, Adebayo AS. Development and Characterization of Optimized Drug-Loaded Niosomes for Delivery of 5-FU and Irinotecan. Pharmaceutics. 2025;17(7). doi:10.3390/pharmaceutics17070900

171. Liu Y, Dan Y, Yang J, He X, Liu J, Yi Y, et al. Clinical Efficacy of a Salicylic Acid–Containing Gel on Acne Management and Skin Barrier Function: A 21-Day Prospective Study. J Cosmet Dermatol. 2025;24(7):e70353.

doi:10.1111/jocd.70353 PubMed PMID: 40682377; PubMed Central PMCID: PMC12274963.

172. Li D, Martini N, Wu Z, Chen S, Falconer JR, Locke M, et al. Niosomal Nanocarriers for Enhanced Dermal Delivery of Epigallocatechin Gallate for Protection against Oxidative Stress of the Skin. Pharmaceutics. 2022;14(4):726. doi:10.3390/pharmaceutics14040726 PubMed PMID: 35456560; PubMed Central PMCID: PMC9029719.

173. Żmuda A, Kamińska W, Bartel M, Głowacka K, Chotkowski M, Medyńska K, et al. Physicochemical characterization and potential cancer therapy applications of hydrogel beads loaded with doxorubicin and GaOOH nanoparticles. Sci Rep. 2024;14(1):20822. doi:10.1038/s41598-024-67709-z

174. Lian J, Tang X, Gui Y, Lu S, Song Y, Deng Y. Impact of formulation parameters and circulation time on PEGylated liposomal doxorubicin related hand-foot syndrome. International Journal of Pharmaceutics. 2024;665:124659. doi:10.1016/j.ijpharm.2024.124659

175. Choi S, Kang B, Yang E, Kim K, Kwak MK, Chang PS, et al. Precise control of liposome size using characteristic time depends on solvent type and membrane properties. Sci Rep. 2023;13:4728. doi:10.1038/s41598-023-31895-z PubMed PMID: 36959258; PubMed Central PMCID: PMC10036480.

176. Agarwal S, Bakshi V, Vitta P, Raghuram A, Pandey S, Udupa N. Effect of cholesterol content and surfactant HLB on vesicle properties of niosomes. Indian Journal of Pharmaceutical Sciences. 2004;66:121–3.

177. Span 65 for synthesis 26658-19-5 [Internet]. [cited 2026 Jan 27]. Available from: https://www.sigmaaldrich.com/GB/en/product/mm/840122?srsltid=AfmBOoqgSCu7AN5koJ50rNO83-nixlWfXYFhT4rn88YJCf4y5uGHV0qt

178. ZetaPotential-Introduction-in-30min-Malvern.pdf [Internet]. [cited 2026 Mar 1]. Available from: https://www.research.colostate.edu/wp-content/uploads/2018/11/ZetaPotential-Introduction-in-30min-Malvern.pdf

179. Hadia J, Pethani T, Dudhrejiya A. Development of novel injectable formulation of clopidogrel by QbD approach | international journal of pharmaceutical sciences and research [Internet]. 2019 [cited 2026 Feb 27]. Available from: https://ijpsr.com/bft-article/development-of-novel-injectable-formulation-of-clopidogrel-by-qbd-approach/?view=fulltext

180. Danaei M, Dehghankhold M, Ataei S, Hasanzadeh Davarani F, Javanmard R, Dokhani A, et al. Impact of Particle Size and Polydispersity Index on the Clinical Applications of Lipidic Nanocarrier Systems. Pharmaceutics. 2018;10(2):57. doi:10.3390/pharmaceutics10020057 PubMed PMID: 29783687; PubMed Central PMCID: PMC6027495.

181. Alva-Ensastegui JC, Morales-Avila E, de la Luz AP, Bernad-Bernad MJ. Determination of pKa values and deprotonation order of methotrexate using a combined experimental-theoretical study and binding constants of the methotrexate-Laponite complex at different pH values. Journal of Photochemistry and Photobiology A: Chemistry. 2024;449:115406. doi:10.1016/j.jphotochem.2023.115406

182. Pauli G, Tang WL, Li SD. Development and Characterization of the Solvent-Assisted Active Loading Technology (SALT) for Liposomal Loading of Poorly Water-Soluble Compounds. Pharmaceutics. 2019;11(9):465. doi:10.3390/pharmaceutics11090465 PubMed PMID: 31505795; PubMed Central PMCID: PMC6781273.

183. Methotrexate [59-05-2] Clinisciences [Internet]. [cited 2026 Feb 27]. Available from: https://www.clinisciences.com/en/other-products-186/methotrexate-59-05-2-24029304.html?utm_source=chatgpt.com

184. Methotrexate [Internet]. [cited 2026 Feb 27]. Available from: https://go.drugbank.com/drugs/DB00563

185. Bai M, Shen Q, Wu Y, Ma Z, Wang Y, Chen M, et al. Evaluation of transport mechanisms of methotrexate in human choriocarcinoma cell lines by LC-MS/MS. Journal of Pharmaceutical and Biomedical Analysis. 2024;247:116268. doi:10.1016/j.jpba.2024.116268

186. Drugs.com [Internet]. [cited 2026 Feb 28]. Ketorolac: Package Insert / Prescribing Information. Available from: https://www.drugs.com/pro/ketorolac.html

187. Agents Used for Treatment of Hyperkeratosis [Internet]. [cited 2026 Feb 28]. Available from: https://www.sciencedirect.com/science/chapter/monograph/abs/pii/B9780323612111000553 doi:10.1016/B978-0-323-61211-1.00055-3

188. Lee CY, Tsai T, Peng PC, Chen CT. Fabrication of Doxorubicin-Loaded Lipid-Based Nanocarriers by Microfluidic Rapid Mixing. Biomedicines. 2022;10(6):1259. doi:10.3390/biomedicines10061259 PubMed PMID: 35740280; PubMed Central PMCID: PMC9219747.

189. Seleci DA, Maurer V, Stahl F, Scheper T, Garnweitner G. Rapid Microfluidic Preparation of Niosomes for Targeted Drug Delivery. International Journal of Molecular Sciences. 2019;20(19). doi:10.3390/ijms20194696

190. Obeid MA, Khadra I, Aljabali AA, Amawi H, Ferro VA. Characterisation of niosome nanoparticles prepared by microfluidic mixing for drug delivery. International Journal of Pharmaceutics: X. 2022;4:100137. doi:10.1016/j.ijpx.2022.100137 PubMed PMID: 36386005.

191. Cheng Y, Hay CD, Mahuttanatan SM, Hindley JW, Ces O, Elani Y. Microfluidic technologies for lipid vesicle generation. Lab Chip. 2024;24(20):4679–716. doi:10.1039/D4LC00380B

192. Machado ND, García-Manrique P, Fernández MA, Blanco-López MC, Matos M, Gutiérrez G. Cholesterol free niosome production by microfluidics: Comparative with other conventional methods. Chemical Engineering Research and Design. 2020;162:162–71. doi:10.1016/j.cherd.2020.08.002

193. Obeid MA, Gebril AM, Tate RJ, Mullen AB, Ferro VA. Comparison of the physical characteristics of monodisperse non-ionic surfactant vesicles (NISV) prepared using different manufacturing methods. International Journal of Pharmaceutics. 2017;521(1):54–60. doi:10.1016/j.ijpharm.2017.02.007

194. DOXORUBICIN HYDROCHLORIDE- doxorubicin hydrochloride injection, solution Pfizer Laboratories Div Pfizer Inc [Internet]. [cited 2026 Mar 1]. Available from: https://labeling.pfizer.com/ShowLabeling.aspx?id=530#section-3

195. caelyx-pegylated-liposomal-epar-product-information_en.pdf [Internet]. [cited 2026 Mar 1]. Available from: https://www.ema.europa.eu/en/documents/product-information/caelyx-pegylated-liposomal-epar-product-information_en.pdf

196. Dehghan S, Naghipour A, Anbaji FZ, Golshanrad P, Mirazi H, Adelnia H, et al. Enhanced *in vitro* and *in vivo* anticancer activity through the development of Sunitinib-Loaded nanoniosomes with controlled release and improved uptake. International Journal of Pharmaceutics. 2023;640:122977. doi:10.1016/j.ijpharm.2023.122977

197. Dimov N, Kastner E, Hussain M, Perrie Y, Szita N. Formation and purification of tailored liposomes for drug delivery using a module-based micro continuous-flow system. Sci Rep. 2017;7:12045. doi:10.1038/s41598-017-11533-1 PubMed PMID: 28935923; PubMed Central PMCID: PMC5608873.

198. NanoAssemblr™ GMP System for nanoparticle formulation | Cytiva [Internet]. [cited 2026 Mar 1]. Available from: https://www.cytivalifesciences.com/en/pl/products/items/nanoassemblr-gmp-system-for-nanoparticle-formulation-p-45347?selectedProduct=31125573